NOTICE

The quality of this microform is heavily dependent upon the quality of the original thesis submitted for microfilming. Every effort has been made to ensure the highest quality of reproduction possible.

If pages are missing, contact the university which granted the degree.

Some pages may have indistinct print especially if the original pages were typed with a poor typewriter ribbon or if the university sent us an inferior photocopy.

Reproduction in full or in part of this microform is governed by the Canadian Copyright Act, R.S.C. 1970, c. C-30, and subsequent amendments.

AVIS

La qualité de cette microforme dépend grandement de la qualité de la thèse soumise au microfilmage. Nous avons tout fait pour assurer une qualité supérieure de reproduction.

S'il manque des pages, veuillez communiquer avec l'université qui a conféré le grade.

La qualité d'impression de certaines pages peut laisser à désirer, surtout si les pages originales ont été dactylographiées à l'aide d'un ruban usé ou si l'université nous a fait parvenir une photocopie de qualité inférieure.

La reproduction, même partielle, de cette microforme est soumise à la Loi canadienne sur le droit d'auteur, SRC 1970, c. C-30, et ses amendements subséquents.

THE UNIVERSITY OF ALBERTA

THE EXPRESSION AND ASSEMBLY OF *ESCHERICHIA COLI* FUMARATE REDUCTASE

by

© David John Latour

A THESIS

SUBMITTED TO THE FACULTY OF GRADUATE STUDIES AND RESEARCH IN PARTIAL FULFILLMENT OF THE REQUIREMENTS FOR THE DEGREE OF Doctor of Philosophy

DEPARTMENT OF BIOCHEMISTRY

EDMONTON, ALBERTA

FALL, 1988

ISBN 0-315-52760-9

"It is a profound and necessary truth that the deep things in science are not found because they are useful; they are found because it was possible to find them."

R. Oppenheimer

"One of the most insidious and nefarious properties of scientific models is their tendency to take over, and sometimes supplant, reality."

E. Chagraff

"The perversity of the Universe tends towards a maximum."

L. Niven

IN MEMORIAM

Jean-Paul André Latour,
B. Sc., M.D., C.M., F. R. C. P. S., F. A. C. S.
1915-1987

Father and mentor.

ABSTRACT

Fumarate reductase of *Escherichia coli* is a membrane bound electron transport enzyme composed of four different subunits. The 69 000 Da FrdA contains covalently bound flavin adenine dinucleotide. The 27 000 Da FrdB contains three iron-sulphur centres. The 15 000 Da FrdC and 13 000 Da FrdD are hydrophobic and serve to anchor the enzyme to the membrane.

Using Tn*5* mutagenesis it has been shown that FrdA was flavinylated in the absence of FrdB, and that FrdAB was the minimal catalytic domain. The FrdAB dimer was stimulated by anions and was both thermal and alkaline labile. The holoenzyme was stable in both conditions and was insensitive to anions. A Tn*5* mutation in *frdD* truncated the polypeptide and this allowed a FrdABC trimer to accumulate in the cytoplasm, indicating that FrdC alone was inadequate for membrane attachment. The trimer was not activated by anions and it was thermolabile. It was stable to alkali. The truncated FrdD [FrdD'] could associate with the trimer in the membrane. This tetramer could couple to the electron transport chain or to quinone analogues, unlike the dimeric or trimeric forms. It was still thermolabile.

An *in vivo* T7 phage transcription/translation system allowed probing of the assembly pathway of the holoenzyme. Flavinylation of FrdA was by flavin adenine dinucleotide and not by a precursor. The two membrane anchor subunits associated immediately with the membrane and then were capped by FrdB. The addition of FrdA completed the assembly. FrdD' was required for FrdC to interact with FrdAB, but once assembled, the FrdABC trimer could be dissociated from FrdD'. .

Control of the *frd* operon was examined *in vitro* in an S-30 extract. Three hairpin loops can form in the mRNA in a region encoding an alanine rich segment of the FrdA N-terminal region. The level of alanine in the medium controlled expression of the operon in a fashion similar to attenuation of the amino acid biosynthetic operons. The Fnr protein caused termination at several sites, and six potential binding sites for Rho were identified in the *frd* mRNA.

ACKNOWLEDGEMENTS

I would like to thank my supervisor, Joel Weiner for his patience and his willingness to share his thoughts, ideas and experience. His support during my foray into the uncharted wilderness of *frd* regulation was particularly encouraging. I would also like to thank the members of my committee; Bill Parachych, Wolfgang Schneider and Glen Armstrong for their direction and interest in my progress.

Many past and current members of this department have lent advice, assistance or materiel; Brett Findlay, Britt Pasloske, Colin MacAulay, Chris Upton, Clive Sanders, Gillian Henry and Charles Séguin. I thank you all for your time and effort.

It has been my pleasure to work with the many and varied people who have passed through this lab during my tenure here; graduate students John Robinson, Bernie Lemire, Stuart Lee and Monica Varga; post-doctoral Fellows Bob Jones, Peter Bilous, Caro Condon, Lynn Elmes and Sambu Damarajau. These people have all made a contribution to the way I see and do science, as well as being friends. Lynn's editorial skills and chocolate thumb are, in particular, sorely missed.

Reinhardt Reithmeier, Brian Sykes, Bill Bridger and Dick Morgan of this department have given freely of their time and knowledge. I thank them, also. Glen Armstrong deserves additional thanks for the work he and his people did in raising antisera to our various proteins.

I would like to thank my family for their moral and financial support over the years and for helping to lay the foundations of my life which led me eventually to this time and place.

Last in place but first in my thoughts, I would like to thank Carolyn Aks for her love and support, and her absolute faith in my abilities and future prospects. May we always be as we have been these past nine years; lovers and friends.

This work has been supported by a grant from the Medical Research Council to Joel Weiner.

TABLE OF CONTENTS

LIST OF TABLES

LIST OF FIGURES

LIST OF ABBREVIATIONS AND SYMBOLS

A	adenosine
ADP	adenosine-5'-diphosphate
AMP	adenosine-5'-monophosphate
Ap^r	ampicillin resistance
ATP	adenosine-5'-triphosphate
bla	β-lactamase gene
bp	basepair
C	cytosine
$C_{12}E_8$	octaethyleneglycol dodecyl ether
cAMP	adenosine-3',5'-cyclic monophosphate
Cm^r	chloramphenicol resistance
Da	dalton
DCCD	dicyclohexylcarbodiimide
DMN/H_2	2,3-dimethyl-1,4-naphthoquinone/quinol
DMSO	dimethylsulphoxide
EDTA	ethylenediaminetetraacetate
ESR	electron spin resonance
ETC	electron transfer chain
F_0	membrane domain of the ATP synthase
F_1	catalytic domain of the ATP synthase
FAD	flavin adenine dinucleotide
FeS	iron-sulphur cluster
FRD	fumarate reductase
G	guanosine
GF	glycerol-fumarate medium
HEPES	N-2-hydroxyethyl-piperazine-N'-2-ethane sulphonic acid

kbp	kilobasepair
kDa	kilodalton
K_m	Michaelis constant
Km^r	kanamycin resistance
LB-B_1	Luria broth supplemented with thiamin
memb	membrane
MK	menaquinone
NAD^+/NADH	nicotine adenine dinucleotide, oxidized/reduced
NMR	nuclear magnetic resonance spectroscopy
nt	nucleotide
PBS	phosphate buffered isotonic saline
PMSF	phenylmethylsulphonyl fluoride
SDH	succinate dehydrogenase
SDS-PAGE	polyacrylamide gel electrophoresis using sodium dodecyl sulphate
Sm^r	streptomycin resistance
sol	soluble
T	thymidine
TCA^1	trichloroacetic acid
TCA^2	tricarboxylic acid cycle
Tc^r	tetracycline resistance
TLCK	*p*-tosyllysylchloromethylketone
TMAO	trimethylamine-*N*-oxide
TPCK	*p*-tosylyphenylalanylchloromethylketone
U^1	unit
U^2	uridine
UQ	ubiquinone

vol	volume
Δp	proton motive force
ΔpH	proton chemical differential
$\Delta \psi$	electrical potential differential

I. INTRODUCTION

Escherichia coli, a gram-negative bacterium can derive energy for growth both by fermentation through glycolysis and by oxidative phosphorylation *via* an assortment of electron transport chains. Oxidative phosphorylation can be driven by a number of primary dehydrogenases coupled to a variety of terminal electron acceptors; oxygen, nitrate, nitrite, trimethylamine-*N*-oxide and dimethylsulphoxide [1-5]. This facultative anaerobe lives in a variety of environments, from well-oxygenated river water to the mammalian colon, which is poor in oxygen but rich in organic compounds. To adapt to such a wide range of environments*E. coli* has evolved an array of electron transport proteins to allow the use of alternate electron acceptors, as required.

A. MECHANSIM OF ENERGY COUPLING

ATP synthesis can be coupled directly or indirectly to substrate oxidation. Direct coupling is known as substrate-level phosphorylation and is exemplified by the reaction of pyruvate kinase. This form of energy coupling supplies up to 15% of the total ATP pool, depending on the growth substrate [6]. Indirect coupling of substrate oxidation is called oxidative phosphorylation and is mediated by the various electron transport chains. These electron transport, or respiratory chains generate a charged state of the cytoplasmic membrane, often termed 'squiggle', or more correctly, the proton motive force [Δp]. This generated potential can then be used to drive energy dependent processes such as ATP synthesis, substrate transport and flagellar rotation.

The chemiosmotic model of the coupling of the energised state of the membrane to the various processes it drives was first proposed by Dr. Peter Mitchell [7]. His hypothesis was that the respiratory chains used the energy of electron transport to exude protons to the external medium, generating a potential gradient across the membrane. This potential can be described mathematically as:

$$\Delta p = \Delta\Psi - Z\Delta pH$$

where Z is 2.303 RT/nF. At 37°C Z is approximately equal to 62 mV for protons and other monovalent cations. It can be seen that the potential has both an electrical component, $\Delta\Psi$ which arises from the accumulation of positive charges outside and a chemical component, ΔpH which is due to the higher concentration of protons outside.

Mitchell proposes four essential postulates for the chemiosmotic hypothesis [8]. The first is that the coupling membrane must be topologically closed and relatively impermeable to both protons and hydroxyl ions, in order that a gradient can be established and maintained across the membrane. The second is that the respiratory chains are capable of generating a differential of proton concentration across the membrane, either through vectorial reactions or by a pumping mechanism. The third is the existance of a reversible membrane-spanning ATPase which could use the potential gradient to drive ATP synthesis or use ATP hydrolysis to generate the proton motive force. The fourth postulate is that the other energy dependent processes such as substrate transport and flagellar rotation should also be capable of using the proton gradient directly.

Figure I.1 shows a general picture of the chemiosmotic hypothesis as applicable to *E. coli*. A simple respiratory chain is depicted which expels protons by transport of hydrogen from the substrate inside to the outside of

the membrane, deposition of the protons to the external medium in a scalar reaction and transport of the electrons back to the cytoplasmic side of the membrane where they are used to reduce the final electron acceptor in another scalar reaction, along with protons from the internal medium. The proton gradient thus generated is shown generating ATP *via* the F_1F_0 ATP synthase, driving the uptake of an anionic substrate and powering bacterial motility *via* the flagellar motor.

E. coli growing anaerobically on glycerol and fumarate uses a respiratory scheme as simple as that depicted in Fig. I.1 [9]. Glycerol diffuses inwards across the cytoplasmic membrane and is phosphorylated to glycerol-3-phosphate by glycerol kinase [10]. There it is oxidized to dihydroxyacetonephosphate by the anaerobic glycerol-3-phosphate dehydrogenase. The hydrogen is donated to menaquinone [11] which in turn donates the electrons to fumarate reductase [10]. During this process the protons are left in the external medium. A *b*-type cytochrome has been implicated in this disproportionality [12] but all attempts to isolate this protein have failed to date, and its existance in this respiratory chain must remain moot.

The glycerol to fumarate electron transport chain can generate $\Delta\rho$, as shown by the accumulation of sugars [13] and amino acids in cells [10] or in right-side-out vesicles [14,15], by the fumarate dependent quenching of atebrin fluorescence in inside-out vesicles [16], by the fumarate dependent translocation of protons in cells [17] and by isolation of an enzyme complex which catalyses glycerol-3-phosphate dependent fumarate reduction which is capable of driving ATP synthesis [18].

B.THE ATP SYNTHASE

The Mg^{2+} dependent ATP synthase is found in all energy transducing membranes from sources such as mitochondria, chloroplasts and bacteria [19]. The enzyme is a complex oligomer of eight different subunits, of similar composition and structure in the membranes of diverse organisms [20].

The ATP synthase of *E. coli* is divided into two functional domains, a water soluble F_1 portion and a membrane bound F_0 domain. F_1 corresponds to the knob seen on the internal surface of energy transducing membranes [22] and is responsible for the catalytic intercoversion of ATP and ADP plus inorganic phosphate [21]. This domain contains five different polypeptides with an aggregate weight of approximately 360 000 Da. The generally accepted stoichiometry of the subunits is $\alpha_3\beta_3\gamma\delta\varepsilon$ [20]. The α and the β subunits may be all that is required for ATP hydrolysis [23], but the γ subunit may be needed as well [24].

The membrane bound F_0 portion contains three polypeptides in the ratio of $\mathbf{a}_1\mathbf{b}_2\mathbf{c}_{10\text{-}15}$ [25,26]. F_0 can be shown to act as a proton channel across biological or artificial lipid membranes [27,28]. Binding of the F_1 head on the F_0 stalk blocks the proton pore of the latter domain [20].

Reaction of the hydrophobic subunit **c** with dicyclohexylcarbodiimide modifies an aspartyl residue proposed to be located in the middle of a transmembrane α-helix [29] and blocks the conduction of protons through F_0 [30]. Mutations affecting this particular aspartyl residue result in an impermeable F_0 domain [31].

The **a** and **b** subunits appear to function in the proper assembly of F_0 and the attachment of F_1 [32]. Mutants in subunit a prevent the modification of subunit **c** by DCCD and reduce the proton conductance of

F_0 [33,34]. In these mutants the F_1 portion could be more easily dissociated. Mutants in subunit **b** result in a proton impermeable F_0 and an F_1 free in solution [35].

It is the ATP synthase which is responsible for coupling the proton gradient to the formation of the γ-phosphate bond of ATP, even in artificial liposomes [36] and it is capable of using either the $\Delta\Psi$ or the ΔpH component of Δp for this purpose [37]. It is the magnitude of Δp, rather than its source, which is responsible for driving ATP synthesis. A minimum driving force of 150mV is required.

The primary role of the ATP synthase during oxidative growth is to make ATP from the energy of the electr chemical potential, while during fermentation its function is to produce a Δp from ATP derived t th substrate level phosphorylation [37].

C.THE ELECTROCHEMICAL PROTON GRADIENT

The gradient of protons across the coupling membrane is used to power a variety of energetic processes. These include active transport of solutes, motility, transhydrogenation, phage infection, reverse electron transport and ATP synthesis [38]. Figure I.2 shows a general scheme of energy transduction in *E. coli.*

Either component of Δp will drive ATP synthesis, with a proton to ATP ratio of between two and three. Some types of active transport require either $\Delta\Psi$ or ΔpH specifically. Anions or neutral molecules are taken up with protons [symport]. Cation export is also coupled to the proton gradient by an electroneutral exchange of proton for cation [antiport]. The potassium antiporter is $\Delta\Psi$ dependent while the lactose permease is a ΔpH dependent symporter [39].

D.THE AEROBIC ELECTRON TRANSPORT CHAIN

The membranes of aerobically grown *E. coli* contain seven cytochromes; five *b*-type cytochromes, cytochrome *d* and cytochrome a_1 [40,41]. There appear to be two branches of the aerobic chain, one used at high oxygen tension and one used at low oxygen tension. There are two cytochromes which function as terminal oxidases; the *b*-type cytochrome *o* and cytochrome *d* [41]. The pathways of electron transport are shown in Fig. I.3.

Cells grown at high oxygen concentrations show two cytochrome peaks in reduced minus oxidized spectra taken at 77 K. One has a λ_{max} of 556nm while the other, cytochrome *o* has a split α-band with peaks at 555 and 562nm [41]. As oxygen tension in the culture is reduced, other cytochromes become visible; cytochrome a_1, with an α-band between 590 and 595nm and cytochrome *d* with an absortion band at 630nm.

Ubiquinone-8 is the hydrogen carrier in aerobically grown cells. With a decrease in oxygen tension, significant amounts of menaquinone-8 appear in the membrane. Under anaerobic conditions only menaquinone is detectable [41].

Cytochrome *o* and cytochrome *d* are the terminal oxidases in aerobically grown *E. coli.* Cytochrome *o* binds CO and CN at high affinity and is considered to be the major cytochrome oxidase. Under low oxygen tension cytochrome *o* still persists, but with altered spectral properties [41]. A complex of cytochrome b_{562} and cytochrome *o* has been isolated by Kita and co-workers [42] and contains equimolar amounts of two proteins of 55 kDa and 33 kDa as well as heme and Cu but no non-heme Fe or quinone. Matsushita *et al* report an additional two polypeptides of 22 kDa and 17

kDa in a purified cytochrome *o* complex [43]. This segment of the electron transport chain can generate Δp in the presence of ubiquinone and a suitable electron donor [43,44]. Redox titration of cytochrome *o* gives a mid-point potential of +260mV [41]. The K_m for O_2 consumption of cytochrome *o* has been reported to be in the range of 0.74 to 2.9 μM [41].

Cytoc' me *d* is the other major oxidase of *E. coli* grown in oxygen limiting c ions [41,45]. Its expression is apparently linked to that of cytochromes a_1 and b_{558} [1]. Cytochrome *d* has a much lower K_m for oxygen than does cytochrome *o* [0.23-0.38μM *versus* 0.74-2.9μM [41]], in accord with its function at low oxygen tension *in vivo*. A purified complex of cytochrome *d* together with cytochrome b_{558} has been described [46]. SDS-PAGE of such complexes showed the presence of two polypeptides reported variously as 70 kDa and 43 kDa, 57 kDa and 43 kDa [41] or 51 kDa and 26 kDa [47]. There were equimolar amounts of protoheme-IX and heme chlorin in the preparation [47]. There was no copper. The mid-point potential of cytochrome *d* has been measured both in membrane preparations and purified complexes and was found to be between +232 and +280mV [41]. Reconstituted cytochrome *d* can generate a Δp across the membrane [47].

E. CHEMIOSMOTIC COUPLING OF THE AEROBIC RESPIRATORY CHAINS

Measurements of the stoichiometry of proton extrusion driven by respiration suggest that there are two energy conserving sites in the aerobic electron transport chains [17,41]. Oxidation of malate gives a proton to oxygen ratio of four while oxidation of succinate or lactate results in a proton to oxygen ratio of two. This would suggest that one site is between

NADH dehydrogenase and quinone and one is between quinone and the terminal oxidase [48].

The low value of two protons per oxygen per site bears on models of electron transport and the generation of Δp. Vectorial reactions of the respiratory chain components suffice to provide this stoichiometry without the need for Q-cycles or proton pumps. These stoichiometries are valid whether grown at high or low oxygen tension [17], suggesting that cytochrome *o* and cytochrome *d* have similar reaction mechanisms.

F. THE ANAEROBIC RESPIRATORY CHAINS

E. coli growing anaerobically can use any of five primary substrates for energy production; H_2, formate, nicotine adenine dinucleotide, glycerol-3-phosphate and lactate, and five terminal oxidants in lieu of oxygen; nitrate, nitrite, fumarate, TMAO and DMSO [49]. For each primary substrate there is a primary dehydrogenase and for each oxidant there is a separate terminal reductase. The primary dehydrogenases are each induced by their substrates, while the terminal oxidases can best described as being repressed by the presence of a better oxidant than their own substrates. Coupling of the dehydrogenases to the reductases is mediated by menaquinone-8 and in some cases by a *b*-type cytochrome specific to the chain involved [49].

G. PRIMARY DEHYDROGENASES

ENZYMES OF THE AEROBIC PATHWAY

sn-GLYCEROL-3-PHOSPHATE DEHYDROGENASE.

E. coli can grow with glycerol as sole carbon and energy source both aerobically and anaerobically [9,41,49]. The aerobic and the anaerobic pathways use different dehydrogenases. The aerobic enzyme is encoded by *glpD* and *glpD* mutants can grow on fumarate or nitrate but not oxygen [50]. Mutants in *glpABC*, which encodes the anaerobic dehydrogenase, can grow with oxygen or nitrate but not with fumarate. That the aerobic enzyme couples to oxygen or nitrate while the anaerobic enzyme couples to nitrate or fumarate may be due to the fact that the aerobic respiratory chain is dependent on ubiquinone while the anaerobic chains use menaquinone. Nitrate reductase can use either hydrogen carrier [41].

The aerobic enzyme is abundantly produced during growth on glycerol or glycerol-3-phosphate [41,51]. Its active site is on the cytoplasmic side of the membrane [52]. It is composed of a single polypeptide of 58 kDa which probably associates as a homodimer [53]. The cofactor for this enzyme is non-covalently bound flavin adenine dinucleotide, one molecule per dimer. The activity of the enzyme is modulated by detergent or phospholipid.

SUCCINATE DEHYDROGENASE

Succinate dehydrogenase is an enzyme of the tricarboxylic acid cycle and functions at the point where the TCA cycle couples to the electron transport chain. The enzyme is expressed during growth without glucose on either O_2 or NO_3^- [41,53,54]. Succinate dehydrogenases from a variety of eukaryotic and prokaryotic sources contain covalently bound FAD [56] and three iron-sulphur clusters termed centres 1, 2, and 3 [57]. The holoenzyme consists of four polypeptides of 71 kDa, 26 kDa, 17 kDa and

15 kDa [SdhA, B, C and D]. SdhA contains the FAD, while SdhB contains the three iron-sulphur centres, based on the nucleotide sequence. Electron spin resonance spectra of SDH showed the presence of an Fe_2S_2 cluster [centre 1] and an Fe_3S_X cluster [centre 3]. Centre 2, an Fe_4S_4 cluster, is detectable only as an alteration of the relaxation properties of centre 1 at low redox potentials [58,59]. The redox potentials of centres 1, 2 and 3 have been variously reported as -20mV, -220mV and +100mV [41] or +10mV, -175mV and +65mV, respectively [58,59]. The detergent solubilised enzyme contains cytochrome *b556*. This is verified by chromosomal mapping of the cytochrome *b556* gene to the region of *sdh* [60] and N-terminal analysis of purified cytochrome *b556* [61] which revealed that the first 27 residues of the protein match the sequence of *sdhC*.

NADH DEHYDROGENASE

The respiratory NADH dehydrogenase has been cloned, isolated and characterized [41]. It is a single polypeptide of 47 kDa containing tightly bound but not covalently attached FAD. In the membrane it may be associated with an iron-sulphur protein which is detectable by ^{59}Fe radiography. Evidence for the association with another factor comes from the coprecipitation of NADH dehydrogenase and an FeS protein by crossed immunoelectrophoresis and the fact that NADH oxidation in normal cells results in the translocation of four protons while in cells grown in sulphate-limited medium the stoichiometry is two. Additionally, reversed electron transport from ATP to NAD^+ can be supported by lactate and succinate, suggesting a coupling site between these dehydrogenases and NADH dehydrogenase.

D-LACTATE DEHYDROGENASE

E. coli produces four lactate dehydrogenases, two of which are soluble enzymes using NADH as cofactor. The membrane bound respiratory lactate dehydrogenases are specific for either D- or L-lactate. D-lactate dehydrogenase is constitutive while L-lactate dehydrogenase is inducible by growth on DL-lactate [41].

D-lactate dehydrogenase has a molecular weight of 73 kDa and has a noncovalently bound FAD prosthetic group. The enzyme has two regions of low polarity and one of high polarity and secondary structure prediction by hydrophobic moment analysis indicates several possible amphipathic α-helices. Oxidation of D-lactate proceeds with the translocation of two protons in intact cells.

L-lactate dehydrogenase is quite distinct from D-lactate dehydrogenase. It consists of a single protein of 43 kDa with one mole of FMN bound per mole of polypeptide. Its synthesis is repressed during growth on glycerol aerobically or glucose anaerobically [62].

ENZYMES OF THE ANAEROBIC PATHWAYS

FORMATE HYDROGEN-LYASE

The formate hydrogen-lyase complex consists of a formate dehydrogenase and an hydrogenase and allows *E. coli* to grow on formate with the production of CO_2 and H_2 [49]. The formate dehydrogenase component is inducible anaerobically by the presence of formate in the medium or by the synthesis of pyruvate formate-lyase induced by excess

pyruvate. The enzyme requires Se for activity and uses the same Mo cofactor as does nitrate reductase. It is a single polypeptide of 80 kDa.

The hydrogenase component of formate hydrogen-lyase accounts for 90% of the hydrogenase activity of *E. coli.* Expression is induced by formate and repressed by nitrate and oxygen. The enzyme requires both Fe and Ni for activity.

When grown on nitrate *E. coli* produces a formate dehydrogenase distinct from the one already discussed [49]. It consists of three polypeptides of 110 kDa, 32 kDa, and 20 kDa. The largest subunit is a selenoprotein while the smallest is a *b*-type cytochrome. This enzyme also has a Mo cofactor and non-heme iron.

The formate induced enzyme does not couple to the electron transport chain, but does remove one proton from the cytoplasm in a scalar reaction

$$HCOO^- + H^+ \rightleftharpoons CO_2 + H_2$$

The nitrate induced enzyme, in contrast, donates the hydrogen extracted from formate to the quinone pool, thereby giving rise to the extrusion of two protons per formate oxidized.

sn-GLYCEROL-3-PHOSPHATE DEHYDROGENASE

The anaerobic glycerol-3-phosphate dehydrogenase is distinct from the aerobic enzyme and is encoded by the *glpABC* operon [49,63]. Only about 5-10% of the enzyme is bound to the cytoplasmic membrane, the rest is soluble in the cytoplasm [64]. The enzyme consists of a 62 kDa protein containing FAD as a dissociable cofactor and a 43 kDa subunit that had been assumed to be an FeS protein [65]. A 41 kDa polypeptide is the membrane anchor subunit [49] and comparison of the sequence [Cole *et al,*

in press] and electron spin resonance spectroscopy [R. Cammack, personal communication] has shown it to be, in fact, the iron-sulphur subunit.

H. TERMINAL REDUCTASES OF THE ANAEROBIC PATHWAYS

NITRATE REDUCTASE

Nitrate reductase is a complex membrane bound enzyme which catalyses the reduction of NO_3^- to NO_2^- [9,49]. The enzyme consists of two α-subunits of 150 kDa, two β-subunits of 60 kDa and four γ-subunits of 20 kDa. The α-subunits carry the Mo cofactor while the γ-subunits have been identified as the nitrate reductase specific cytochrome, cytochrome b_{556}^{NR}. The role of the β-subunit is unclear, but it exists in two interconvertible forms with different mobilities on SDS-PAGE gels [60 kDa and 58 kDa [55]]. Subunits α and β appear to be acylated by fatty acids. They are exposed on the cytoplasmic face of the membrane while the γ-subunits span the membrane and serve to anchor the complex there [49].

TMAO REDUCTASE

Four proteins with TMAO reductase activity have been identified; isozyme I [200 kDa], isozyme II [70 kDa], isozyme III [70 kDa] and isozyme IV [100 kDa] [49,66]. The major enzyme is probably isozyme I, which accounts for 93% of TMAO reductase activity [67]. It requires the same Mo cofactor as does nitrate reductase and induces the expression of four new cytochromes with α-bands at 548, 552, 554 and 557 nm [68].

DMSO REDUCTASE

An enzyme which allows the anaerobic growth of *E. coli* on dimethyl-sulphoxide [68] has recently been cloned and purified [69]. The purified enzyme consists of three polypeptides , DmsA, B and C of 82 kDa, 24 kDa and 23 kDa, respectively. It contains non-heme iron and uses the same Mo cofactor as does nitrate reductase, formate dehydrogenase and TMAO reductase.

FUMARATE REDUCTASE

The fumarate reductase of *E. coli* is a membrane bound enzyme induced during anaerobic growth on fumarate [9]. The holoenzyme contains four different subunits in equimolar ratio [Fig. I.4] and catalyses the interconversion of fumarate and succinate using electrons donated from the electron transport chain.

$$2e^- + 2H^+ + HOOC\text{-}CH{=}CH\text{-}COOH \rightleftharpoons HOOC\text{-}CH_2\text{-}CH_2\text{-}COOH$$

The 69 kDa FrdA subunit contains an FAD molecule covalently bound to His^{44} *via* an 8α-[N3]-histidyl linkage [70]. The 27 kDa FrdB subunit is thought to contain the three known iron-sulphur clusters, based on the primary sequence of the protein [3]. The iron-sulphur centres have been identified and characterized to be one each of an Fe_2S_2 [centre 1], an Fe_3S_4 [centre 3] and an Fe_4S_4 [centre 2] by electron spin resonance and magnetic circular dichroism spectra [71,72,73]. The 15 kDa and 13 kDa subunits FrdC and FrdD function to anchor the enzyme to the cytoplasmic membrane and to allow oxidation of quinols [74,75,76].

The *frd* operon maps at 94 min of the *E. coli* chromosome and has been cloned and sequenced [58,82,83]. It is composed of the four cistrons for the fumarate reductase subunits in the order *frdABCD* with a single

promoter upstream [84] and a strong terminator downstream [83]. The operon is transcribed as a single polycistronic messenger RNA [84]. The expression of the *frd* operon is modulated by fumarate [3,49], cAMP [113,116], NarL [115] and Fnr [3,97,113, 114].

Fumarate reductase is composed of two functional domains; a catalytic domain consisting of FrdA and FrdB and a membrane anchor domain consisting of FrdC and FrdD which is required for association with the membrane [79]. The FrdC and FrdD polypeptides are basic and quite hydrophobic [81]. Models of their secondary structure based on Kyte-Doolittle analysis [85] of the primary sequence show that each has three potential transmembrane segments and a pair of small loops on the cytoplasmic side of the membrane.

The catalytic domain can be purified in a water soluble form [77,78,79]. This FrdAB dimer is dependent on anions such as phosphate for maximal activity and stability [79]. In the absence of anions the activity of FrdAB is labile at pH 8.6 with a halflife of seven minutes [76]. On heating to greater than 45°C at pH 6.8 the dimer was rapidly denatured in 25 mM HEPES buffer but not in 200 mM phosphate buffer. The specific activity of the dimer is greater in sodium phosphate buffer [550 U mg^{-1}] than in HEPES buffer [100 U mg^{-1}] [79]. In contrast, the specific activity of the tetramer is 200 U mg^{-1} and is independent of anionic buffers. The tetramer is stable to alkaline denaturation and resistant to thermal denaturation [86]. The K_m for succinate is 2 mM while that for fumarate is 420 µM.

Fumarate reductase is a flavoenzyme. The flavin cofactor is not released from FrdA by treatment with denaturants such as trichloroacetic acid or KBr, as it is from most flavoenzymes [70]. Digestion with

proteases renders the FAD moiety TCA soluble. SDS-polyacrylamide gels fixed in TCA and viewed under UV illumination show a fluorescent band corresponding to FrdA. The fluorescence is quenched at high pH, is sensitive to dithionite but not borohydride and shows a hypochromic shift of the UV absorption peak from 325 to 350 nm. These features are characteristic of an 8α-substituted flavin.

The flavin attachment site of bovine succinate dehydrogenase has been determined by protein sequencing [129] A sequence of nine amino acids around the attachment site is perfectly conserved in FrdA, indicating that the first histidyl residue, His^{44}, is the site of attachment in fumarate reductase [3]. Sequence comparisons with glutathione reductase, whose structure is known [130] shows two regions of homology with FrdA at residues 6 to 37 and 359 to 379, which mark the bottom and the top of the AMP binding domain, respectively [3]. The bottom fold shows the β-α-β arrangement of the Rossman nucleotide binding fold [3].

Studies on 6-hydroxy-D-nicotine oxidase [131] indicated that covalently bound FAD molecules could be attached co-translationally, but a requirement for a full length FrdA has been demonstrated [132] indicating that in the case of fumarate reductase, at least, the attachment is likely to be post-translational.

Titration of FrdAB with the sulphydryl modifying agent 5,5'-dithiobis(2-benzoic acid) showed the presence of a single Cys residue which is required for activity. Cleavage at the modified residue and labelling of the scissile bond by ^{14}C-cyanide revealed the disappearance of the 69 kDa subunit and appearance of a new polypeptide of 38 kDa, suggesting that the residue was near the middle of FrdA, likely Cys^{247} [78].

The iron-sulphur centres have been localized to the FrdB subunit by comparison of its primary sequence with those of ferrodoxins of known structure and cluster geometry. FrdB has 11 Cys residues in 3 clusters. The first, at residues 56 to 77 resembles the Fe_2S_2 sites of plant ferrodoxins. The other two, between residues 147 to 166 and 204 to 214 resemble bacterial ferrodoxin iron-sulphur centres of the Fe_4S_4 or Fe_3S_4 type [3].

Electron spin resonance studies have shown that iron-sulphur centre 1 is an Fe_2S_2 type with a midpoint potential for reduction of -20 mV. Centre 3 is an Fe_3S_4 cluster with a mipoint potential of -70 mV. Centre 2 can only be visualized as an increase in the electron spin relaxation time of centre 1 and has been identified as an Fe_4S_4 type of cluster with a midpoint potential of -320 mV, a value too low for it to function in electron transport within the enzyme [73].

The separation of catalytic domain from anchor domain has been achieved, but the resolution of individual active subunits has not. The inner membranes of strains amplifying fumarate reductase are studded with 40-50 Å knobs. Washing with 6 M urea removes these knobs. This leaves the anchor subunits embedded in the membrane. Fresh catalytic dimer can then be reconstituted onto the anchors, as shown by the regaining of alkaline stability on formation of the tetramer [86]. Proteinase K digestion removes the 69 and 27 kDa subunits with concommitant loss of the knobs. Anti-fumarate reductase IgG forms a fuzzy coat over knob-studded membranes but not smooth membranes.

Amplification of fumarate reductase in the membrane does not alter the lipid to protein ratio, implying the increased synthesis of membrane lipid. This results in the production of a unique lipoprotein structure

within the cell [81,134]. The cytoplasm becomes filled with long lipoprotein tubules closely studded with a helical array of fumarate reductase knobs. The tubules are enriched in cardiolipin compared with normal membranes.

FrdB is partially inaccessible to labelling by phenylglyoxal, iodosulphanilic acid or iodination by lactoperoxidase [81]. FrdA has been shown to cross-link to both FrdB and FrdC [3]. Deletion of FrdD from the plasmid-borne operon leads to the synthesis of a soluble enzyme, and no amplification of membrane-bound activity, implying that FrdC alone is inadequate for membrane insertion [3]. It is possible to assemble functional fumarate reductase *in vivo* even when each of the subunits are expressed from different replicons, with one exception. Expression of FrdC and FrdD from separate replicons result in a membrane bound but physiologically inactive tetramer, implying that interaction between the two anchor subunits at the time of synthesis is required for proper assembly [133].

A point mutation resulting in the change of FrdC His^{82} to Arg^{82} results in a holoenzyme which is bound to the inner membrane but which can no longer use quinones as electron donors. Additionally, the rate of reduction of the FAD moiety as examined by electron spin resonance spectroscopy is slowed considerably by the mutation [74]. His^{82} is located on the cytoplasmic side of the subunit [81] and it may be involved conformationally in the formation of the quinone binding site or mechanistically in the transfer of electrons from quinones.

I. ASSEMBLY OF MEMBRANE PROTEINS

Membrane proteins can be subdivided into two classes, intrinsic and extrinsic. Extrinsic membrane proteins do not penetrate the lipid bilayer, but rather are associated with the surface of the membrane. This association may be mediated by electrostatic interactions between the protein and the phospholipid headgroups, or they may be bound in turn to intrinsic membrane proteins.

Intrinsic proteins penetrate the core of the lipid bilayer and are bound there by hydrophobic interactions. Most, if not all intrinsic proteins span the bilayer. They are readily distinguishable from extrinsic proteins by the requirement for detergents, organic solvents or strong chaotropes to solubilize them, as compared with extracting extrinsic proteins with changes of pH or ionic strength.

STRUCTURE OF INTRINSIC MEMBRANE PROTEINS

The prototype membrane protein is bacteriorhodopsin from *Halobacterium halobium*. This protein is an major component of the bacterial membrane, organised in a two-dimensional array known as the purple membrane. Because it exists in an ordered packing state, it was possible to produce a low-resolution three dimensional structure by using image reconstruction techniques on electron micrographs taken at various angles [87]. Each bacteriorhodopsin molecule appears to have seven transmembrane α-helices inclined at small angles to the perpendicular of the membrane. Examination of the amino acid sequence revealed seven regions where there were stretches of about 24 mainly hydrophobic amino acids which could believably be transmembrane segments [88].

The *E. coli* ATP synthase is another well-studied membrane protein. Like fumarate reductase there is an extrinsic catalytic domain composed of five subunit types and an intrinsic membrane anchor domain composed of three subunit types. Each of the anchor subunits has a sequence which could give rise to transmembrane helices and hydrophilic regions which could interact with the catalytic head [20].

Porin spans the outer membrane of *E. coli* and forms voltage dependent gated channels [89]. This very polar protein does not contain regions which could be transmembrane α-helices. It consists primarily of antiparallel β-sheets, proposed to be arranged perpendicular to the membrane [90,91]. This structure places the side chains of hydrophobic residues towards the outside while those of hydrophilic residues point primarily towards the interior, forming a hydrophilic pore through the centre of the molecule.

MEMBRANE PROTEINS AND SIGNAL SEQUENCES

Like all Gram-negative bacteria *E. coli* has an inner membrane, an outer membrane and a peptidoglycan layer within the periplasmic space between the two membranes. Proteins which belong in the outer membrane or periplasm must cross the inner membrane. All periplasmic and outer membrane proteins are synthesised as precursors with an N-terminal extension of 15-25 residues termed the signal sequence. The initiating Met residue is followed by a short stretch of charged residues. Next is a stretch of very hydrophobic residues followed in turn by a small uncharged amino acid such as Gly, Ala or Ser which serves as a cleavage site for a specific signal peptidase [90]. There is probably a protein transloctation complex involved in the export of periplasmic and outer

membrane proteins [92], as these proteins require a signal sequence for localization [93].

Most proteins of the inner membrane of *E. coli* are synthesised without a signal sequence. It is suggested that the hydrophobic domains of these proteins form hairpin loops which spontaneously partition into the membrane during synthesis [91]. This assembly may be independent of receptors or transport machinery and may be driven entirely by the enthalpy of membrane insertion.

J. METABOLISM OF *E. COLI*

AEROBIC METABOLISM OF GLUCOSE

E. coli uses glycolysis, the tricarboxylic acid cycle and the aerobic electron transport chains to derive energy from glucose aerobically [94,95]. Glucose is taken up and phosphorylated by the phospho*enol*pyruvate-dependent phosphotransferase system. Glucose-6-phosphate is isomerised to fructose-6-phosphate by phosphoglucose isomerase. Phosphofructokinase then phosphorylates it to fructose-1,6-diphosphate, using ATP as donor. Fructose-1,6-diphosphate is then split into dihydroxyacetone phosphate and glyceraldehyde-3-phosphate by aldolase. A triose isomerase then converts the dihydroxyacetone phosphate to another molecule of glyceraldehyde-3-phosphate.

Glyceraldehyde-3-phosphate is oxidized to phosphoglycerate by glyceraldehyde dehydrogenase with the production of an NADH. The carboxylic acid group is phosphorylated by inorganic phosphate during the oxidation. This phosphate is then donated to ADP by phosphoglycerate kinase to yield 3-phosphoglycerate and ATP. The 3-phosphoglycerate is

isomerized to 2-phosphoglycerate by phosphoglycerate mutase. Enolase then dehydrates 2-phosphoglycerate to phospho*enol*pyruvate, which is then dephosphorylated to pyruvate by pyruvate kinase with the production of another ATP. The pyruvate is then split oxidatively to yield acetyl-CoA, CO_2 and NADH by the pyruvate dehydrogenase complex.

THE TRICARBOXYLIC ACID CYCLE

The first reaction of the tricarboxylic acid cycle is the condensation of the acetyl group with oxaloacetate to yield citrate by the enzyme citrate synthase. Citrate is converted to 2-oxoglutarate by aconitase and isocitrate dehydrogenase with the production of NADH. The 2-oxoglutarate is converted to succinyl-CoA and CO_2 by 2-oxoglutarate dehydrogenase with the production of another NADH. Succinyl-CoA synthetase then generates free CoA and succinate with the generation of an ATP. Succinate is oxidized to fumarate by succinate dehydrogenase with the donation of the reducing equivalents to the electron transport chain. The fumarate is recycled to oxaloacetate by fumarase and malate dehydrogenase with the production of an NADH.

As mentioned above the primary coupling of the TCA cycle to electron transport occurs *via* succinate dehydrogenase, but the NADH generated in the cycle and in glycolysis can also feed into the electron transport chain *via* NADH dehydrogenase, discussed in Section G.

Glycerol can be fed into glycolysis and the TCA cycle at the level of triose isomerase. Glycerol is first phosphorylated at the expense of an ATP by glycerol kinase and then oxidized to dihydroxyacetone phosphate by the aerobic glycerol-3-phosphate dehydrogenase.

ANAEROBIC METABOLISM OF GLYCEROL AND FUMARATE

Figure I.5 shows the pathways of metabolism of *E. coli* grown anaerobically on glycerol and fumarate. Glycerol is taken up and phosphorylated at the expense of an ATP and then oxidized to dihydroxyacetone phosphate by the anaerobic glycerol-3-phosphate dehydrogenase [Fig. I.5]. The reducing equivalents are fed to the electron transport chain. The dihydroxyacetone phosphate is converted to pyruvate with the production of an NADH and two ATP, as in the terminal portion of the glycolytic pathway. The pyruvate is then oxidized to acetate in a three step process generating one ATP [96]. First, pyruvate is converted to acetyl-CoA and formate by an anaerobic pyruvate formate-lyase. This requires electrons donated by flavodoxin. The formate is then drawn off by conversion to CO_2 and H_2 by formate hydrogen-lyase. The acetyl group is then transferred from CoA to inorganic phosphate by phosphotransacetylase. Finally, the phosphate group is donated to ADP by acetate kinase and the acetate is excreted.

Fumarate is used to oxidize the electron transport chain, giving rise to an energized membrane, as well as being converted in two steps to oxaloacetate for biosynthetic purposes with the concommitant production of an NADH. The succinate formed by the reduction of fumarate is used for biosynthesis and the excess is excreted.

K. GENETIC REGULATION IN *E. COLI*

DIVERSITY OF REGULATORY MECHANISMS

The expression of many operons in *E. coli* is regulated at the transcriptional level by a number of mechansisms. There are positive and

negative effectors, alternate components of the RNA polymerase, small molecule cofactors and translationally-coupled mechanisms used in a wide variety of forms and combinations.

The primary level of control involves the recognition of the promoter for an operon by the RNA polymerase. This is mediated by a specific DNA sequence upstream [5'] of the start of transcription. The promoter is divided into two regions of six basepairs [bp] separated by 17 bp [97]. The first region in centred 10 bp upstream of the start of transcription [-10 region] and the second is centred 35 bp 5' to the start of transcription [-35 region]. The conserved sequences are TTGaca for the -35 region and TAtaaT for the -10 region [98], where capitals indicate strong conservation and small letters indicate weak conservation of residues. The 17 bp separation of the regions must be preserved within ±1 residue. The strength of the promoter is inversely related to its departure from the consensus sequence [99].

Until recently it was assumed that the well characterised RNA polymerase of *E. coli* had only one protein cofactor needed for recognition of the promoter; σ^{70}. This is indeed the form used to recognise the consensus promoter discussed above. However, alternate σ-factors have been discovered which function in the global regulation of nitrogen metabolism and heat shock response [97] termed σ^{60} and σ^{32}, respectively. The promoters using the alternate σ-factors also have altered consensus sequences.

Auxilliary proteins can affect the binding of RNAPolσ^{70} to specific consensus promoters. An example is the cAMP receptor protein [CRP] which has the effect of enhancing initiation of some operons, inhibiting the initiation of others and decreasing the termination of transcription in still

other operons [100]. CRP exists as a homodimer and binds both DNA and cAMP, its effector molecule. The binding of cAMP increases the affinity of complex for specific DNA sequences [the CAT box]. The CAT sequence can occur up to 92 bp 5' to the start of transcription. CRP may stimulate transcription by hiding a high-affinity but non-productive promoter. It may inhibit transcription by binding to a productive promoter. In both cases the CRP excludes the binding of the RNApolσ^{70} to the promoter in question.

LexA is a repressor protein involved in the regulation of several operons for DNA repair [97]. It binds to an AT-rich sequence which overlaps the various σ70 promoters, either upstream, centrally or downstream. It may function by preventing the binding of RNApolσ^{70} to the promoter or by preventing bound polymerase from moving downstream.

LacI is the repressor of the *lac* operon. In the absence of its inducer LacI binds to the operator region of the operon and blocks the access of RNApolσ^{70} to the promoter. Binding an inducer such as isopropyl-β-D-thiogalactoside releases LacI from the operator, allowing access to the promoter by the initiation complex. CRP and cAMP are required for full activation of *lac* transcription [101].

ATTENUATION

The regulation of several operons is affected early in transcription, rather than at the time of initiation. This involves the formation of a specific mRNA conformation which signals the termination of transcription and the release of the truncated messenger. This is termed attenuation [102]. This mechanism was first described in the biosynthetic operon for

tryptophan, *trp*, and then for other amino acid biosynthetic operons, *his*, *leu*, *thr*, *ilv* and *phe*, and has been detected in other operons not involved in amino acid metabolism as well.

The basic model of attenuation in the amino acid biosynthetic operons is as follows [103,104]. The first region of the mRNA encodes a very short polypeptide followed by a stop codon. The first cistron of the operon begins a little way downstream. The mRNA region encoding this leader sequence has four regions of inverse repeat symmetry which can fold into three mutually exclusive hairpin-like structures. The most proximal pairing, of regions 1 and 2 forms a loop which causes the RNA polymerase to pause momentarily. A ribosome binds and begins to translate the leader sequence. When the ribosome approaches the polymerase it is released to continue transcription through regions 3 and 4. Within region 1 are one or more of the codons for the amino acid whose operon is being regulated. If amino acid levels are low and tRNAs are not fully charged, the ribosome will stall, waiting for a charged tRNA. This blocks the formation of the region 1:2 loop, but allows formation of the 2:3 loop. This structure does not impede the polymerase and the operon is transcribed.

If, on the other hand, amino acid levels are high and the tRNAs are fully charged, the ribosome will read through region 2, thus preventing the formation of the 2:3 loop. This allows a weaker pairing to form the 3:4 loop which functions as a simple transcription terminator, ending the mRNA transcript upstream of the first cistron of the operon. This sensitiviy to the relative abundance of the charged tRNAs allows a close match of amino acid biosynthesis to amino acid requirements.

SIMPLE TERMINATION

In simple termination the 3' end of the mRNA occurs at a single site whose location is specified by the sequence and secondary structure immediately upstream. This region contains a GC-rich inversely repeated sequence which is capable of forming a stable hairpin loop. Immediately downstream of the loop is a short stretch of uridine residues within which the transcript ends [103]. This type of termination has been well characterized in 30 operons and by sequence comparison only in another 20. The loop is thought to cause the polymerase to pause long enough for the reduced binding energy of the polyU:dA sequence to allow release of the transcript from the transcription bubble. Simple termination occurs at the end of most operons.

A number of accessory proteins can modulate the efficiency of the simple terminator. Tau is required for efficient termination at the simple terminators of bacteriophage T3 and T7 in *E. coli*. In the absence of this host cell protein termination occurs less than 60% of the time [105]. NusA can also increase the efficiency of termination at the λ t_{R2} terminator and the T_1 terminator of the *E. coli rrnB* operon [106]. N protein operates to cause antitermination at the λt_{L2} terminator in a fashion which is dependent on both NusA and NusB [103]. A 6S RNA is produced by phage λ from the $p_{R'}$ promoter and terminated at the t_{6S} terminator. Q protein functions to reduce the efficiency of termination, and this effect is enhanced by NusA.

RHO-DEPENDENT TERMINATION

Nonsense polarity is the term used to describe the effect that a nonsense mutation in one cistron has of decreasing the transcription of

other cistrons downstream of it. This type of termination is mediated by Rho [10..07]. Rho termination is imprecise, in that it does not occur at a specific site, but at a cluster of residues within a large region. The necessary conditions for Rho termination are a stretch of mRNA at least 100 nucleotides long that is free of ribosomes and strong secondary structure, followed by a secondary structure or pause sequence that halts the polymerase momentarily. Rho then acts to release the mRNA from the paused transcription complex. The mechanism of Rho action most likely involves the disruption of the transcription bubble within the elongation complex. This could explain the requirement for ATP hydrolysis in Rho termination [108].

In low salt buffers or in the presence of RNA Rho exists as a hexamer and it is believed that this is the form in which it binds to the messenger RNA[103]. The hexamer bound to mRNA, but not alone, possesses the ATPase activity. The interaction with the mRNA requires cytosine residues within the binding region. Replacement with 5-bromocytosine abolishes Rho binding [109]. Using a fluorescent nucleotide, 1,N^6-ethenoadenosine, it has been shown that the minimal Rho binding site is 78±6 nucleotides, or 13±1 nucleotides per monomer [110]. A spacing of cytosine residues of 12±1 nucleotides within Rho binding regions has been reported [111]. There is evidence that NusA can decrease the efficiency of Rho termination in the intercistronic region of the *rplL-rpoB* operons of *E. coli* [112]. Conformational changes resulting in altered trypsin sensitivity occur when mRNA-bound Rho binds ATP [103].

REGULATION OF *FRD*.

At least four regulators have been identified in the anaerobic induction of fumarate reductase; Fnr [3,97,113,114], a pleiotropic affector of all the terminal reductases, NarL [115], which activates expression of nitrate reductase and suppresses production of fumarate reductase, fumarate [3] and cyclic AMP [113,116], both of which can stimulate the expression of fumarate reductase under anaerobic conditions.

In cells grown on glucose media anaerobically, the addition of 20mM fumarate stimulated the induction of the fumarate reductase operon 12-16 fold over the basal level, as reported by *frd-lacZ* fusion strains [117]. In cells harbouring a *frd-galK* fusion on a plasmid, the increase in galactokinase activity by anaerobiosis alone was 15 fold, while the addition of fumarate to the medium increased the level of induction another 1.8 fold over that seen in the presence of oxygen [84]. When *frd* is present on a high-copy-number plasmid it can be expressed to moderate levels aerobically [118], while the other anaerobic genes remain repressed. This has led to the suggestion that a fumarate-sensitive repressor protein affects transcription from the *frd* promoter, and that this protein is titrated out by the high number of *frd* promoters in the strains bearing plasmids [3].

The anaerobic expression of the *frd* operon in glycerol-fumarate medium is dependent on the presence of cyclic AMP [116]. Mutants in *cya*, the adenylate cyclase gene, suppress fumarate reductase activity 13.5 fold. Addition of 5 mM cAMP to the medium restores expression. This effect is not mediated by the global effector of catabolite repression, the cAMP receptor protein, as *crp* mutants express fumarate reductase with or without exogenous cAMP. The Fnr protein has structural similarities to CRP, especially in a domain thought to bind to DNA and in a domain

reminiscent of the cAMP-binding pocket [119]. The residues directly involved in binding cAMP are not conserved in Fnr, however. Purified Fnr does not bind cAMP [113,120]. It should be noted that purified Fnr migrates as a smaller protein on SDS-PAGE than does the cellular form identified in maxicells [113,123].

Fumarate reductase is not expressed anaerobically if nitrate is present in the medium [3,84]. NarL is a protein required for the induction of nitrate reductase by nitrate anaerobically [121]. *NarL* maps at 27 min of the *E. coli* chromosome. It has been demonstrated that a *narL* mutation prevents the stimulation of expression of nitrate reductase [*narC*] and the supression of fumarate reductase activity in the presence of nitrate anaerobically [115]. NarL also suppresses the expression of *tor*, the gene for trimethylamine-*N*-oxide reductase, and the gene for alcohol dehydrogenase. It seems apparent that NarL mediates the choice between low potential electron acceptors like fumarate and TMAO and the high potential electron acceptor, nitrate. *NarL* has also been called *frdR* for its role in regulating fumarate reductase [122]. It has been reported that the NarL effect on *frd* and *narC* is synergistically affected by molybdate as well as nitrate [122A].

Fnr was the designation used for mutations which prevented anaerobic growth on both fumarate and nitrate [114]. *Fnr* maps at 29.3 min of the *E. coli* chromosome and the gene has been cloned and sequenced [124]. It has also been implicated genetically in the regulation of the *hyd, fdh* and *tor* operons of anaerobic electron transport proteins [97]. Fnr has a molecular weight of 28 kDa and as mentioned above it has sequence similarities with DNA binding regulatory proteins [124,119]. Fnr is constitutively expressed aerobically but there is some controversy as to its expression

anaerobically. Two groups have reported no change in Fnr levels under anaerobic conditions by immunoblotting [113] or by *fnr-lacZ* fusions [120]. Spiro and Guest [125] using a defined *fnr-lacZ* fusion containing 117 bp of *fnr* sequence and 91 bp of upstream sequence showed a 2.7 fold decrease in β-galactosidase activity under anaerobic conditions. This downregulation was increased if wild-type *fnr* was also present, implying an autoregulation of Fnr levels. This was also seen by Pascal *et al* [120].

In a wild-type strain anaerobiosis induces a nine fold increase in *frd* expression which is enhanced to 15 fold in the presence of fumarate [126]. In an *fnr* background the anaerobic induction of the *frd* operon is reduced 6 fold compared to wild-type and the enhancement of expression by addition of fumarate is abolished. Repression of *frd* expression by nitrate is as efficient in the *fnr* strain as in the wild-type strain.

Two classes of *frd* mutants with altered responses to anaerobiosis have been isolated [127]. They were isolated by conferring the ability to grow aerobically on an Sdh⁻ strain, as it has been shown that fumarate reductase can take over the function of succinate dehydrogenase under appropriate conditions [128]. The first class, designated Oxr for oxygen resistance, expresses 18 fold more fumarate reductase aerobically than do wild-type strains. The level of enzyme activity is equivalent to that obtained anaerobically in the wild-type strain grown without fumarate. Expression in the Oxr mutant increased 3-6 fold when grown anaerobically without fumarate. Addition of fumarate to the medium resulted in a 4 fold enhancement of activity in both wild-type and Oxr strains. Addition of nitrate to the medium suppressed activity to the same extent in wild-type and Oxr strains. The Oxr mutation behaves as an upregulation of basal expression with oxygen, fumarate and nitrate sensitivities intact.

The second class of mutants were termed Con, for constitutive. These strains grown aerobically expressed fumarate reductase to twice the level found in Oxr strains, or 50% of that seen in wild-type anaerobic cells. When grown anaerobically, expression increased to the maximum level found in wild-type cells; about a two fold increase. The addition of fumarate to the medium aerobically or anaerobically did not change the level of expression. Nitrate was as effective at supressing expression as it was in wild-type cells. The Con mutation behaves as an upregulation of expression with no senstivity to fumarate and reduced sensitivity to oxygen. Both Con and Oxr mutants have lost sensitivity to *fnr*.

L. THESIS PROBLEM

In attempting to understand the structure, organization and function of electron trnasport chains in general, we have focused our efforts on a relatively simple system as a model. The anaerobic electron transport chain from glycerol-3-phosphate dehydrogenase to fumarate reductase is composed of only three known components; the primary dehydrogenase, menaquinone and the terminal reductase. The purification and partial characterization of both the dehydrogenase and the reductase had been accomplished, yet our understanding of the ways these proteins are expressed and assembled in the inner membrane of *E. coli* remained inadequate. Our ultimate goal of reconstituting an entire electron transport chain seemed unobtainable in the near future.

A combination of biochemical and molecular biological techniques were applied to the study of fumarate reductase. The gene for fumarate reductase, *frd*, had just been cloned and sequenced when I joined the lab, largely as the result of the work of Drs. S. Cole and B. Jaurin. The

sequence revealed four open reading frames which coded for proteins of 69 kDa, 27 kDa, 15 kDa and 13 kDa; FrdA, B, C and D, respectively.

An enzyme composed of the two larger proteins had been purified as a water soluble entity and characterized by Peter Dickie and John Robinson. The dimer was shown to be an active reductase using reduced dyes as artificial electron donors. It required high anion concentrations for both thermal and alkaline stability and for maximal activity. Bernie Lemire and John Robinson showed that the two smaller polypeptides were part of the holoenzyme, which were lost during the hydrophobic exchange chromatography which was part of the original purification protocol. They isolated the tetrameric form of the enzyme and showed that the 15 kDa and 13 kDa subunits served to anchor the enzyme to the inner membrane and served to confer stability and anion insensitivity on the catalytic domain. It was not apparent why two dissimilar subunits were required, however.

In Chapter II I used transposon insertions to prepare mutants of the *frd* operon carried on the multicopy plasmid, pBR322 and isolated plasmids with polar mutations in *frdA*, *frdB* and *frdD*. With these mutants I showed that the minimal catalytic unit was the FrdAB dimer, that FrdA could be covalently modified by flavin adenine dinucleotide in the absence of the other subunits and that the two anchor subunits were necessary for coupling to the electron transport chain. I was able to distinguish properities of the individual small subunits; FrdC for anion insensitivity and alkaline stability and FrdD for proper assembly, thermal stability and quinol oxidase activity. I was further able to implicate the C-terminal portion of FrdD as being required for proper assembly and thermal stability.

Bernie Lemire constructed a plasmid bearing only the *frdA* and *frdB* genes and showed that this produced and assembled the catalytic dimer in the absence of the two anchor polypeptides. He also showed that the catalytic heads could be stripped away from the anchors in the inner membrane, and that the anchors remained competent to bind fresh catalytic dimer produced by the *frdAB* plasmid. We wished to know whether the normal pathway of assembly involved the coordinate assembly of all four subunits in the membrane, or if it was as Bernie had suggested, that the FrdAB dimer was assembled in the cytoplasm and then attached to the preassembled anchor domain in the membrane.

In Chapter III I used a phage T7-based *in vivo* transcription/ translation system developed by Dr. S. Tabor and monospecific antibodies directed against FrdA and FrdB to examine the synthesis and assembly of fumarate reductase holoenzyme and the modified enzyme produced from the operon bearing the transposon insertion in *frdD*. The T7 system allowed me to examine early events in the assembly of fumarate reductase. The monospecific antibodies allowed me to show which of the other subunits were stably associated with either FrdA or FrdB in a coprecipitable manner. This study indicated that the membrane anchor domain was rapidly assembled into the membrane and that the two large subunits were added individually, rather than as a preformed dimer. The truncated FrdD' in one of the plasmid-borne operons showed that assembly to the membrane was impaired, and that a soluble trimer was produced as the result of proteolysis of FrdD' from assembled, but not inserted, tetramer.

In the course of the study on assembly I noted that the ratio of subunits synthesised varied with changes in the temperature at which the experiment

was run. This gave rise to the suspicion that mRNA secondary structure might be important in the expression of the *frd* operon. Computer-assisted examination of the DNA sequence revealed a pattern of potential hairpin loop-forming regions in a stretch which encoded the alanine-rich N-terminus of FrdA which was reminiscent of the attenuator regions of the amino acid biosynthetic operons. The pattern suggested that alanine levels might affect *frd* expression. In Chapter IV I used a commercial *in vitro* translation system based on an S-30 extract to show that alanine did indeed affect transcription of the *frd* operon in a manner consistent with the attenuation model.

The Fnr protein is a pleiotropic effector of anaerobic expression from a number of operons, including *frd.* Using a plasmid carrying the *fnr* operon, supplied to us by Dr. R. P. Gunsalus, I showed that Fnr served to induce termination of transcription in a manner similar to that of Rho, and computer analysis of the fumarate reductase operon indicated several regions which resembled Rho-binding sites.

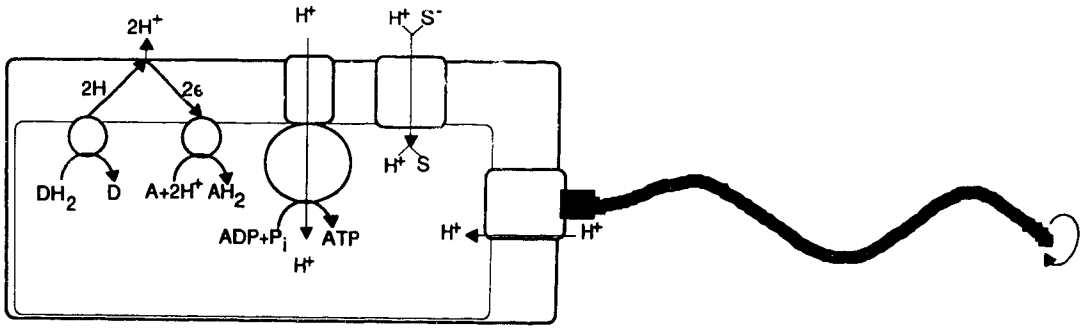

Figure I.1. A general view of the chemiosmotic systems in *E. coli*.

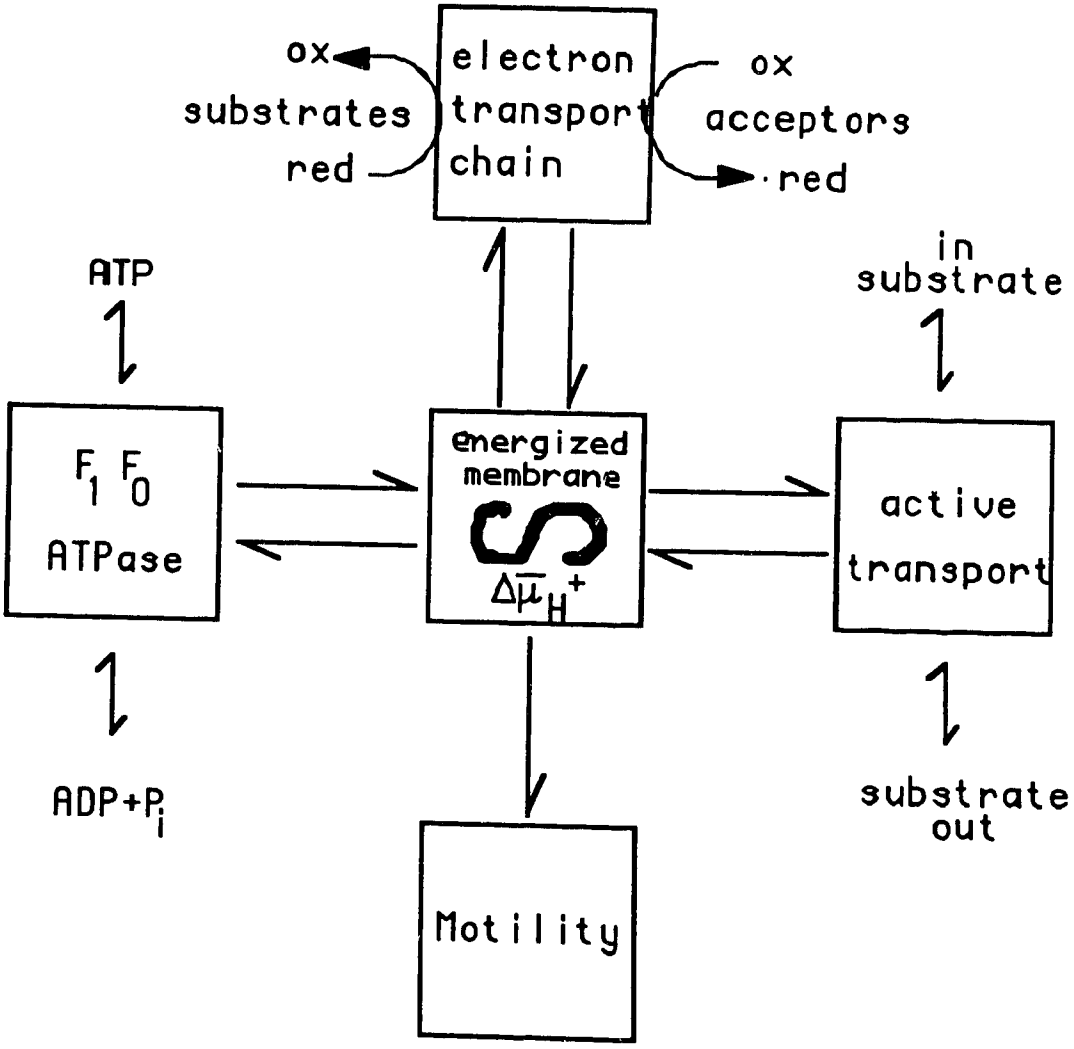

Figure I.2. General scheme of energy transduction in *E. coli*.

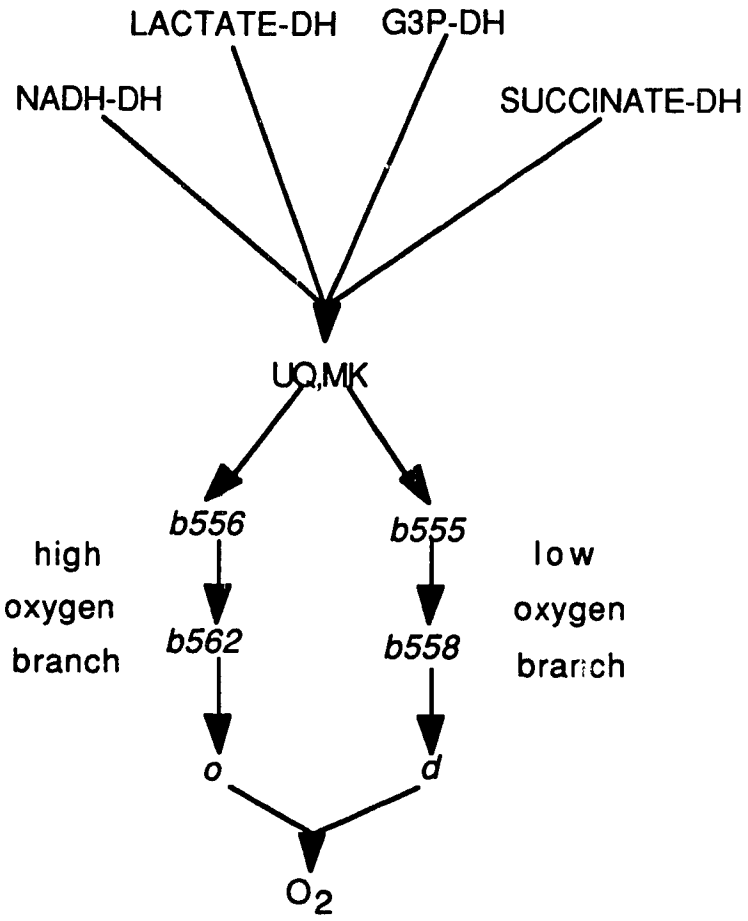

Figure I.3. Pathways of electron transport through the aerobic respiratory chains of *E. coli*.

PAGE 39 REMOVED DUE TO COPYRIGHT RESTRICTIONS

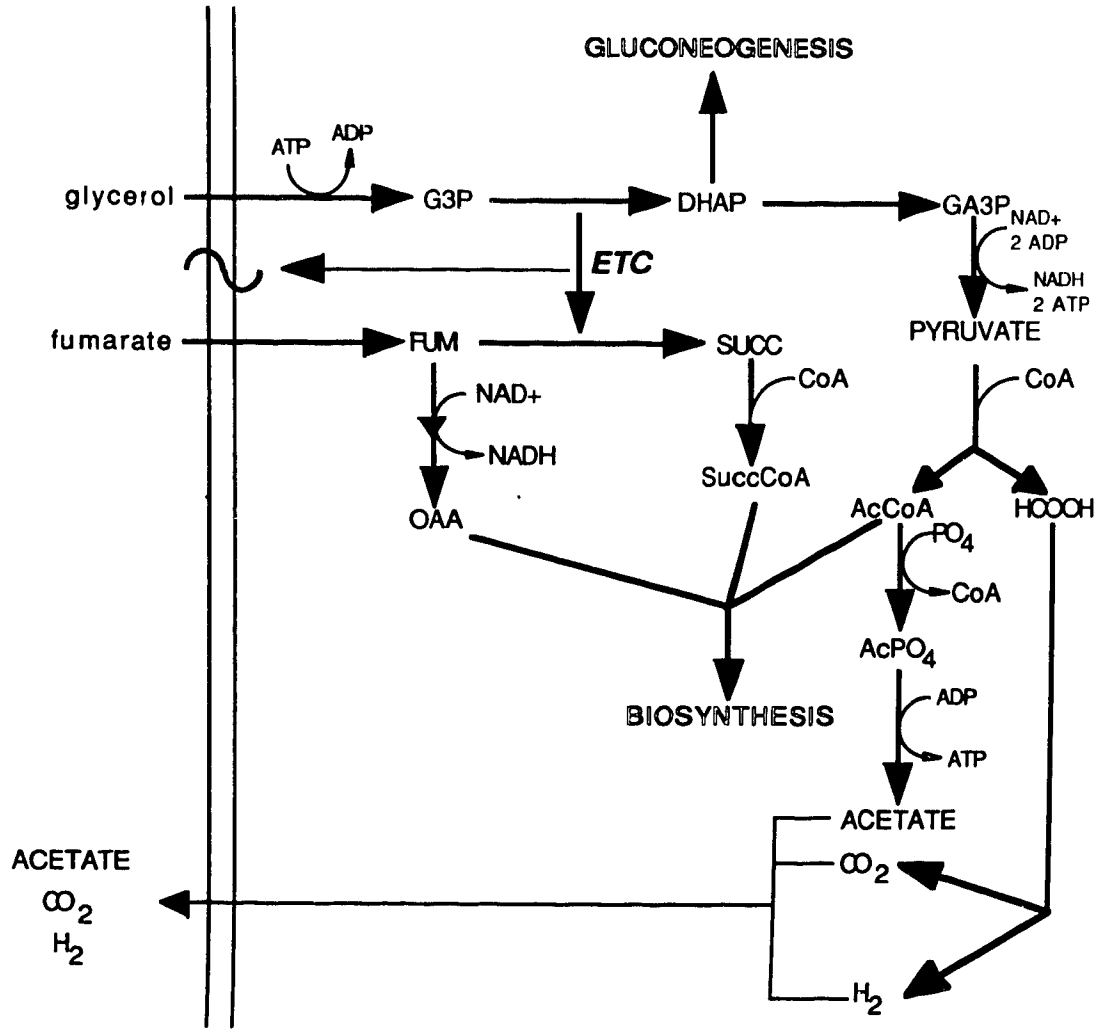

Figure I.5. Pathways of anaerobic metabolism in *E. coli*.

Bibliography

1. Ingledew, W. J. & Poole, R. K. 1984. Microbiol. Rev. **48**:222-271
2. Bilous, P. T. & Weiner, J. H. 1985. J. Bacteriol. **162**:1151-1155
3. Cole, S. T., Condon, C., Lemire, B. D. & Weiner, J. H. 1985. Biochim. Biophys. Acta **811**:381-403
4. Bragg. P. D. 1980. p. 115-136. *In* Diversity of Bacterial Respiratory Systems, Vol. I. C. J. Knowles [ed.]. CRC Press, Boca Raton.
5. Kröger, A. 1980. p.1-17. *In* Diversity of Bacterial Respiratory Systems, Vol. II. C. J. Knowles [ed.]. CRC Press, Boca Raton
6. Holmes, W. H., Hamilton, I. D. & Robertson, A. G. 1972. Arch. Microbiol. **83**:95-101
7. Mitchell, P. 1961. Nature **191**:144-148
8. Mitchell, P. 1979. Science **206**:1148-1159
9. Haddock, B. A. & Jones, C. W. 1977. Bacteriol. Rev. **41**:47-99
10. Lin, E. C. C. 1976. Ann. Rev. Microbiol. **30**:535-578
11. Newton, N. A., Cox, G. B. & Gibson, F. 1972. Biochim. Biophys. Acta **244**:155-165
12. Singh, A. P. & Bragg, P. D. 1976. Biochim. Biophys. Acta **423**:450-461
13. Rosenberg, H., Cox. G. B.. Butlin, J. D. & Gutowski, S. J. 1975. Biochem. J. **146**:417-423
14. Boonstra, J., Huttunen, M. T. & Konings, W. N. 1975. J. Biol. Chem. **250**:6792-6798
15. Miki, K. & Lin, E. C. C. 1975. J. Bacteriol. **124**:1282-1287
16. Haddock, B. A. & Kendall-Tobias, M. W. 1975. Biochem. J. **152**:655-659

17. Brice, J. M., Law, J. W., Meyer, D. J. & Jones, C. W. 1974. Biochem. Soc. Trans. **2**:523-526

18. Miki, K. & Lin, E. C. C. 1972. Fed. Proc. Amer. Soc. Exp. Biol.**32**:632

19. Hinkle, P. C. and McCarty, R. E. 1978. Sci. Amer. **238**:104-123

20. Futai, M. & Kanazawa, H. 1983. Microbiol. Rev. **47**:285-312

21. Downie, J. A., Gibson, F. & Cox, G. B. 1979. Ann. Rev. Biochem. **48**:103-131

22. Racker, E. 1976. *In* A New Look at Mechanisms in Bioenergetics. Academic Press Inc., New York

23. Nelson, N., Kanner, B. I. & Gutnick, D. L. 1974. Proc. Natl. Acad. Sci. USA. **71**:2720-2724

24. Smith, J. B. & Sternweis, P. C. 1982. Arch. Biochem. Biophys. **217**:376-387

25. von Meyenburg, K., Nielson, J., Jorgensen, B. B. Michaelsen, O. & Hansen, F. 1983. Tokai J. Exp. Clin. Med. Sp. Symp. **7**:23-31

26. Foster, D. L. & Fillingame, R. H. 1982. J. Biol. Chem. **257**:2009-2015

27. Fillingame, R. H., Mosher, M. E., Negrin, L. S. & Peters, L. K. 1983. J. Biol. Chem. **258**:604-609

28. Foster, D. L. & Fillingame, R. H. 1979. J. Biol. Chem. **254**:8230-8236

29. Solioz, M. 1984. Trends in Biochem. Sci. **9**:309-312

30. Rosen, B. P. 1973. Biochem. Biophys. Res. Comm. **53**:1289-1296

31. Hoppe, J., Schairer, H. U., Friedl, P. & Sebald, W. 1982. FEBS Lett. **145**:21-24

32. Klionsky, D. J., Brusilow, W. S. A. & Simoni, R. D. 1983. J. Biol. Chem. **258**:10136-10143

33. Fillingame, R. H. , Mosher, M. E., Negrin, L. S. & Peters, L. K. 1983. J. Biol. Chem. **258**:604-609

34. Hasan, S. M., Tsuchiya, T. & Rosen, B. P. 1978. J. Bacteriol. **133**:108-113

35. Downie, J. A., Cox, G. B., Langman, G. A., Becker, M. & Gibson, F. 1981. J. Bacteriol. **145**:200-210

36. Sone, N., Yoshida, M., Hirata, H. & Kagawa, Y. 1977. J. Biol. Chem. **252**:2956-2960

37. Jones, C. W. 1982. *In* Aspects of Microbiology, Vol. 5., J. A. Coles & C. J. Knowles [eds.] Nelson Canada Ltd., Don Mills

38. Bragg, P. D. 1979. p.341-449. *In* Membrane Proteins in Energy Transduction. R. A. Capaldi. [ed.] Marcel Dekker AG , Basel

39. Maloney, P. C. 1987. p.222-243. *In Escherichia coli* and *Salmonella typhimurium* Cellular and Molecular Biology. F. C. Neidhardt. [ed. in chief.] ASM, Washington

40. Scott, R. I. & Poole, R. K. 1982. J. Gen. Microbiol. **128**:1685-1696

41. Poole, R. K. & Ingledew, W. J. p. 170-200. *In Escherichia coli* and *Salmonella typhimurium* Cellular and Molecular Biology. F. C. Neidhardt. [ed. in chief.] ASM, Washington

42. Kita, K. Konishi, K. & Anraku, Y. 1984. J. Biol. Chem. **259**:3368-3374

43. Kita, K., Kasahara, M. & Anraku, Y. 1982. J. Biol. Chem. **257**:7933-7935

44. Matsushita, K. , Patel, L., Gennis, R. B. & Kaback, H. R. 1983. Proc. Natl. Acad. Sci. USA. **80**:4889-4893

45. Haddock, B. A., Downie, J. A. & Garland, P. B. 1976. Biochem. J. **154**:285-294

46. Findlayson, S. D. & Ingledew, W. J. 1985. Biochem Soc. Trans. **13**:632-633

47. Kita, K., Konishi, K. & Anraku, Y. 1984. J. Biol. Chem. **259**:3375-3381

48. Lawford, H. G. & Haddock, B. A. 1973. Biochem. J. **136**:217-220

49. Lin, E. C. C. & Kuritzkes, D. R. 1987. p. 201-221 *In Escherichia coli* and *Salmonella typhimurium* Cellular and Molecular Biology. F. C. Neidhardt. [ed. in chief.] ASM, Washington

50. Kistler, W. S.& Lin, E. C. C. 1972. J. Bacteriol. **108**:1224-1234

51. Weiner, J. H. & Heppel, L. A. 1972. Biochem. Biophys. Res. Comm. **47**:1360-1365

52. Weiner, J. H. 1974. J. Memb. Biol. **15**:1-14

53. Schryvers, A. , Lohmeier, E. & Weiner, J. H. 1978. J. Biol. Chem. **253**:783-788

54. Ruiz-Herrera, J. & Garcia, L. G. 1972. J. Gen. Microbiol. **7**:29-35

55. Ingledew, W.J. & Poole, R. K. 1984. Microbiol. Rev. **48**:222-271

56. Ohnishi, T. & Salerno, J. C. 1982. p.285-327. *In* Iron Sulfur Proteins. Metals in Biology. T. G. Spiro [ed.] Vol. IV, John Wiley & Sons, New York

57. Condon, C., Cammack, R., Patil, D. S. & Owen, P. 1985. J. Biol. Chem. **260**:9427-9434

58. Cole, S. T. 1982. Eur. J. Biochem. **122**:479-484

59. Darlison, M. G. & Guest, J. R. 1984. Biochem. J. **223**:507-517

60. Murakami, H., Kita, K., Oya, H. & Anraku, Y. 1985. Mol. Gen. Genet. **196**:1-5

61. Murakami, H., Kita, K. Oya, H. & Anralu, Y. 1985. FEMS Microbiol. Lett. **30**:307-311

62. Futai, M. & Kimura, H. 1977. J. Biol. Chem. **252**:5820-5827

62A. Zinoni, F. Birkman, A., Stadtman, T. C. & Böck, A. 1986. Proc. Natl. Acad. Sci. USA. **83**:4650-4654

63. Ehrman, M. Boos, W., Ormseth, E., Schweizer, H. & Larson, T. J. 1987. J. Bacteriol. **169**:526-532

64. Kistler, W. S. & Lin, E. C. C. 1972. J. Bacteriol. **112**:539-547

65. Schryvers. A. & Weiner, J. H. 1981. J. Biol. Chem. **256**:9959-9966

67. Pascal, M-C., Burini, J-F. & Chippaux, M. 1984. Mol. Gen. Genet. **195**:351-355

66. Shimokawa, O. & Ishimoto, M. 1979. J. Biochem. **86**:1709-1717

68. Bilous, P. T. & Weiner, J. H. 1985. J. Bacteriol. **162**:1151-1155

69. Weiner, J. H., MacIsaac, D. P., Bishop, R. E. & Bilous, P. T. 1988. J. Bacteriol. **170**:1505-1510

70. Weiner, J. H. & Dickie, P. 1979. J. Biol. Chem. **254**:8590-8593

71. Morningstar, J. E., Johnson, M. K., Cecchini, G., Ackrell, B. A. C. & Kearney, E. B. 1985. J. Biol. Chem. **260**:13631-13638

72. Johnson, M. K., Morningstar, J. E., Cecchini, G. & Ackrell, B. A. C. 1985. Biochem. Biophys. Res. Comm. **131**:653-658

73. Cammack, R., Patil, D. S. & Weiner, J. H. 1986. Biochim. Biophys. Acta. **870**:545-551

74. Weiner, J. H., Cammack, R., Cole, S. T., Condon, C., Honoré, N., Lemire, B. D. & Shaw, G. 1986. Proc. Natl. Acad. Sci. USA. **83**:2056-2060

75. Cecchini, G., Ackrell, B. A. C., Gunsalus. R. P. & Kearney, E. B. 1984. ICSU Reports **38**:575-576

76. Latour, D. J. & Weiner, J. H. 1987. J. Gen. Microbiol. **133**:597-607

77. Dickie, P. & Weiner, J. H. 1979. Can. J. Biochem. **57**:813-821

78. Robinson, J. J. & Weiner, J. H. 1982. Can. J. Biochem. **60**:811-816

79. Lemire, B. D., Robinson, J. J. & Weiner, J. H. 1982. J Bacteriol. **152**:1126-1131

80. Cecchini, G., Ackrell, B. A. C., Kearney, E. B. & Gunsalus, R. P. 1984. p.555-558. *In* Flavins and Flavoproteins. R. C. Bray, P. C. Engel & S. G. Mayhew [eds.] Walter deGruyter & Co., Berlin

81. Weiner, J. H., Lemire, B. D., Jones, R. W., Anderson, W. F.& Scraba. D. G. 1984. J. Cell. Biochem. **24**:207-216

82. Cole, S. T., Grundström, T., Jaurin, B., Robinson, J. J. & Weiner, J. H. 1982. Eur. J. Biochem. **126**:221-216

83. Grundström, T. & Jaurin, B. 1982. Proc. Natl. Acad. Sci. USA. **79**:1111-1115

84. Jones, H. M. & Gunsalus, R. P. 1985. J. Bacteriol. **164**:1100-1109

85. Kyte, J. & Doolittle, R. F. 1982. J. Mol. Biol. **157**:105-118

86. Lemire, B. D., Robinson, J. J., Bradley, R. D., Scraba, D. G. & Weiner, J. H. 1983. J. Bacteriol. **155**:391-397

87. Unwin, P. N. T. & Henderson, R. 1975. J. Mol. Biol. **94**:425-440

88. Engleman, D. M., Henderson, P., McLachlan, P. & Wallace, B. A. 1980. Proc. Natl. Acad. Sci. USA. **77**:2023-2027

89. Schindler, H. & Rosenbusch, J. P. 1978. Proc. Natl. Acad. Sci. USA. **78**:2302-2306

90. Wickner, W. 1979. Ann. Rev. Biochem. **48**:23-46

91. Engleman, D. M. & Steitz, T. A. 1981. Cell **23**:411-422

92. Pugsley, A. P. & Schwartz, M. 1985. FEMS Microbiol. Rev. **32**:3-38

93. Wickner, W. T. & Lodish, H. F. 1985. Science **230**:400-407

94. Fraenkel, D. G. 1987. p.142-150 *In Escherichia coli* and*Salmonella typhimurium* Cellular and Molecular Biology. F. C. Neidhardt. [ed. in chief.] ASM, Washington

95. Lehninger, A. L. 1975. Biochemistry. Second ed. Worth Publishers Inc, New York

96. Knappe, J. 1987. p.151-155. *In Escherichia coli* and*Salmonella typhimurium* Cellular and Molecular Biology. F. C. Neidhardt. [ed. in chief.] ASM, Washington

97. Hoopes, B. C. & McClure, W. R. 1987. p.1231-1240.*In Escherichia coli* and*Salmonella typhimurium* Cellular and Molecular Biology. F. C. Neidhardt. [ed. in chief.] ASM, Washington

98. Hawley, D. K. & McClure, W. R. 1983. Nucl. Acids Res. **11**:2237-2255

99. Mulligan, M. E., Hawley, D. K., Entriken, R. & McClure, W. R. 1984. Nucl. Acids Res. **12**:789-800

100. Adhya, S & Garges, S. 1982. Cell **29**:287-289

101. Beckwith, J. 1987. p.1444-1452.*In Escherichia coli* and*Salmonella typhimurium* Cellular and Molecular Biology. F. C. Neidhardt. [ed. in chief.] ASM, Washington

102. Landick, R. & Yanofsky, C. 1987. p.1276-1301.*In Escherichia coli* and*Salmonella typhimurium* Cellular and Molecular Biology. F. C. Neidhardt. [ed. in chief.] ASM, Washington

103. Yager, T. D. & von Hippel, P. H. 1987. p.1241-1275.*In Escherichia coli* and*Salmonella typhimurium* Cellular and Molecular Biology. F. C. Neidhardt. [ed. in chief.] ASM, Washington

104. Yanofsky, C. 1981. Nature **289**:751-758

105. Briat, J.-F. & Chamberlin, M. J. 1984. Proc. Natl. Acad. Sci. USA. **81**:7373-7377

106. Schmidt, M. C. & Chamberlin, M. J. 1987. J. Mol. Biol. **195**:809-818

107. Wek, R. C., Sameshima, J. H. & Hatfield, G. W. 1987. J. Biol. Chem. **262**:15256-15261

108. Richardson, J. P. & Conaway, R. 1980. Biochem. **19**:4293-4299

109. Adhya, S, Sarkar, P., Valenzuela, D. & Maitra, U. 1979. Proc. Natl. Acad. Sci. USA. **76**:1613-1617

110. McSwiggen, J. A., Bear, D. G. & von Hippel, P.H. 1988. J. Mol. Biol.**199**:609-622

111. Platt, T. 1986. Ann. Rev. Biochem. **55**:339-372

112. Ralling, G. & Linn, T. 1987. J. Bacterial. **169**:2277-2280

113. Unden, G. & Duchene, A. 1987. Arch. Microbiol. **147**:195-200

114. Lambden, R. R. & Guest, J. R. 1976. J. Gen. Microbiol. **97**:145-160

115. Iuchi, S. & Lin, E. C. C. 1987. Proc. Natl. Acad. Sci. USA. **84**:3901-3905

116. Unden, G. & Guest, J. R. 1984. FEBS Lett. **170**:321-325

117. Ruch, F. E., Kuritzkes, D. R. & Lin, E. C. C. 1979. Biochem. Biophys. Res. Comm. **91**:1365-1370

118. Cole, S. T. & Guest, J. R. 1980. Mol. Gen. Genet. **179**:377-385

119. Shaw, D. J., Rice, D. W. & Guest, J. R. 1983. J. Mol. Biol. **166**:241-247

120. Pascal, M.-C., Bonnefoy, V., Fons, M. & Chippaux, M. 1986. FEMS Microbiol. Lett. **36**:35-39

121. Stewart, V. 1982. J Bacteriol. **151**:1320-1325

122. Kalman, L. & Gunsalus, R. P. 1988. J. Bacteriol. **170**:623-629

122A. Iuchi, S. & Lin, E. C. C. 1987. J. Bacteriol. 169:3720-3725

123. Unden, G. & Guest, J. R. 1985. Eur. J. Biochem. **146**:193-199

124. Shaw, D. J. & Guest, J. R. 1982. Nucl. Acids Res. **10**:6119-6130

125. Spiro, S. & Guest, J. R. 1987. J. Gen. Microbiol. **133**:3279-3288

126. Jones, H. M. & Gunsalus, R. P. 1987. J. Bacteriol. **169**:3340-3349

127. Iuchi, S. Kuritzkes, D. R. & Lin, E. C. C. 1986. J Bacteriol. **168**:1415-1421

128. Guest, J. R. 1981. J. Gen. Microbiol. **122**:171-179

129. Kenney, W. C., Walker, W. H. & Singer, T. P. 1972. J. Biol. Chem. **247**:4510-4513

130. Wood, D., Darlison, M. G., Wilde, R. J. & Guest, J. R. 1984. Biochem J **222**:519-534

131. Hamm, H.-H. & Decker, K. 1978. Eur. j Biochem **92**:449-454

132. Cecchini, G., Kearney, E. B., Jones, H. & Gunsalus, R. P. 1985. Fed. Proc. **44**:1766

133. Condon, C. & Weiner, J. H. 1988. Molex. Microbiol. **2**:43-52

134. Elmes, M. L., Scraba, D. G. & Weiner, J. H. 1986. J. Gen. Microbiol. **132**:1429-1439

II. INVESTIGATION OF *ESCHERICHIA COLI* FUMARATE REDUCTASE SUBUNIT FUNCTION USING TRANSPOSON TN5[1]

A. INTRODUCTION

When the facultative anaerobe *Escherichia coli* is grown anaerobically on medium containing glycerol and fumarate, a simple electron transport chain consisting of the anaerobic glycerol-3-phosphate dehydrogenase, menaquinone, a *b*-type cytochrome and fumarate reductase is synthesized and assembled in the cytoplasmic membrane [1,2,3]. Fumarate reductase, the terminal electron transfer enzyme, is composed of four non-identical subunits of 69 kDa, 27 kDa, 15 kDa and 13 kDa [4], encoded by the *frdA,B,C* and *D* genes, respectively. The *frd* operon has been cloned into multicopy plasmids and sequenced [5,6,7]. Strains of *E. coli* harbouring such plasmids amplify fumarate reductase activity in their membranes 5-20 fold [4,8]

The holoenzyme has been purified and characterised [4]. The 69 kDa [Da] polypeptide [FrdA] contains a catalytically essential sulfhydryl group [9] and a covalently-bound 8α-[N3-histidyl]-flavin adenine dinucleotide cofactor [10]. The 27 kDa [FrdB] subunit contains three iron-sulphur centres [3,6,11,12]. Together these two subunits comprise a membrane-extrinsic catalytic domain which can be purified in water-soluble form [10].

The 15 kDa and 13 kDa subunits [FrdC and FrdD, respectively] are basic and extremely hydrophobic in amino acid composition [4]. They

[1]A version of this chapter has been published: Latour, D. J. & Weiner, J. H. 1987. J. Gen. Microbiol. **133**:597-607.

form the membrane-anchor domain of fumarate reductase [13]. The finding that anions or the anchor polypeptides could stabilize the catalytic dimer against denaturation by either alkali [pH≥8.6] or heat [temp. >45°C] has led us to the proposal that the FrdC and D polypeptides serve at least two functions; anchoring and stabilizing the catalytic dimer [9,13,14].

In *E. coli*, transposon Tn*5* confers resistance to the aminoglycoside antibiotics kanamycin and neomycin [15]. It transposes at high frequency [16] and with little or no insertional specificity [17,18,19]. Transposition of Tn*5* into a structural gene causes insertional inactivation, which is normally polar on cistrons located promoter-distal to the site of the insertion [18,20]. Tn*5* mutagenesis has been used to generate correlated physical and genetic maps of DNA segments cloned into multicopy plasmids [21,22,23,24,25].

In this chapter Tn*5* is used to introduce polar mutations into the plasmid-borne *frd* genes. The altered gene products are examined in terms of the known properties of fumarate reductase and the specific functions of individual polypeptides are discussed.

B. MATERIALS AND METHODS

Enzymes and chemicals

Restriction endonucleases *Eco*RI, *Ava*I, *Alu*I and *Sal*I were obtained from Boehringer-Mannheim [Montréal, Québec]. *Bam*HI and *Hin*dIII were from Pharmacia P-L Biochemicals [Dorval, Québec]. Rabbit anti-succinyl CoA synthetase IgG was a gift from W.A. Bridger [this department]. 2,3-dimethyl-1,4-naphthoquinone was a gift from A. Kröger [J.W. Goethe University]. All other chemicals were of the highest grade commercially available.

Strains and plasmids

These are described in Table II.1. pFRD79 is similar to pFRD63 [13] except that the 4.5 kilobasepair *Hin*dIII fragment carrying the *frd* operon is reversed in orientation relative to the *Eco*RI site of pBR322. Expression of the *frd* operon is not altered by this change [B. D. Lemire & J. H. Weiner, unpublished data].

Cell growth

Cells were grown anaerobically for 21 h on glycerol-fumarate medium supplemented with appropriate antibiotics, as previously described [26].

Tn5 mutagenesis and plasmid isolation

HB101[pFRD79] was grown overnight at 37°C on L-broth [27] supplemented with 20 μg ml^{-1} thiamine [LB-B_1], 10 mM $MgSO_4$ and 100 μg ml^{-1} ampicillin. 3×10^9 p.f.u. of λ*b*221cI857*rex*::Tn*5* were added to 6×10^8 cells of bacterial culture. The culture was incubated for 30 min at 24°C, then centrifuged for 5 min at 13 000 x *g*. The pellet was suspended in 10 volumes of LB-B_1 containing ampicillin, and the cells were incubated at 30°C without shaking for 2 hours. The cells were harvested as before, then suspended in 200 μl of medium. 100 μl aliquots of the suspension were spread on LB-B_1 agar plates supplemented with thiamine, ampicillin, and 40 μg ml^{-1} kanamycin, and incubated overnight at 32°C. Resistant colonies were suspended in 2 ml of medium and 250 μl was inoculated into 25 ml of LB-B_1 containing ampicillin and grown to stationary phase. 5 ml of stationary phase culture were inoculated into 1 l M9 medium [27] with suitable supplements and plasmid DNA was amplified by the method of

Clewell and Helinski [28]. Cells were harvested and plasmid DNA was prepared as previously described [8]. HB101 cells treated with $CaCl_2$ [29] were transformed with plasmid DNA and Tn*5*-containing plasmids were selected on LB-B_1 plates supplemented with ampicillin and kanamycin.

Screening Tn*5* insertions

Individual colonies were picked and grown overnight at 37°C in 2ml LB-B_1 supplemented with ampicillin and kanamycin. Plasmid DNA was isolated from 0.5ml of the above cultures by the rapid alkaline extraction method of Birnboim and Doly [30] and digested with 1-3 units of restriction endonuclease, as described previously [8].

Membrane preparations and detergent extractions

Crude cell envelopes were prepared by French pressure cell lysis at 110MPa as previously described [31]. Inner membranes were prepared by a modification of the method of Yamato *et al* [32]. DNAse [10μg ml^{-1}] and $MgCl_2$[25mM] were added before lysis in 30 mM Tris/HCl, pH8.0 at 34MPa. At the final step, isolated inner membranes were suspended in a minimum volume of 200mM $NaPO_4$, pH6.8. Detergent extracts were prepared by suspension of inner membranes [10mg ml^{-1} protein] in 200mM $NaPO_4$, pH6.8, 1% [v/v] Triton X-100. The extract was stirred on ice for 1h. Insoluble debris was removed by centrifugation for 5min at 15000x*g*. All solutions contained 2mM phenylmethylsulphonylfluoride and unless otherwise stated, all procedures were performed at between 0° and 4°C.

Assays

Fumarate reductase was assayed by the method of Dickie and Weiner [31] except that the assay buffer was 200 mM $NaPO_4$, pH6.8, 0.5 mM dithiothreitol. For anion titrations this buffer was changed to 25 mM HEPES, pH6.8, 0.5 mM dithiothreitol. One unit of activity equaled 1 µmol reduced benzyl viologen oxidized per minute. Proteins were estimated by the method of Bradford [33] using crystalline bovine serum albumin [BioRad Laboratories, Mississauga, Ontario] as standard.

Quinol oxidase activity was measured in 4 ml quartz cuvettes sealed with rubber septa. All buffers and solutions were degassed and saturated with O_2-free Ar, and injected through the septa using Hamilton syringes. 2,3-dimethyl-1,4-naphthoquinone [5 mM in ethanol] was reduced by the addition of 2 mol/mol of $NaBH_4$ [28 mM in 0.025 N NaOH] and kept dark and anoxic [$DMNH_2$]. The quinol could be kept stably reduced for at least 3 h. Final substrate concentrations in 3.7 ml 100 mM $NaPO_4$, pH6.8 assay buffer were 50 µM $DMNH_2$ and 200 µM Na fumarate. Oxidation of $DMNH_2$ was followed at 270 nm, using an extinction coefficient of 16000 $l\,mol^{-1}\,cm^{-1}$

SDS-PAGE Procedure

Gels [22 x 15 x 0.15 cm] were linear gradients of 12-17% [w/v] acrylamide, 0.32-0.45% [w/v] bis-acrylamide and 0-6% [w/v] sucrose. All solutions were prepared according to Laemmli [34]. Gels were stained and destained as described previously [13].

Thermal stability studies

Fumarate reductase catalytic dimer or mutant enzymes were stored in 200 mM $NaPO_4$, pH6.8. Immediately prior to assay the buffer was exchanged by chromatography through 1 ml Sephadex G-25 Fine columns equilibrated with 25 mM HEPES, pH6.8 and coloured fractions pooled for assay. Membrane-bound forms were sedimented for 20 min at 105 000 x *g* in a Beckman Airfuge [Beckman Instruments, Palo Alto, Ca.] and suspended by homogenization in 25 mM HEPES, pH6.8. Incubations were done at 47°C for up to 60 min at a protein concentration of 1-3 mg ml^{-1}. Aliquots were removed at intervals and assayed for fumarate reductase activity.

Anion titrations

Samples were prepared in 25 mM HEPES, pH6.8 as described for thermal stability studies. Enzyme assays were performed as described in the presence of increasing concentrations of $NaPO_4$, pH6.8.

^{35}S-Labelling

2 ml of stationary phase LB-B_1 culture were washed twice with 5 ml of 50 mM Tris/HCl, pH7.2 by centrifugation at 5 000 x *g* for 10 min followed by resuspension, and inoculated into 60 ml M9 medium supplemented with thiamine, kanamycin, ampicillin and 40 µg ml^{-1} each of 19 amino acids [lacking methionine]. [^{35}S]methionine [1.0 MBq, 46.6 TBq mol^{-1}]was added and the culture grown anaerobically for 21 h at 37°C.

Immunoprecipitations

FrdA and FrdB polypeptides were isolated by excision from Coomassie Blue stained SDS-PAGE gels. The polyacrylamide slices were finely minced and emulsified with Freund's complete adjuvant. Catalytic dimer was purified by phenyl-Sepharose chromatography [31] and emulsified in Freund's complete adjuvant at 1 mg protein ml^{-1}. Rabbit antisera to FrdA, FrdB and purified catalytic dimer were raised by standard methods [14]. Serum [75 mg ml^{-1} protein] was pretreated with 2 mM *p*-tosyllysylchloromethylketone, *p*-tosylphenylalanylchloro-methylketone and benzamidine hydrochloride, 1 U ml^{-1} aprotinin and 1/10 volume of cytoplasmic extract from a culture not expressing fumarate reductase. Following incubation for 2 h at room temperature the serum was cleared by centrifugation at 20 000 x *g* for 20 min. Cleared antiserum or control IgG [15 mg ml^{-1} rabbit anti-succinyl-CoA synthetase] was mixed 5 to 1 with unlabelled or ^{35}S-labelled cytoplasmic fraction [20-25 mg ml^{-1}] and incubated 5 h at 4°C. 0.2 mg ml^{-1} bovine serum albumin was added to the ^{35}S-labelled samples. Unlabelled immunoprecipitates were harvested by centrifugation at 13 000 x *g* for 5 min, sonicated at 10 mW for 60 sec in 5 volumes 10 mM phosphate-buffered isotonic saline, pH 7.4 [PBS], 0.5% $C_{12}E_8$ and sedimented as before. For labelled samples, *S. aureus* protein A was added to 0.1 mg ml^{-1} and incubated a further 2 h at 4°C. The co-precipitates were collected as above. The pellets were homogenised in 25 µl PBS, 25 µl solubilization buffer [34] and boiled for 2 min.

Immunoblotting analysis

Gels were prepared as described above in slabs of 11 x 15 x 0.15 cm. 10 µg protein was loaded per well. Protein was transferred to BA85

nitrocellulose paper [Schleicher & Schuell, Keene, NH] by passive diffusion [35,36] for 24 hours. The nitrocellulose-bound protein was decorated by the method of Johnson *et al* [37] with rabbit antisera raised against FrdA or FrdB. Bands were visualized with horseradish peroxidase-coupled goat-antirabbit antibody [BioRad Laboratories, Mississauga, Ontario].

C. RESULTS

Isolation of Tn*5* insertion mutants

302 colonies exhibiting both ampicillin and kanamycin resistance were screened. The *Eco*RI restriction digestion patterns were compared to that of the parent plasmid, pFRD79 [Fig. II.1a]. Loss of the 3.4 kilobasepair [kbp] fragment and appearance of a 9 kbp fragment indicated insertion of Tn*5* into the *frd* operon distal to the *Eco*RI site in *frdA*. 72 colonies [23.8%] showed this pattern. An additional 112 [37.1%] colonies showed a pattern consistent with Tn*5* insertions in the pBR322 vector or the promoter-proximal region of FrdA, while the remainder [39.1%] showed a pattern which indicated the presence of both a wild-type pFRD79 and a transposon-carrying plasmid.

The location of the Tn*5* insertion in the *frd* operon was mapped for each of the 72 *frd*::Tn*5* plasmids by digestion with *Sal*I, *Bam*HI and *Hin*dIII. Insertions in the *frdC* and *D* region were further mapped with *Ava*I and *Alu*I digestions [Fig. II.1c]. 37 [51.4%] insertions mapped in *frdA*, 28 [38.9%] in *frdB*, 3 [4.2%] in *frdC* and one [1.4%] in *frdD*. An additional 2[2.8%] were found to be in the *ampC* region [Fig. II.1b]. Mutant pFRD79::Tn*5*-239 as chosen as an insertion in *frdA* [*frdA*::Tn*5*], pFRD79::Tn*5*-260 as an insertion in *frdB* [*frdB*::Tn*5*], pFRD79::Tn*5*-233

as an insertion in *frdC* [*frdC*::Tn*5*], and pFRD79::Tn*5*-299 as the sole example of an insertion in *frdD* [*frdD*::Tn*5*].

The expression of fumarate reductase polypeptides by *frd* mutants

Each of the selected *frd* mutations was examined for expression and cellular localization of Frd polypeptides. When Tn*5* was inserted within *frdA* [*frdA*::Tn*5*] no fumarate reductase subunits were detected in the cytoplasm by immunoprecipitation. [Fig. II.2a, lane 1], or immunoblotting [Fig. II.3a, compare lanes 1 and 2]. Similar results were seen with other Tn*5* insertions in *frdA*. Following insertion of Tn5 within *frdB* [*frdB*::Tn*5*], intact FrdA was detected by immunoblotting [Fig. II.3, lanes 1 and 3] and by immunoprecipitation [Fig. II.2a, lane 2], but no fragments of FrdB were seen [Fig. II.3b, lanes 1 and 3] The antibodies raised against FrdB exhibited some cross-reactivity with FrdA [Fig. II.3b, lanes 1 and 3]. The FrdA polypeptide accumulated in the cytoplasm and contained the covalent flavin co-factor characteristic of fumarate reductase [10] [data not shown]. When Tn*5* was inserted near the middle of *frdC* [*frdC*::Tn*5*], both FrdA and FrdB accumulated in the cytoplasm [Fig. II.2a, lane 3] but a FrdC fragment could not be detected on the gels. The insertion mutation in *frdD* [*frdD*::Tn*5*] gave rise to a unique phenotype. Immunoprecipitation of Triton X-100 extracts of inner membrane fraction indicated that a tetramer consisting of FrdA,B,C and a truncated FrdD [FrdD'] migrating at an apparent molecular weight of 12 kDa was amplified in the membrane [Fig. II.2a, lane 4]. No wild-type FrdD could be visualized in the membrane fraction. Furthermore, examination of Fig. II.2b, lane 1 shows that a fumarate reductase trimer composed of FrdA, B and C accumulated

in the cytoplasm of a strain which does not carry a chromosomal copy of *frd* [MI1443, Table II.1]. This trimer apparently reacted poorly with the antisera available, and could only be visualized in radiolabelled immunoprecipitates.

Amplification of fumarate reductase activity in *frd* mutants

The presence of a complete *frd* operon on a plasmid vector [pFRD79] results in an amplification of membrane-bound fumarate reductase activity over wild-type [Table II.2]. The presence of a plasmid carrying only *frdA* and *frdB* [pFRD117] results in a substantial expression of soluble activity. Insertion of a transposon into *frdA* or *frdB* did not give rise to detectable activity in the cytoplasm, but normal levels of activity were observed in the cytoplasmic membrane of HB101, due to the intact chromosomal copy of *frd*. HB101 harbouring mutation *frdC*::Tn*5* produce large quantities of soluble, cytoplasmic enzyme activity and normal levels of membrane associated activity. Phenotypically, this plasmid is indistinguishable from pFRD117 [13].

In transposon mutation *frdD*::Tn*5* both the cytoplasmic and membrane fractions of HB101 had amplified levels of fumarate reductase activity. Nearly 80% of the total activity was soluble, while the remainder was bound to the inner membrane [Table II.2].

Properties of fumarate reductase produced in strains harbouring *frdC*::Tn*5* and *frdD*::Tn*5*

The catalytic dimer and holoenzyme forms of fumarate reductase can be easily distinguished [4,13]. *E. coli* MI1443 is deleted for *frd* and *ampC* and cannot grow anaerobically on GF. pFRD117, which produces dimer,

does not permit growth on GF, while pFRD79, which codes for wild-type tetramer, does [37A]. The activity of the dimer, but not the tetramer is stimulated 5-fold by addition of anions to the assay buffer [38]. Additionally, the catalytic dimer is rapidly denatured by incubation in alkaline solution [pH8.6] or at elevated temperature [>45°C]. Holoenzyme, but not dimer is capable of accepting reducing equivalents from quinone analogues [39,40]. These observations have led to the proposal that the anchor polypeptides [FrdC and FrdD] induce an optimal conformation of the catalytic subunits [4] and are essential for the physiological functions of fumarate reductase. The properties of the two Tn*5* insertions in FrdC and D provide further evidence for this model.

Transposon mutation *frdC*::Tn*5* produced catalytic dimer in the cytoplasm, while *frdD*::Tn*5* produced soluble trimer. These two enzyme forms showed different anion dependence. *FrdC*::Tn*5* enzyme was stimulated 5-fold by anions [Fig. II.4], as expected for catalytic dimer and in agreement with the results reported previously [13]. *FrdD*::Tn*5* trimeric enzyme was not activated by anions. This result indicates that although the *frdD*::Tn*5* enzyme lacked FrdD, it behaved like tetramer with respect to anion dependence.

To examine this further the thermal and alkaline labilities of the *frdC*::Tn*5* and *frdD*::Tn*5* activities from the cytoplasm and *frdD*::Tn*5* activity from the membrane were measured. Fig. II.5a shows that both cytoplasmic enzymes were denatured by incubation at 47°C with a half-life of about 7 min. The *frdC*::Tn*5* dimer was rapidly denatured following incubation at pH8.6 [Fig. II.5b] while the *frdD*::Tn*5* trimer was stable. The *frdD*::Tn*5* tetramer in the inner membrane has stability properties indistinguishable to those of the soluble trimer. It is thermolabile

[Fig. II.6a], unlike wild-type tetramer and stable to alkaline conditions [Fig. II.6b].

The *frdD*::Tn*5* plasmid complements MI1443 to growth on GF. The trimeric enzyme has no detectable fumarate reductase activity in the $DMNH_2$ assay, while membrane bound FrdABCD' has 2-[n-heptyl]-4-hydroxyquinoline-N-oxide sensitive fumarate-dependent $DMNH_2$ oxidase activity. The ratio of specific activity of the BV to $DMNH_2$ assays is 9 for the two membrane-bound enzymes. Thus, the altered tetramer with the truncated FrdD subunit retains physiological activity, while the soluble FrdABC trimer does not. Together these results discriminate the functions of FrdC and FrdD.

D. DISCUSSION

72 Tn*5* insertions [23.8% of the total] in the *frd* operon distal to the *Eco*RI site in *frdA* were isolated. If Tn*5* had transposed completely at random, 37% of insertions would be expected to lie in this 3.4 kbp region of pFRD79 [9.1 kbp total size]. While the transposition of Tn*5* is not site-specific [17,18,19], there is a preference for insertion at GC [41]. Moreover, it was shown that there is a hotspot for insertion of Tn*5* at nucleotide 31 of pBR322, which is part of the *Hin*dIII site into which *frd* is cloned in pFRD79. This may account for the apparent bias for insertion in the vector compared to *frd*. Bossi and Ciampi [42] reported that Tn*5* inserts preferentially at a concensus sequence which is homologous to a 12 bp region in the terminal repeats of the transposon. The *frd* sequence has been computer-searched for this concensus sequence, and while it was found 7 times when 4 mismatches were allowed, the locations did not

match any of the insertions mapped [V. Paetkau, personal communication]. The selectivity of Tn*5* insertion is exemplified in Fig. II.1, which shows a striking paucity of insertions within the *frdCD* region, compared to flanking sequences. The length of DNA coding for the small polypeptides and FrdB is similar, yet 28 insertions were mapped in *frdB* and only 4 in the *CD* region. A possibility which cannot be ruled out at this time is that insertions did occur in this region, but the resulting mutations were lethal.

Expression analysis of a number of insertions within *frdA* and *frdB* indicated that truncated fragments were never detected by the methods used. One possibility is that the cell recognized these aberrant polypeptides and rapidly cleared them by proteolysis [43]. Hederstedt and co-workers have detected truncated fragments of succinate dehydrogenase flavoprotein and iron-sulfur protein subunits in the cytoplasm of *Bacillus subtilis*, but note that they are unstable unless special precautions are taken to preserve them [44,45]. Intact FrdA accumulated in the cytoplasm of strains carrying Tn*5* mutations in *frdB*, although neither fumarate reductase [fumarate-dependent benzyl viologen oxidase] activity [Table II.2] nor succinate dehydrogenase [succinate-dependent 3-[4,5-dimethylthiazolyl-2]-2,5-diphenyltetrazolium bromide [MTT] reductase] activity [data not shown] was observed. This is in agreement with the results of Cecchini *et al* [39], who also showed that the FrdA subunit was inactive as succinate dehydrogenase, but in contrast to the results reported by Unden and Kröger [46] for the fumarate reductase of *Wolinella succinogenes.* They observed that the isolated 79kDa covalent-flavin containing subunit [equivalent to *E. coli* FrdA] was catalytically active, but only when associated as a homodimer. The monomer itself was inactive. This leads to

the suggestion that the minimal catalytic unit for the *E. coli* enzyme is the FrdAB dimer.

It was previously shown that FrdC plus FrdD anchor and stabilize the catalytic dimer and permit fumarate-dependent oxidation of quinone analogues [39,40]. However, although these 2 subunits appear structurally similar [4] no information has been available as to why two different polypeptides are needed. The Tn*5* insertion in *frdD* addresses this question. The FrdABC trimer found in the cytoplasm of strains harbouring the *frdD*::Tn*5* plasmid has properties intermediate between those of dimer and tetramer. The presence of FrdC confers stability at high pH, but not at high temperature. It renders the catalytic domain insensitive to anion stimulation by phosphate. It is not sufficient to allow binding of fumarate reductase to the inner membrane. It does not allow fumarate-dependent oxidation of quinone analogues.

The membrane-bound mutant tetramer expressed by the *frdD*::Tn*5* plasmid elucidates the role of FrdD. The truncated FrdD' is capable of allowing membrane insertion of the complex, but at an apparently reduced efficiency [21.5% membrane-bound in *frdD*::Tn*5* vs 100% membrane-bound in pFRD79, Table II.2]. This effect could also be due to competition between proteolysis of the FrdD' fragment, giving rise to soluble trimer, and insertion of the mutant tetrameric complex into the membrane [47]. It has already been noted that intact Frd subunits tend to accumulate, while truncated polypeptides do not. FrdD' does not confer thermal stability on the catalytic domain, implicating the missing C-terminal fragment in this role. FrdD' together with FrdC permit the use of quinone analogues as reducing agents, and apparently normal physiological activity of the fumarate reductase complex. It cannot be distinguished whether FrdD'

alone is responsible, or the interaction between it and the rest of the subunits forms the site of interaction with the quinones of the electron transport chain.

It is interesting to note that in strains bearing the *frdD*::Tn*5* plasmid there is only trimer in the cytoplasm and only tetramer in the cytoplasmic membrane. It is inferred from this that FrdA and B are assembled from a cytoplasmic pool, and that the hydrophobic FrdC polypeptide can associate with this dimer in a soluble form. Upon addition of the FrdD [or FrdD'] polypeptide the complex becomes membrane bound, but the order of subunit assembly or membrane insertion remains unclear. It is not known why this putative assembly pathway produces only mutant tetramer in a strain that harbours both *frdD*::Tn*5* and a wild-type *frd* operon [HB101], unless over-production of mRNA from the multicopy plasmid overwhelms that from the chromosome. Experiments to further elucidate this pathway and the role of FrdC and FrdD in quinone binding are being conducted.

The authors wish to thank Dr. M. Iwaya for supplying MI443 and Dr. G.D. Armstrong for assistance with raising antisera.

Table II.1 Bacterial strains, phage and plasmids

Bacteria	Genotype/phenotype	Source
E. coli HB101	F- *hsdR hsdM pro leu gal lac thi recA rpsL*	G. McFadden
E. coli MI1443	Δ[*frdABCDampC*] Sm^r	M. Iwaya
Phage and plasmids		
λ*b*221 c1857*rex*::Tn*5*	Km^r	P. P. Dennis
pBR322	Ap^rTc^r	Boehringer
pFRD117	Ap^r *frdAB*	This laboratory
pFRD79	Ap^r *frdABCD*	This laboratory
pFRD79::Tn*5*-233	Ap^r *frdC*::Tn*5*	This work
pFRD79::Tn*5*-239	Ap^r *frdA*::Tn*5*	This work
pFRD79::Tn*5*-260	Ap^r *frdB*::Tn*5*	This work
pFRD79::Tn*5*-299	Ap^r *frdD*:Tn*5*	This work

Table II.2 Expression and localization of fumarate reductase

Cells were grown as described in Methods and lysed by two passages through a French pressure cell. Crude envelopes were separated from cytoplasm by centrifugation at 150 000 x *g* for 60 min and the envelopes suspended by homogenization in a minimal volume of 200 mM sodium phosphate buffer, pH 6.8. Data are representative of four independent experiments.

	Specific activity [units mg protein^{-1}]		Percentage of total activity	
Strain	Envelopes	Cytoplasm	Envelopes	Cytoplasm
HB101/pBR322	21	ND	100	ND
HB101/pFRD117	11.5	42.3	0.6±0.3	99.4±0.6
HB101/pFRD79	76.7	3.2	56.8±5.0	43.2±4.5*
HB101/*frdC*::Tn*5*	19	70.8	0.9±0.5	99.1±0.5
HB101/*frdA*::Tn*5*	16	ND	100	ND
HB101/*frdB*::Tn*5*	12	ND	100	ND
HB101/*frdD*::Tn*5*	45	32.7	21.5±5.3	78.5±5.2

ND = Not detected

*Fumarate reductase in the cytoplasm of this strain is not soluble. It is holoenzyme bound into tubular lipoprotein structures induced by over-expression of the enzyme [4]

Specific activities were reproducible within 10% variability.

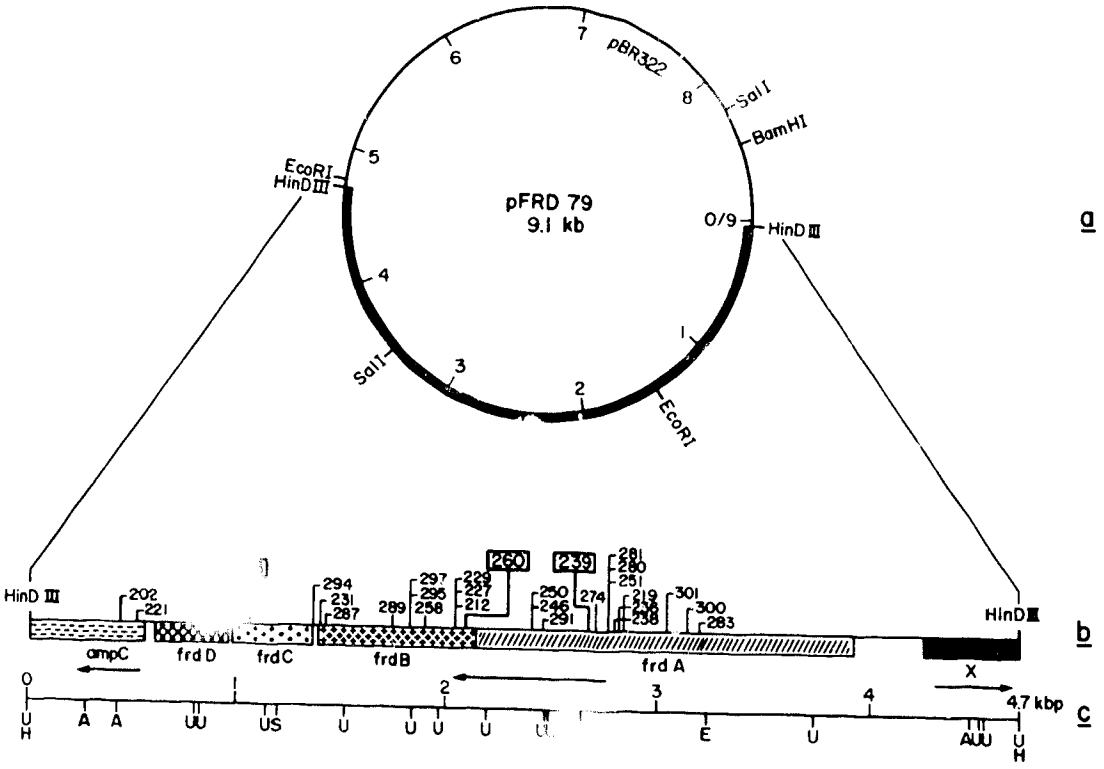

FigureII.1 [a] **Restriction map of pFRD79**. Heavy line is the *Hin*dIII fragment carrying *frd*. Thin line is pBR322. [b] **Genetic map of *Hin*dIII fragment.** Arrows show direction of transcription. Numbers mark locations of Tn*5* insertions. Boxed are the mutants discussed. [c] Restriction map of *Hin*dIII fragment: A, *Ava*I, E, *Eco*RI, H, *Hin*dIII, S, *Sal*I, U, *Alu*I

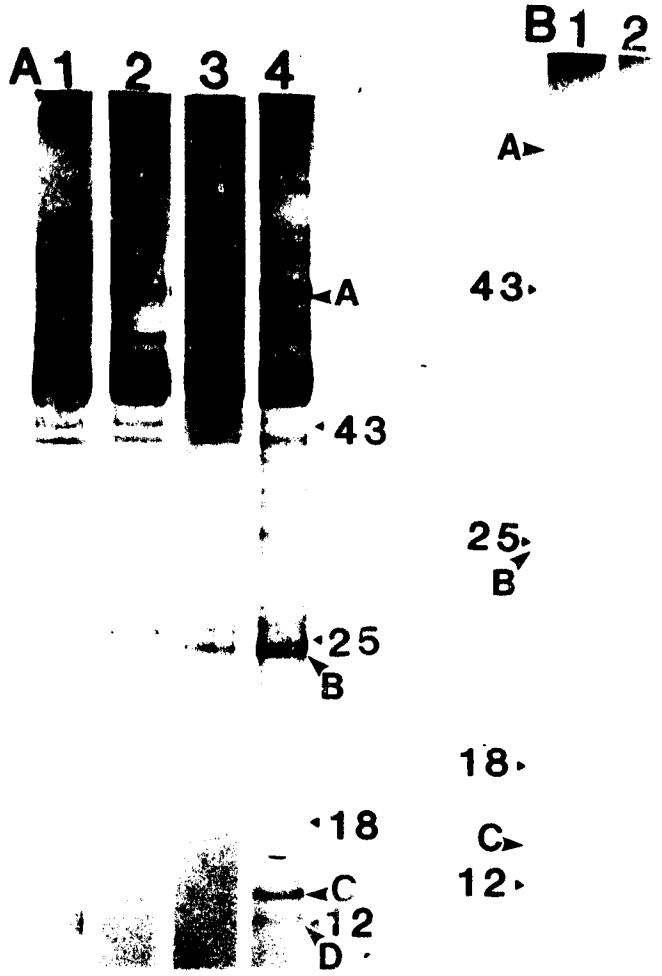

Figure II.2. [a] SDS-PAGE of unlabelled immunoprecipitates, Coomassie Blue staining. Cytoplasmic fractions and Triton X-100 extracted inner membranes were precipitated with anti-FrdAB serum and separated as described in Methods on 12-17% polyacrylamide gels. Lane [1] HB101 [*frdA*::Tn*5*] cytoplasmic fraction; Lane [2] HB101 [*frdB*::Tn*5*] cytoplasmic fraction; Lane [3] HB101 [*frdC*::Tn*5*] cytoplasmic fraction Lane [4] HB101 [*frdD*::Tn*5*] Triton X-100 extract. **[b] SDS-PAGE of ^{35}S-labelled immunoprecipitates**, autoradiograph. Lane [1] MI1443 [*frdD*::Tn*5*] cytoplasmic fraction precipitated with anti-FrdAB serum. Lane [2] MI1443 [*frdD*::Tn*5*] cytoplasmic fraction precipitated with control immunoglobulin. Molecular weight markers are chick ovalbumin [43 kDa], α-chymotrypsinogen [25 kDa], β-lactoglobulin [18 kDa] and cytochrome *c* [12 kDa]. Letters mark the positions of the Frd subunits.

Figure II.3. Immunoblotting analysis of fumarate reductase polypeptides. Immunoblotting was carried out as described in Methods. In [**a**] anti-FrdA gamma-globulin was used, in [**b**] anti-FrdB gamma-globulin was used. Lane [1] SDS-solubilized membranes from HB101 [pFRD79]; Lane [2] cytoplasm from HB101 [*frdA*::Tn*5*]; Lane [3] cytoplasm from HB101 [*frdB*::Tn*5*]. Molecular weight markers are chick ovalbumin [43 kDa], α-chymotrypsinogen [25 kDa], β-lactoglobulin [18 kDa] and cytochrome *c* [12 kDa]. Letters mark locations of Frd subunits.

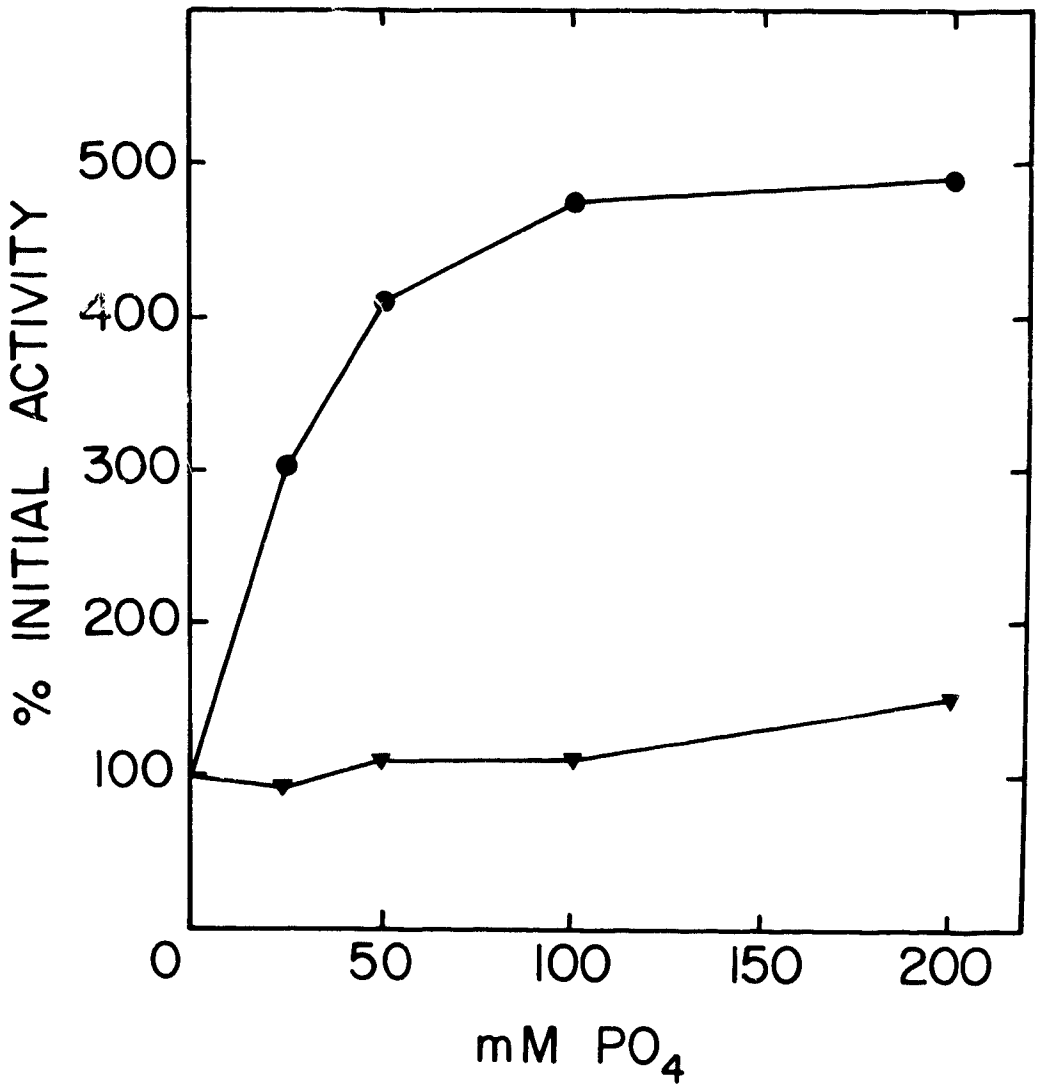

Figure II.4. Anion titration of the cytoplasmic fumarate reductase activity produced by HB101 [*frdC*::Tn*5*], [●] and HB101 [*frdD*::Tn*5*] [▼]. Assays were carried out in 25 mM Hepes, pH6.8, 0.5 mM DTT with increasing concentrations of $NaPO_4$ buffer, pH6.8.

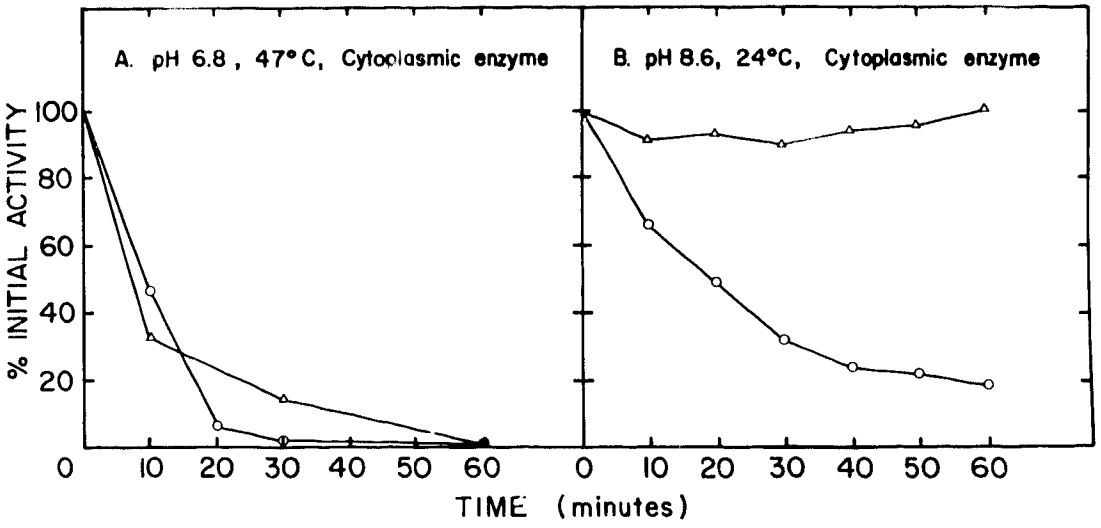

Figure II.5. [**a**] **Thermal stability** [47°C, pH6.8] of the cytoplasmic fumarate reductase activity produced by HB101 [*frdC*::Tn*5*] [o] and HB101 [*frdD*::Tn*5*] [Δ]; [**b**] **Alkaline stability** [pH8.6, 24°C] of the cytoplasmic fumarate reductase activity produced by HB101 [*frdC*::Tn*5*] [o] and HB101 [*frdD*::Tn*5*] [Δ]. Samples were treated and assays were carried out as described in Methods.

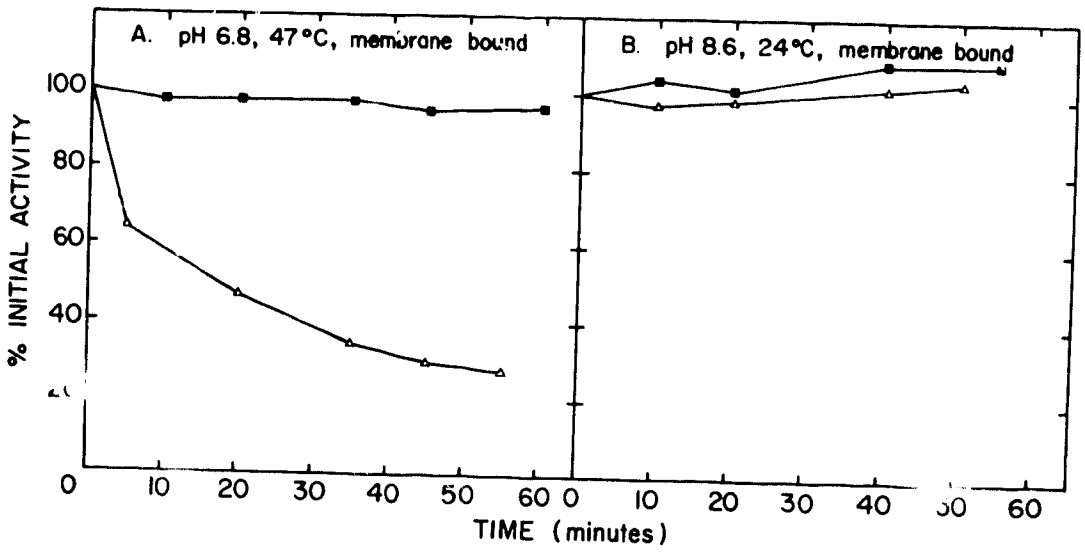

Figure II.6. [a] **Thermal stability** [47°C, pH6.8] of inner membrane-bound enzyme produced by HB101 [pFRD79] [■] or by HB101 [*frdD*::Tn*5*] [Δ]; [b] **Alkaline stability** [pH8.6, 24°C] of inner membrane-bound enzyme produced by HB101[pFRD79] [■] or by HB101 [*frdD*::Tn*5*] [Δ].

Bibliography

1. Singh, A.P. & Bragg, P.D. 1975. Biochim. Biophys. Acta **396**: 229-241.
2. Haddock, B.A. & Jones, C.W. 1977.Bacteriol. Rev.**41**: 47-99.
3. Ingledew, W.J. & Poole, R.K. 1984. Microbiol. Rev. **48**:222-271.
4. Weiner, J.H., Lemire, B.D., Elmes, M.L., Bradley, R.D. & Scraba, D.G. 1984. J. Bacteriol. **158**:590-596.
5. Cole, S.T 1982. Eur. J. Biochem. **122**:479-484.
6. Cole, S.T., Grundström, T., Jaurin, B., Robinson, J.J. & Weiner, J.H. 1982. Eur. J. Biochem. **126**:211-216.
7. Grundström, T. & Jaurin, B. 1982. Proc. Natl. Acad. Sci. USA. **79**:1111-1115.
8. Lohmeier, E., Hagen, D.S., Dickie, P. & Weiner, J.H. 1981. Can. J. Biochem. **59**:158-164.
9. Robinson, J.J. & Weiner, J.H. 1982.Can. J. Biochem. **60**:811-816.
10. Weiner, J.H. & Dickie, P. 1979. J. Biol. Chem. **254**:8590-8593.
11. Cole, S.T., Condon, C., Lemire, B.D. & Weiner, J.H. 1986. Biochim. Biophys. Acta Rev. Bioenerg. **811**:381-403.
12. Cammack, R., Patil, D.S. & Weiner, J.H. 1986. Biochim. Biophys. Acta **870**:538-544.
13. Lemire, B.D., Robinson, J.J. & Weiner, J.H. 1982. J. Bacteriol. **152**:126-1131.
14. Lemire, B.D., Robinson, J.J., Bradley, R.D., Scraba, D.G. & Weiner, J.H. 1983. J. Bacteriol. **155**:391-397.

15. Berg, D.E. 1977. pp. 205-212.*In* Bukhan, A.I., Shappiro, J.A. & Adhya, S.L. [eds.] *DNA Insertion Elements, Plasmids and Episomes* Cold Spring Harbor Laboratory Press, N.Y.
16. Johnson, R.C., Yin, J.C.P. & Reznikoff, W.S. 1982. Cell **30**:873-882.
17. Shaw, K.J. & Berg, C.M. 1979.Genetics **92**:741-747.
18. Berg, D.E., Forgerson, R. & Davies, J. 1978. pp. 13-15. *In* Schlesinger, D. [ed.], *Microbiology-1978.* American Society for Microbiology, Washington.
19. Miller, J.H., Calos, M.P., Galas, D., Hofer, M., Buchel, D.E. & Muller-Hill,B. 1980. J. Molec. Biol. **144**:1-18.
20. Berg, D.E., Weiss, A. & Crossland, L. 1980. J. Bacteriol. **142**:439-446.
21. Laird, A.J. & Young, I.G. 1980. Gene **11**:359-366.
22. Pannekoek, H., Hillie, J., & Noordermeer, I. 1980. Gene **12**:51-61.
23. de Bruijn, F.J. & Ausubel, F.M. 1981. Molec. Gen. Genet. **183**:289-297.
24. Lupski, J.R., Smillie, B.L., Blattner, F.R. & Godson, G.N. 1982. Molec. Gen. Genet. **185**:120-128.
25. de Bruijn, F.J., Stroke, I.L., Marvel, D.J. & Ausubel, F.M. 1983. EMBO J. **2**:1831-1838.
26. Spencer, M.E. & Guest, J.R. 1974. J. Bacteriol. **117**:954-959.
27. Miller, J.H. 1972. pp431-435.*Experiments in Molecular Genetics* Cold Spring Harbor Laboratory Press, N.Y. .
28. Clewell, D.B. & Helinski, D.R. 1972. J. Bacteriol. **110**:1135-1146.
29. Mandel, M. & Higa, A. 1970. J. Molec. Biol. **53**:159-162.
30. Birnboim, H.C. & Doly, J. 1979. Nucl. Acids Res. **7**:1513-1523.

31. Dickie, P. & Weiner, J.H. 1979. Can. J. Biochem. **57**:813-821.
32. Yamato, I., Anraku, Y. & Hirosawa, K. 1975. J. Biochem. **77**:705-718.
33. Bradford, M.M. 1976. Anal. Biochem. **72**:248-254.
34. Laemmli, U.K. 1970. Nature **227**:680-685.
35. Renart, J., Reiser, J. & Stark, G.R. 1979. Proc. Natl. Acad. Sci USA. **76**:3116-3120.
36. Bowen, B., Steinberg, J., Laemmli, U.K. & Weintraub, H. 1980. Nucl. Acids Res. **8**:1-20.
37. Johnson, D.A., Gautsch, J.W., Sportsman, J.R. & Elder, J.H. 1984. Gene Analysis Techniques 1:3-8.
38. Robinson, J.J. & Weiner, J.H. 1981. Biochemi. J. **199**:473-477.
39. Cecchini, G., Ackrell, B.A.C., Deshler, J.O. & Gunsalus, R.P. 1986. J. Biol. Chem. **261**:1808-1814
40. Weiner, J.H., Cammack, R., Cole, S.T., Condon, C., Honoré, N., Lemire, B.D. & Shaw, G. 1986. Proc. Natl. Acad. Sci. USA. **83**:2056-2060.
41. Berg, D.E., Schmandt, M.A. & Lowe, J.B. 1983. Genetics **105**:813-828.
42. Bossi, L. & Ciampi, M.S. 1981. Molec.Gen. Genet. **183**:406-408.
43. Goldberg, A.L. 1972. Proc. Natl. Acad. Sci. USA. **69**:422-426.
44. Hederstedt, L. 1983. Eur. J. Biochem. **132**:589-593.
45. Hederstedt, L., Maguire, J.J., Waring, A.J. & Ohnishi, T. 1985. J. Biol. Chem. **260**:5554-5562.
46. Unden, G. & Kröger, A. 1981.Eur. J. Biochem. **120**:577-584.
47. Oliver, D. 1985. Ann. Rev. Microbiol. **39**:615-648.

III. ASSEMBLY OF FUMARATE REDUCTASE HOLOENZYME

A. INTRODUCTION

When *Escherichia coli* is grown anaerobically on media containing glycerol and fumarate it produces a simple electron transport chain which terminates in the enzyme fumarate reductase [12,13,14]. Fumarate reductase is composed of four subunits of 69 kDa, 27 kDa, 15 kDa and 13 kDa encoded by the *frdA, B, C* and *D* genes, respectively [15].

FrdA and FrdB together comprise a membrane extrinsic domain which can be purified in a water soluble form [16]. FrdA contains a flavin adenine dinucleotide cofactor which is covalently attached *via* an 8α-[N3-histidyl] bond to His^{44} [9]. FrdB contains three iron-sulphur centres [14,17].

FrdC and FrdD together form a membrane anchor domain which serves to hold the enzyme to the cytoplasmic side of the inner membrane [10,18]. Deletion of FrdD results in the expression of a soluble enzyme [14] indicating that FrdC alone is incapable of anchoring the enzyme to the membrane. Truncation of FrdD by transposon insertion in the gene results in production of a soluble trimer of FrdA, B and C accumulating in the cytoplasm, as well as a membrane bound tetramer containing the shortened FrdD' [19], implying a role for FrdD in the proper assembly of fumarate reductase in the inner membrane.

Here I report the *in vivo* assembly of fumarate reductase from wild-type and Tn*5*-mutated operons in a conditional expression system based on the phage T7 RNA polymerase [1].

B. MATERIALS AND METHODS.

Strains and plasmids

The T7 expression system consisting of pGP1-2 bearing the T7-phage *gene1* for its own RNA polymerase under the control of λ P_L and *c*I857and pT7-4 and pT7-6 bearing the T7 *ϕ10* promoter upstream of a multicloning site was obtained from Dr. S. Tabor [Harvard Medical School][1]. pGP1-2 was supplied already transformed into *Escherichia coli* K38 [2]. All strains and plasmids are described in Table III.1

Construction of *E. coli* DLT111

To stabily maintain recombinant plasmids over extended periods of time *E. coli* strain K38 was made *recA* . Bacteriophage P1 was propagated on *Escherichia coli* strain RG51[*srl::*Tn*10*[Tc^r]*recA*56] and used to transduce strain K38 to Tc^r[4]. Mid-log K38/pGP1-2 cells [Tc^s Km^r] were sedimented and suspended in 100 mM $MgSO_4$, 5 mM $CaCl_2$. After gentle aeration at 37°C for 15 min the cells were mixed 1:1 with a 1000-fold dilution of transducing phage, incubated 20 min at 37°C, treated with one vol of 1M Na citrate and spread onto LB-B_1 agar plates [4] for selection of Tc^r Km^r colonies. As this selection is for *srl::*Tn*10,* colonies displaying the Tc^r Km^r phenotype were tested for *recA* by demonstrating no growth on L-broth agar plates containing 0.08% methylmethanesulphonate, a DNA methylating agent. One such colony, DLT111/pGP1-2, was transformed to Tc^r Km^r Ap^r with the various pDJL plasmids, each bearing a combination of *frd* cistrons downstream of the T7 phage *ϕ10* promoter.

Transformation of competent cells

E. coli strains HB101 or DLT111 were made competent by the $CaCl_2$ method of Mandel and Higa [20].

Construction of pDJL1

A plasmid bearing the *frd* operon with the Tn*5*-truncated *frdD* cistron was constructed from pFRD79::Tn*5*-299 [chapter II] by digesting 10 µg of plasmid DNA with 36 U of *Bam*HI for 3 h at 37°C. The digestion products were separated on a 1.2% low-melting point agarose gel in 40mM Tris/acetate, pH8.0, 20mM Na acetate, 2mM EDTA for 18 h at 50 V constant voltage. The 7.2 kbp band carrying *frd* and the left terminal repeat of the inserted transposon Tn*5* was excised and purified.

The gel slice was melted at 70°C for 5 min and was diluted with 5 vol 10 mM Tris-HCl pH7.2, 1 mM EDTA, 0.5 M NaCl. A NACS™-52 column [Bethesda Research Laboratories] was equilibrated in 10 mM Tris-HCl pH7.2, 1 mM EDTA, 0.5 M NaCl at 45°C. The melted agarose and DNA mixture was run through the column and the resin was washed thrice with 1.0 ml of equilibration buffer. The bound DNA was eluted with 600 µl 10 mM Tris-HCl pH7.2, 1 mM EDTA, 2.0 M NaCl. 5 µg of *E. coli* tRNA was added to the eluant as carrier and the DNA fragment was precipitated in 2 vol of ethanol at -70°C for 20 min. The 7.2 kbp fragment was suspended and digested 4 h at 37°C with 6 U *Xho*I to remove the bulk of the Tn*5* insert.

One µg of pT7-6 was digested for 6 h at 37°C with 6 U of *Sal*I and then dephosphorylated by treating with 0.5 U of calf intestinal alkaline phosphatase for 20 min at 37°C. The vector DNA was extracted once with 1/4 vol of phenol and twice with 1/4 vol of diethyl ether[6]. The treated

vector DNA was mixed with the *Xho*I digested fragment and the pooled DNA was precipitated with 2 vol of ethanol at -70°C.

The pellet was suspended and digested with 6 U of *Hin*dIII for 3.5 h at 37°C. After precipitating with 2 vol of cold ethanol to remove the restriction enzyme, the mixture of DNA fragments was suspended in ligase buffer [6] and ligated for 14 h at 14°C with 0.2 U of T4 DNA ligase.

The ligated DNA was used to transform *E. coli* strain HB101 to ampicillin resistance and 150 colonies were screened by the rapid alkaline method of Birnboim and Doly [3]. One clone, pDJL1, showing the proper digestion pattern with *Hin*dIII and *Eco*RI was selected and used for expression studies [Fig. III.1].

Construction of pDJL6

Plasmid pDJL6 was constructed from the Cm^r plasmid pFRD708, which carries the intact *frd* operon on a 4.9 kbp fragment in pACYC184, [7] by digesting 1 μg of pFRD708 for 4 h at 37°C with 5 U *Hin*dIII. 0.5 μg of pT7-4 was also digested for 4 h at 37°C with 5 U of *Hin*dIII. The cut vector DNA was treated with 0.5 U of calf intestinal alkaline phosphatase for 20 min at 37°C, extracted once with 1/4 vol phenol and twice with 1/4 vol diethyl ether.

The two digested DNA mixtures were pooled and precipitated by the addition of two vol of ethanol and incubation at -70°C. The pellet was suspended in ligase buffer and ligated overnight at 14°C with 0.2 U of T4 DNA ligase. The ligated DNA was used to transform HB101 to ampicillin resistance and suitable clones were identified by mapping with *Hin*dIII and *Eco*RI. One clone, pDJL6, was selected for use [Fig. III.1].

Construction of pDJL22

Plasmid pDJL22 was constructed from pDJL6 to contain *frdCD* alone under *ϕ10* control. Three μg of plasmid DNA was digested with 5 U of *Sst*II for 2.5 h at 37°C to remove the bulk of *frdA* and *frdB* on two *Sst*II fragments. *Sst*II is an isoschizomer of *Sac*II. The DNA was extracted once with 1/2 vol of phenol:chloroform [24:1] and once with 1/2 vol of chloroform. The extracted DNA was dialysed against 2.5 mM Tris-HCl, pH 8.0 on a Millipore 0.05 μm VM filter membrane. The dialysed samples were diluted 1:1 with 2X ligase buffer and ligated overnight at 14°C. The ligated DNA was used to transform HB101 to ampicillin resistance and suitable clones were identified by mapping with *Hin*dIII. One clone, pDJL22, was selected for use [Fig. III.1]

Plasmid DNA from each of the above constructions was obtained from the HB101 host by the rapid alkaline extraction method of Birnboim and Doly [3] and used without further purification to transform DLT111/pGP1-2 to Tc^r Km^r Ap^r.

Pulse/chase experiments

Expression from the various pDJL plasmids was achieved by the method of Tabor and Richardson [1]. DLT111 bearing pGP1-2 and the appropriate *frd* plasmids was grown overnight at 32°C in LB-B_1 [4] supplemented with 100 μg ampicillin, 12.5 μg tetracycline, and 40 μg kanamycin ml^{-1}. The cultures were diluted with 4 vol of fresh LB-B_1 and grown for 2 h at 32°C, until they had reached mid-log phase [OD_{550}=0.6]. The cells were sedimented for 5 min at 12 000 x *g*, washed with 5 vol 10mM phosphate buffered isotonic saline, pH7.4 [PBS], sedimented as before and suspended to the original volume in labelling medium [M9

medium [4] supplemented with 1% glucose and 1% Difco methionine assay powdered medium]. The cells were incubated, shaken, for 90 min at 32°C to starve them for methionine.

The temperature was shifted to 42°C for 15 min to induce the expression of T7 RNA polymerase from pGP1-2. Methanolic rifampicin was added to 250 μg ml^{-1} final concentration to stop host cell transcription and the cells were incubated a further 20 min at 42°C and 10 min at 32°C. The cells were then chilled to the desired labelling [illegible] in a refrigerated waterbath and held at that temperature a further 10 min.

370KBq of [^{35}S]methionine [Amersham, 46.6 TBq mol^{-1}] was added per ml of culture and the cells were swirled once. After a 60 sec pulse cold methionine was added to 0.1% final concentration, the cells were swirled once to mix and the 500 μl zero time sample was removed. Further 500 μl aliquots were removed at the times indicated in the figure legends. The samples were pipetted directly into 500 μl of ice-cold stop buffer [100 mM $NaPO_4$, pH6.8, 20 μM PMSF, TLCK, TPCK, benzamidine; 3 mg chloramphenicol and 200 μg streptomycin ml^{-1}] and held on ice until the chase was complete.

The treated cells were lysed by two passages through a French pressure cell at 110 MPa, and unbroken cells were removed by centrifugation for 2 min at 13 000 x *g* at 4°C. The membranes were separated from the soluble fraction by ultracentrifugation at 396 000 x *g* for 30 min at 4°C. The sedimented membranes were suspended in 20 μl PBS by homogenization.

The soluble fraction was treated with 200 μl of 50% TCA and incubated 20 min on ice. The precipitated proteins were sedimented by centrifuging for 15 min at 13 000 x *g* at 4°C. The pellets were washed

once with 200 µl methanol to remove precipitated rifampicin and suspended in 20 µl PBS by homogenization.

All the samples received 20 µl of cracking buffer [60 mM Tris-HCl, pH 6.8, 1% SDS, 1% 2-mercaptoethanol, 10% glycerol, 0.01% bromophenol blue] [1] and were heated to 95°C for 2 min. Half of each sample was loaded onto 22 x 15 x 0.15 cm double gradient acrylamide gels and subjected to electrophoresis for 230 mA·h. The gels were fixed in 10% acetic acid, 30% methanol, dried and autoradiographed at -70°C on Kodak XAR-5 film.

Immunoprecipitations

Monospecific rabbit antibodies directed against purified FrdA and FrdB were prepared as described in Material and Methods, Chapter II. Soluble and membrane fractions were prepared from pulse/chase experiments as described above. Instead of precipitating with TCA, the soluble fractions were treated with 50 µg of monospecific antibodies.

The membrane fractions were suspended in 100 µl of stop buffer and 10µl of 10% Triton X-100. After extracting on ice for 20 min with frequent vortexing the insoluble debris was removed by centrifugation at 13 000 x *g* for 10 min at 4°C. The detergent extract was then treated with 10 µg of monospecific antibodies.

The samples were incubated overnight at 4°C. The soluble fractions received 3 µg of *Staphylococcus aureus* protein A and the membrane fractions received 0.5 µg of protein A. The samples were incubated for 3 h at 4°C before the immunoprecipitates were harvested by centrifugation at 13 000 x *g* for 20 min at 4°C. The pellets were homogenized in 50 µl of

PBS and 50 µl of Laemmli solubilization buffer [21] and heated to 95°C for 2 min.

Temperature profile of protein expression from pDJL6.

In order to examine the synthesis, assembly and insertion into the membrane of the fumarate reductase subunits on a reasonable time-scale, the expression of *frd* polypeptides was conducted at reduced temperatures.

After inducing T7 RNA polymerase expression at 42°C and poisoning the *E. coli* RNA polymerase with rifampicin for 20 min at 42°C, the cells were held at 32°C for 10 min and then chilled to 5°, 10° or 15°C in a refrigerated waterbath for a further 10 min. The cells were pulse-labelled with 370 KBq of ^{35}S-methionine. 100 µl samples were taken at 0, 5,10, 20 and 30 min [the 30 min point was omitted for the 15°C chase] and pipetted directly into an equal vol of cracking buffer at 95°C and heated for 2 min. The cell extracts were separated on 22 x 15 x 0.15 cm double gradient acrylamide gels [chapter IV].The gels were fixed in 10% acetic acid, 30% methanol, dried and autoradiographed at -70°C on Kodak XAR-5 film.

^{32}P-Labelling of FrdA

E. coli HB101 alone or harbouring pFRD79 was grown overnight in LB-B$_1$ [4] supplemented with 100 µg ampicillin ml^{-1} as needed. The cells were harvested by centrifugation at 12 000 x *g* for 10 min, washed with 5 vol PBS and sedimented as described before. The cells were suspended by homogenization in GF medium [22] in which the total phosphate had been reduced to 5 mM. 740 KBq of $Na_2H^{32}PO_4$ [New England Nuclear, 135 MBq ml^{-1}] was added and the 160 ml flask was filled to the neck with

medium and sealed. The anaerobic culture was stirred slowly on a magnetic stirrer at 37°C for 36h.

The labelled cells were harvested by centrifugation at 12 000 x *g* for 10 min, washed in 200 ml PBS and sedimented. The cell paste was suspended in 5 ml 50mM Tris-HCl, pH7.5, 0.1 mg DNAse ml^{-1}, 0.1 mg RNAse ml^{-1}, 20 mM $MgCl_2$ and lysed by two passages through a French pressure cell at 110 MPa. Unbroken cells were removed by centrifugation for 10 min at 15 000 x *g* and the supernatant solution was ultracentrifuged for 60 min at 150 000 x *g* to retrieve the membrane fraction.

The sedimented crude membrane fraction was suspended in 50 µl 200 mM $NaPO_4$, pH6.8 and mixed 1:1 with Laemmli solubilization buffer [21]. After boiling for 3 min the labelled proteins were run out on a 22 x 15 x 0.15 cm 15% Laemmli gel until the tracking dye reached the bottom of the gel. The gel was fixed in 10% acetic acid, 30% methanol, dried and autoradiographed at - 70°C.

Expression of fumarate reductase for activity assays.

DLT111/pDJL6 was grown overnight at 32°C in LB-B_1 with 100 µg ampicillin and 40 µg kanamycin ml^{-1}. 3.5 ml of the overnight culture was inoculated into 50 ml LB-B_1 and was shaken 4 h at 32°C until the OD_{550}=1.0. The cells were shaken for 15 min at 42°C to induce the expression of T7 RNA polymerase. Rifampicin was added to 250 µg ml^{-1} and the cells were shaken an additional 15 min. The temperature was reduced to 32°C at zero time and 5 ml samples were withdrawn at 0, 60,120 and 180 min. The cells were sedimented by centrifugation at 12 000 x *g* for 10 min at 4°C, washed in 10 ml PBS and sedimented again. The cells were homogenized in 1 ml 25mM HEPES, pH6.8, passed through

the French pressure cell twice at 110 MPa, and unbroken cells were removed by centrifugation at 12 000 x *g* at 4°C for 10 min. The crude membrane fraction was collected by centrifugation of the French press lysate for 20 min at 105 000 x *g* at room temperature in an Airfuge [Beckman Instruments, Palo Alto, CA]. The pellets were suspended in 200 µl 25 mM HEPES, pH6.8 and assayed for fumarate reductase by the benzyl viologen method [19].

C. RESULTS

Temperature profile of expression in *E. coli* DLT111.

The behavior of the expression system was examined at below ambient temperature to determine if any intermediates in processing or assembly could be detected. A pulse/chase experiment was performed as in Materials and Methods with the final 10 min incubation before pulsing being at 5°, 10° or 15°C. After labelling for 60 sec the cells were chased with cold methionine. Samples were withdrawn at 0, 5, 10, 20 and 30 min into the chase and quenched immediately with an equal vol of cracking buffer at 95°C. The 30 min time point was omitted for the 15°C experiment.

At 5°C there was insufficient uptake of [^{35}S]methionine in the initial pulse to give adequate labelling [Fig. III.2], although there were faint bands to show that specific expression was occuring. At 10°C and at 15°C there was adequate labelling by radioactive methionine and good levels of expression of the Frd polypeptides. Note that the first time point after the addition of cold methionine [approximately 12 sec delay] showed little or no FrdA or FrdB, but FrdC and FrdD were readily apparent. Three major

bands migrating above FrdB are products of the pT7-4 plasmid and are presumed to be β-lactamase.

Densitometric scans of the 5 min lanes from the 15°C and 10°C experiments were compared with an identical experiment done for 5 min at 37°C [Fig. III.3]. The ratio of subunits expressed varied from being predominantly FrdA [FrdA:FrdB:FrdCD = 1.8:1:1] at 37°C to being predominantly FrdCD [1:1.8:4.3] at 10°C. At 15°C the subunits were expressed at equimolar ratio. There was no evidence of subunit modification at any of the temperatures, and all further experiments were done at 32°C.

Membrane insertion at 32°C in *E. coli* DLT111.

3.5 ml of cells were preincubated at 32°C before pulsing for 60 sec and chasing with cold methionine for 20 min. 0.5 ml aliquots were taken at 0, 0.5, 1.0, 2.5, 5.0, 10 and 20 min and quenched in ice-cold stop buffer. Soluble and membrane fractions were isolated and run on a double gradient gel [Fig. III.4].

At the earliest time point FrdC and FrdD were the most prominent translation products in either the membranes or the soluble fraction. By far the majority of the anchor polypeptides was already associated with the membrane fraction immediately after pulse labelling. Within one min at 32°C the membrane had obtained a steady-state level of proteins, with FrdCD still predominating. In the soluble fraction, FrdA and FrdB were apparent by 30 seconds together with the soluble portion of FrdC and FrdD. The major bands that migrate above FrdB are encoded by the parent plasmid, while those migrating just below FrdA are presumed to be proteolytic fragments of that subunit.

Immunoprecipitations of the soluble fraction with rabbit IgG directed against either FrdA or FrdB showed that FrdA is predominently precipitated alone, with small amounts of FrdB, FrdC and FrdD, while FrdB predominantly co-precipitated with FrdC and FrdD and sub-stoichiometric quantities of FrdA [Fig. III.5]. The major proteolytic species of FrdA at about 50 kDa is readily apparent, as are numerous other proteolytic bands.

Immunoprecipitations of the Triton X-100 extracts of the membrane fraction from this experiment showed that FrdB was primarily associated with FrdCD, with trace amounts of FrdA. All of the FrdA which reacted with monospecific antibodies co-precipitated with the other three polypeptides [Fig. III.5].

Membrane insertion of FrdABCD' from pDJL1 at 32°C in *E. coli* DLT111

The plasmid pDJL1 bears the *frd* operon with the Tn*5* insertion in *frdD* which was discussed in Chapter II. It expresses FrdABC and a truncated FrdD', and the altered holoenzyme can assemble in the membrane like wild-type fumarate reductase. The cytoplasm of cells bearing this altered operon contain a unique water-soluble trimer composed of FrdA, FrdB and FrdC.

E. coli DLT111 cells harbouring pGP1-2 and pDJL1 were pulsed for 60 sec and chased for 120 min.[Fig. III.6] At the earliest time all four subunits were found in both the membrane and the cytoplasm, as for wild-type enzyme, except that the anchor subunits were present in essentially equal amounts in the two compartments, rather than being primarily in the

membrane fraction. A band at about 50 kDa is identified as a proteolytic fragment of FrdA.

A similar experiment was done in which the membrane and soluble fractions were immunoprecipitated with monospecific antisera to FrdA and FrdB [Fig. III.7], to see which of the subunits in either fraction were physically associated and therefore co-precipitable. In the Triton X-100 extract of the membrane fraction anti-FrdA precipitated a complex which is largely FrdC and FrdD' with lesser amounts of FrdA and still less of FrdB. Anti-FrdB precipitated only FrdBCD', again with the anchor subunits predominating.

More interesting was the pattern of co-precipitation from the soluble fraction. Here it was seen that anti-FrdA precipitated predominantly FrdA and some FrdB and FrdC. Note that the FrdD' band is missing and in its place is one of lower molecular weight which is likely a proteolytic fragment of the truncated anchor polypeptide. Anti-FrdB co-precipitated its specific subunit along with FrdC and intact FrdD' plus trace amounts of FrdA. The 50 kDa major proteolytic product of FrdA is readily apparent, as are numerous other proteolytic bands.

Localization of the membrane anchor subunits at 32°C in *E. coli* DLT111

Fig. III.8 shows a 20 min pulse/chase using pDJL22, which encodes only the fumarate reductase anchor subunits, FrdC and FrdD. At all times the anchor proteins were found primarily in the crude membrane fraction, with trace amounts of each detected in the soluble fraction.

Labelling FrdA with $^{32}PO_4$ in *E. coli* HB101.

Two major bands were apparent [Fig. III.9], one which migrated just above the 68 kDa standard and another which migrated just behind the dye front. The former is identified as FrdA, as it is amplified in a strain bearing a *frd* plasmid [compare Fig. III.9, lanes 1 and 2], labelled at the two phosphate positions on the covalently attached FAD at His^{44}. The identity of the other band is not known.

Expression of fumarate reductase activity in *E. coli* DLT111

The production of native, active fumarate reductase from the *ϕ10* promoter was examined in rich medium at 32°C. Table III.2 indicates that enzyme was being expressed in three hours to levels comparable to those found after overnight anaerobic growth in wild-type *E. coli* [19].

D. DISCUSSION

The results from the temperature profile of expression show that no detectable post-translational processing is occuring at any of the temperatures tried. In particular, FrdA expressed from the *ϕ10* promoter migrates with the same relative mobility as FrdA of fumarate reductase purified from anaerobically grown cells. It is known that FrdA is covalently modified at His^{44} by attachment of FAD through an 8α-[N3]-histidyl linkage [9]. This cofactor can be labelled with ^{32}P at either or both of the phosphate groups it contains, and the labelled FrdA can be detected in anaerobically grown cells [Fig. III.9, lane 2]. When attempts were made to label FAD cofactor in FrdA expressed by the *ϕ10* promoter under aerobic conditions no labelled polypeptides were detected.

Frd expression can be induced in an S-30 extract by the addition of alanine [chapter IV]. If $^{32}PO_4$ or ^{14}C-adenine is added to the extract prior to induction, no label is seen in the 68 kDa region of the SDS-PAGE gels [data not shown]. From this it is inferred that the covalent modification of FrdA is by fully synthesized FAD and not by flavin mononucleotide or riboflavin precursors. This is also seen in 6-hydroxy-D-nicotine oxidase [23]. It is also possible that addition of FAD is dependent on anaerobiosis. *Bacillus subtilis* succinate dehydrogenase can be expressed in *E. coli* but the FAD moiety is not attached [24]. This argues for an enzyme mediated modification. In the 6-hydroxy-D-nicotine oxidase system the attachment of FAD is an energy dependent step [25] which can occur post-translationally or co-translationally [23]. That fumarate reductase does have its FAD in this expression system is demonstrated by the increase in specific activity over a period of 3 h shown in Table III.2.

Also apparent from the temperature profiles is that the ratio of Frd subunits produced is dependent on both temperature and time. This observation of differential expression with temperature could be explained by the effect of secondary and tertiary structure in the mRNA on translation and is what led to the analysis of the putative mRNA secondary structure discussed in Chapter IV.

Figure III.3 shows that when all four fumarate reductase subunits are expressed the membrane anchor polypeptides, FrdC and FrdD associate immediately and preferentially with the membrane fraction. This is hardly surprizing considering their highly hydrophobic nature [10]. There is an apparent lag in the onset of synthesis of the two catalytic subunits compared with the membrane subunits, which may be an artifact of the system whereby smaller polypeptides are synthesised more quickly than large

polypeptides [11]. Immunoprecipitations of the soluble fraction with anti-FrdA antibodies indicated that most of the FrdA in the cytoplasm is not associated with the other Frd polypeptides. Most of the FrdB found in the soluble fraction is already associated with the membrane anchors, even in the absence of the lipid bilayer. The Triton X-100 extracts of the membrane shows FrdB is again bound to the membrane anchors, with little or no FrdA, while all of the FrdA bound to the membrane is in association with the other three subunits.

Taken together, these data indicate an assembly pathway in which the membrane anchors assemble first in the membrane and are capped with FrdB. FrdA with its covalently attached FAD then associates with the membrane-bound trimer. If the membrane assembly pathway is blocked by the removal of the genes specifying the anchor domain then assembly of FrdA and FrdB into a functional catalytic domain can still occur [26].

Figure III.6 shows that when FrdD is truncated by insertion of Tn*5* into the *frdD* cistron the association of the membrane anchors with the cytoplasmic membrane is considerably reduced as compared to wild-type enzyme. The anchors can associate first *in situ* with either FrdA or FrdB with similar affinity, although the percentage of holoenzyme is low [Fig. III.10].

The most interesting result is from the precipitation of Frd subunits from the soluble fraction. Here FrdB is largely associated with FrdC and FrdD' while FrdA is primarily associated with FrdC and a polypeptide of about 10 kDa relative mobility which is likely a proteolytic fragment of the already truncated FrdD'. This indicates that while FrdD' is stable in the membrane whether associated with FrdA or FrdB, in the cytoplasm only

FrdB can protect FrdD' from proteolytic degradation. FrdC seems to be stable under all conditions.

This gives rise to the suggestion that the soluble trimeric enzyme found in strains harbouring pFRD79::Tn*5*-299 discussed in Chapter II arose in the cytoplasm from an assembly pathway in which FrdA first associated with FrdCD' and then FrdD' was proteolysed before FrdB bound to complete the trimer, whereas the membrane bound enzyme is derived from a situation where FrdB bound to the anchors first, thereby stabilizing FrdD' against proteolysis, with FrdA binding later to complete the tetramer.

This compares with the assembly of the F_1F_0 ATP synthase *in vivo*. In the absence of the F_0 subunits in the membrane the five subunits of the F_1 domain still assemble into an active, co-immunoprecipitable complex [27]. Both subunits of the Frd anchor domain are required to allow binding of the catalytic head [26,19]. Loss of the FrdD polypeptide prevents assembly of FrdC to FrdAB [14]. A truncated FrdD allows the assembly of all four subunits at reduced efficiency. The enzyme can then associate with the membrane or the FrdD subunit can be proteolysed away, leaving a trimeric enzyme in the cytoplasm. Thus, FrdD allows for the stable binding of FrdC, which cannot bind to FrdAB by itself [14]. In the ATP synthase the three membrane anchor subunits assemble spontaneously into the membrane. Either a or b alone but not c is capable of binding F_1 to the membrane [28].

It should be noted that the time for assembly seen in the T7 system can be as much as 2 h, and that it was not possible to chase the assembly to completion. *In vivo* one would expect that the time for assembly should be on the order of minutes, and that all of the subunits synthesised would be

assembled into holoenzyme. It may be that the excess of anchor subunits compared to catalytic subunits affects the assembly pathway adversely, or that one or more of the prosthetic groups [FAD or FeS] is not being added, with adverse effects on assembly of the tetramer.

Table III.1 Bacterial Strains and Plasmids

Strains	Phenotype	Selection marker	Reference
HB 101	F$^-$, *gal , lac, leu, pro, thi* $r_B^-m_B^-$, *recA, rpsL*	Sm^r	Lab collection
RG 51	F$^-$, *hsdR, supE, supF, lacY, galK, galT, met, trp,* λ^-, *ΔuncB-uncD, srl*::Tn*10 recA*	Tc^r	R.P. Gunsalus
K38	HfrC, λ^-		S. Tabor
DLT 111	HfrC, λ, *srl*::Tn*10 recA*	Tc^r	This work
Plasmids			
pGP1-2	*c*I857, P_L*gene1*	Km^r	S. Tabor
pFRD79	*frdABCD*	Ap^r	This lab.
pFRD708	*frdABCD*	Cm^r	This lab.
pFRD79::Tn*5*-299	*frdABCD::Tn5*	Ap^r, Km^r	This author
pDJL1	*ϕ10 frdABCD'*	Ap^r	This work
pDJL6	*ϕ10 frdABCD*	Ap^r	This work
pDJL22	*ϕ10 frdCD*	Ap^r	This work

Table III.2. Expression of fumarate reductase from the *ϕ10* promoter.

DLT111/pDJL6 was grown in LB-B_1 and expression was induced by temperature shift. After cooling to 32°C cells were sampled and lysed in the French pressure cell. Crude membranes were isolated and assayed by the benzyl viologen method. One unit represents the oxidation of 1 μmol of benzyl viologen per min.

hours	total units	specific activity
0	1.25	2.5
1	5.00	5.6
2	5.70	6.4
3	6.30	7.0

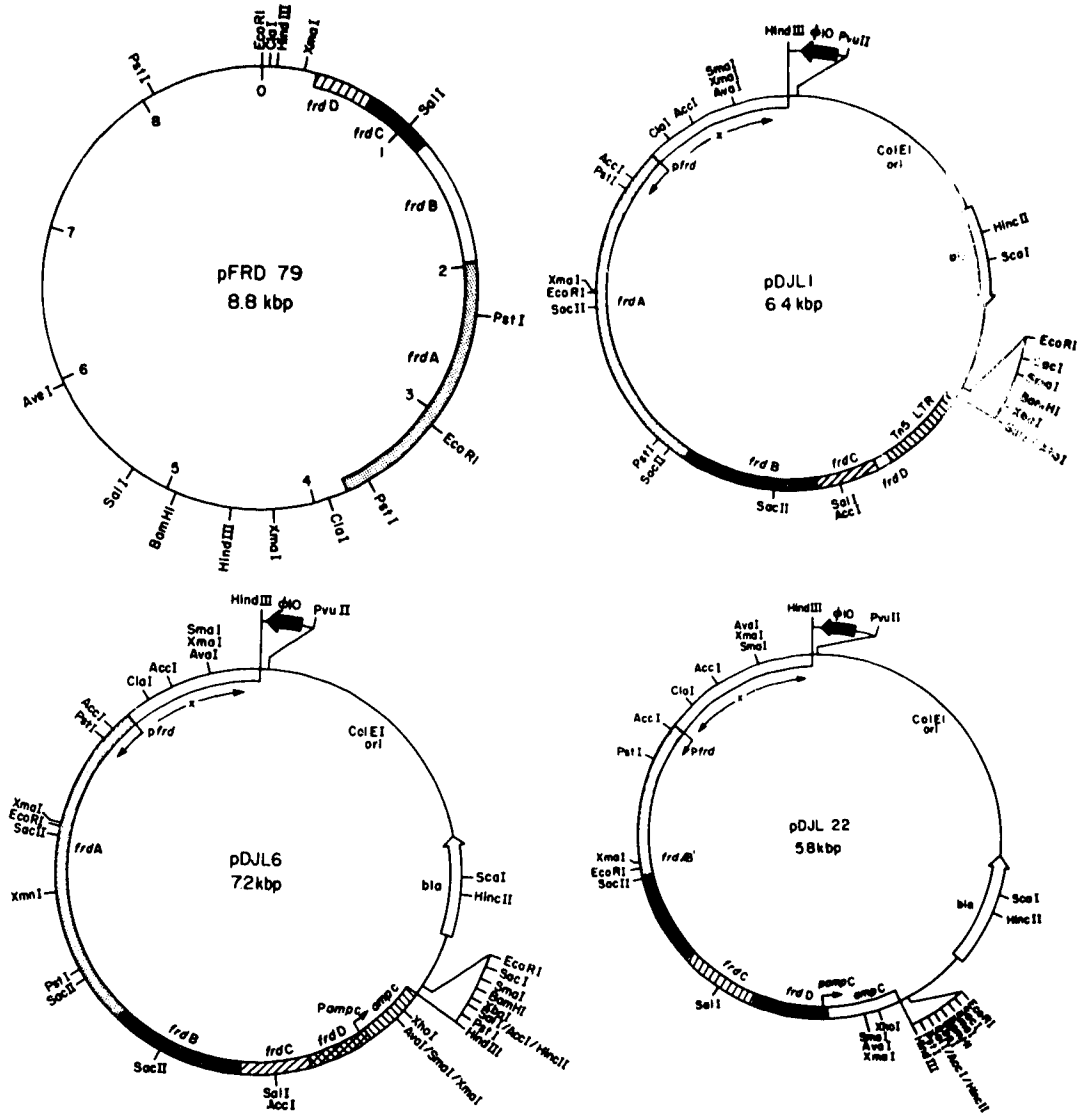

Figure III.1. Maps of pDJL plasmids. Plasmids were constructed and mapped as described in Materials and Methods. The thin line marks the vector sequences. The wide open or shaded line marks the *frd* sequences. Tn5 LTR marks the Tn*5* sequences. Bla marks the β-lactamase gene.

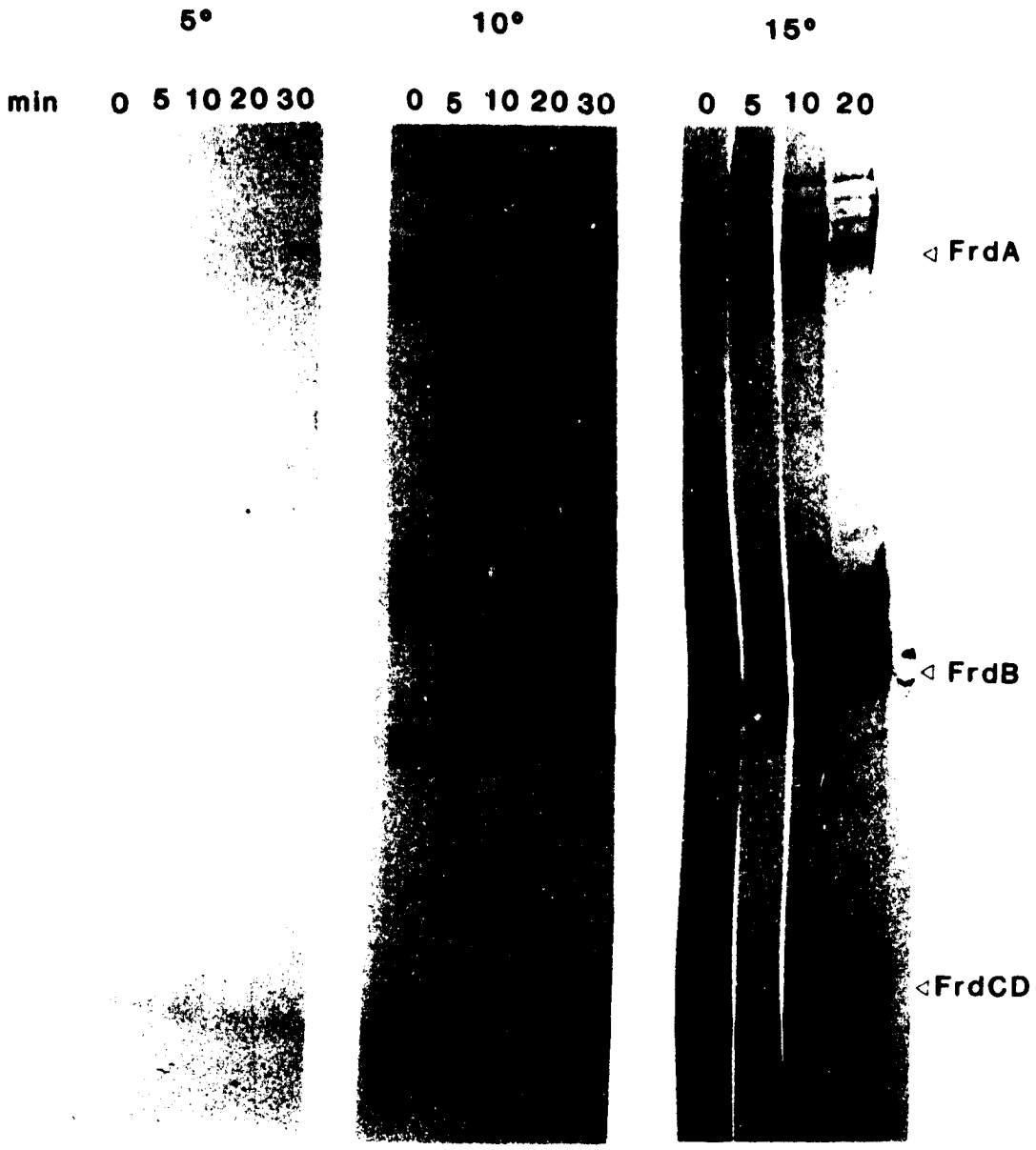

Figure III.2. Temperature profile of protein expression in *E. coli* K38. Cells were pulse labelled with [^{35}S]methionine for one min at the indicated temperatures and chased with 0.1% cold methionine. Aliquots were withdrawn at the indicated times and quenched in cracking buffer at 95°C. Proteins were separated on double gradient gels. Markers show the position of the subunits of purified fumarate reductase.

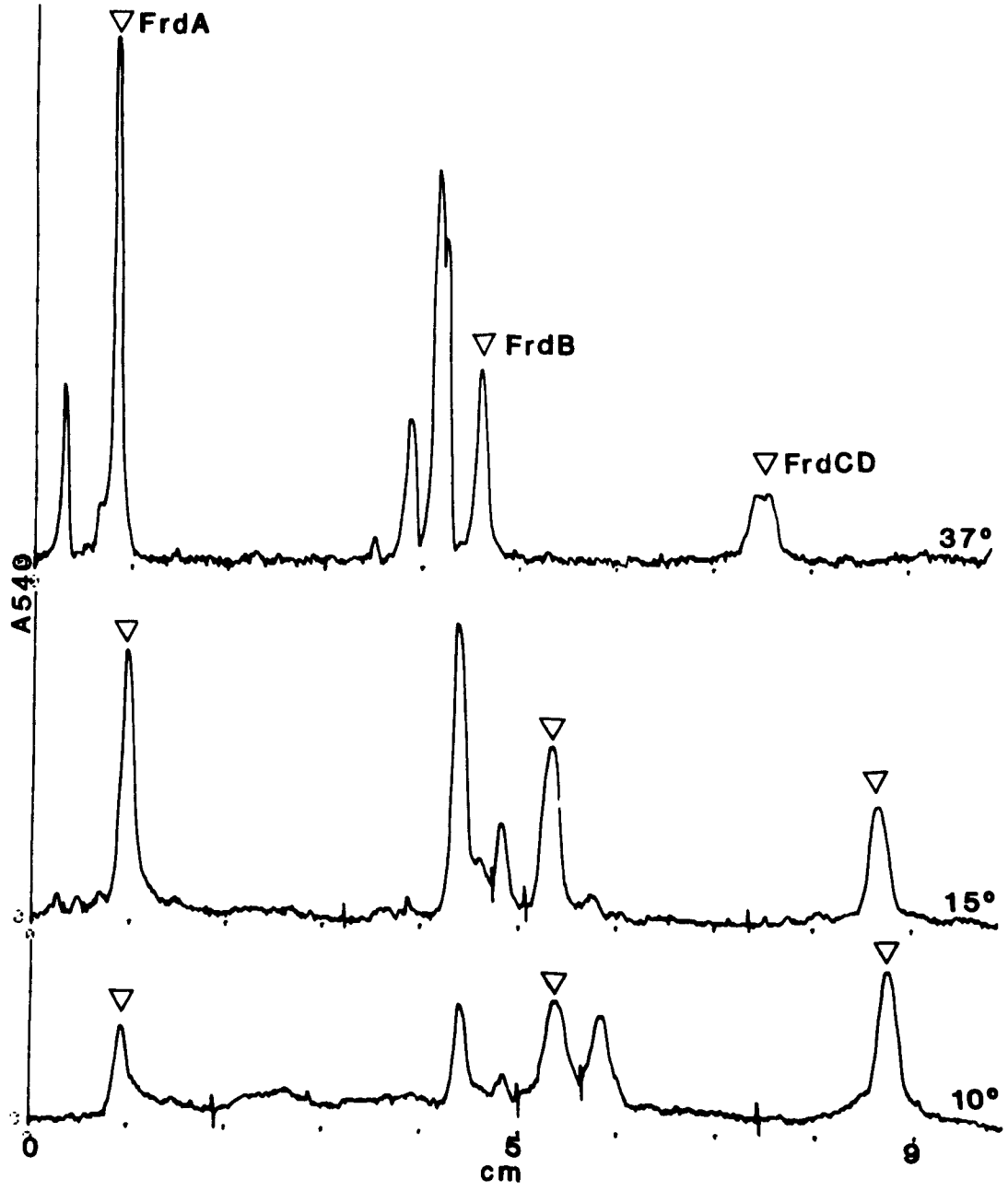

Figure III.3. Subunit ratios at different temperatures. The five minute lanes of the 10°C and 15°C experiments in Figure III.2 and an autoradiograph of an identical experiment performed at 37°C for five min are compared. The positions of the fumarate reductase subunits are marked [▽].

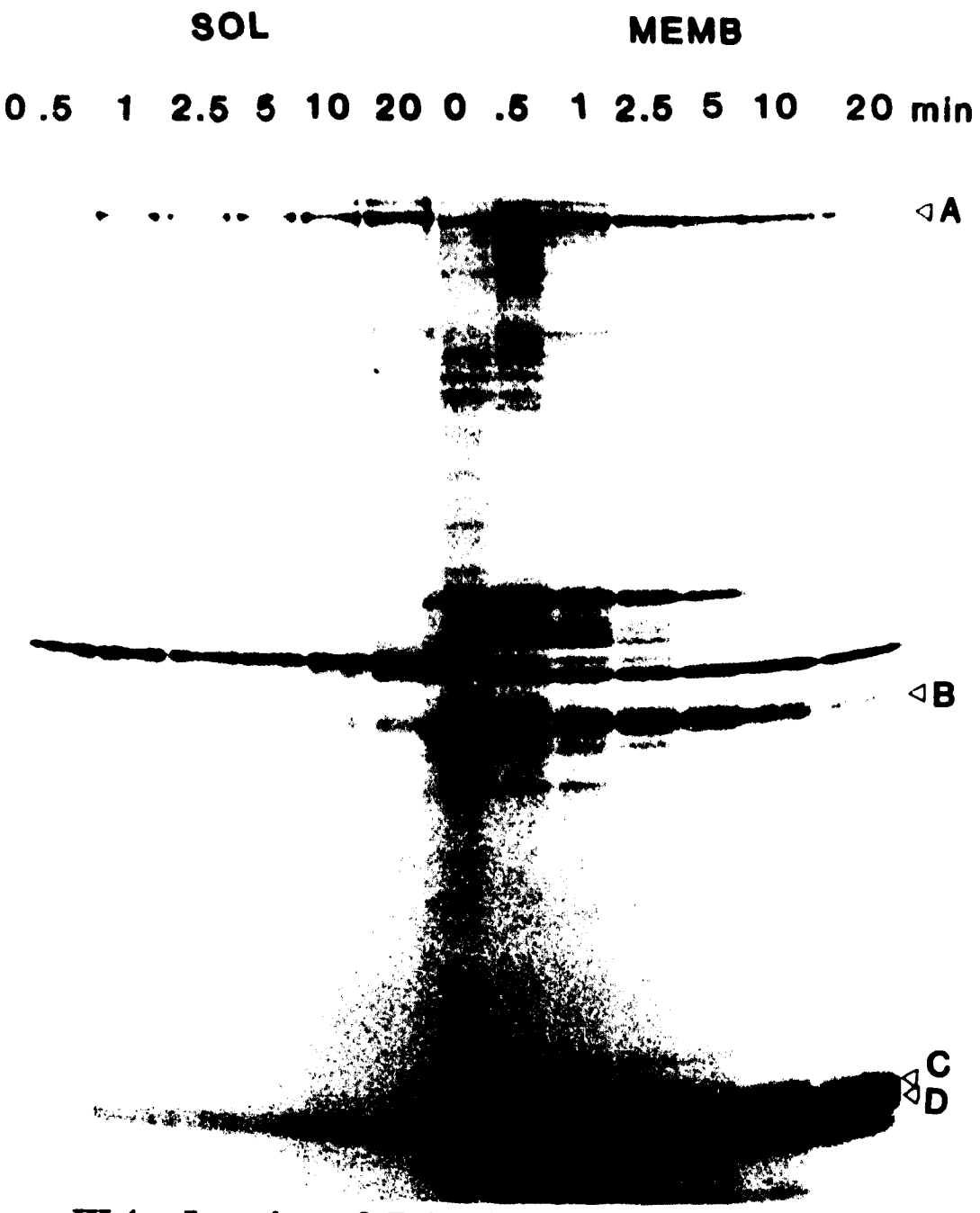

Figure III.4. Insertion of Frd subunits into the membrane at 32°C. DLT111/pDJL6 was pulse labelled with [^{35}S]methionine for one min and chased with 0.1% cold methionine. Aliquots were withdrawn at the indicated times and quenched in ice cold stop buffer. The cells were lysed in a French pressure cell and the soluble fraction and membranes were separated by centrifugation. The soluble fraction was precipitated in 10% TCA. Soluble and membrane fractions were suspended in solubilization buffer. Electrophoresis was on a double gradient gel. Markers show the position of the subunits of purified fumarate reductase.

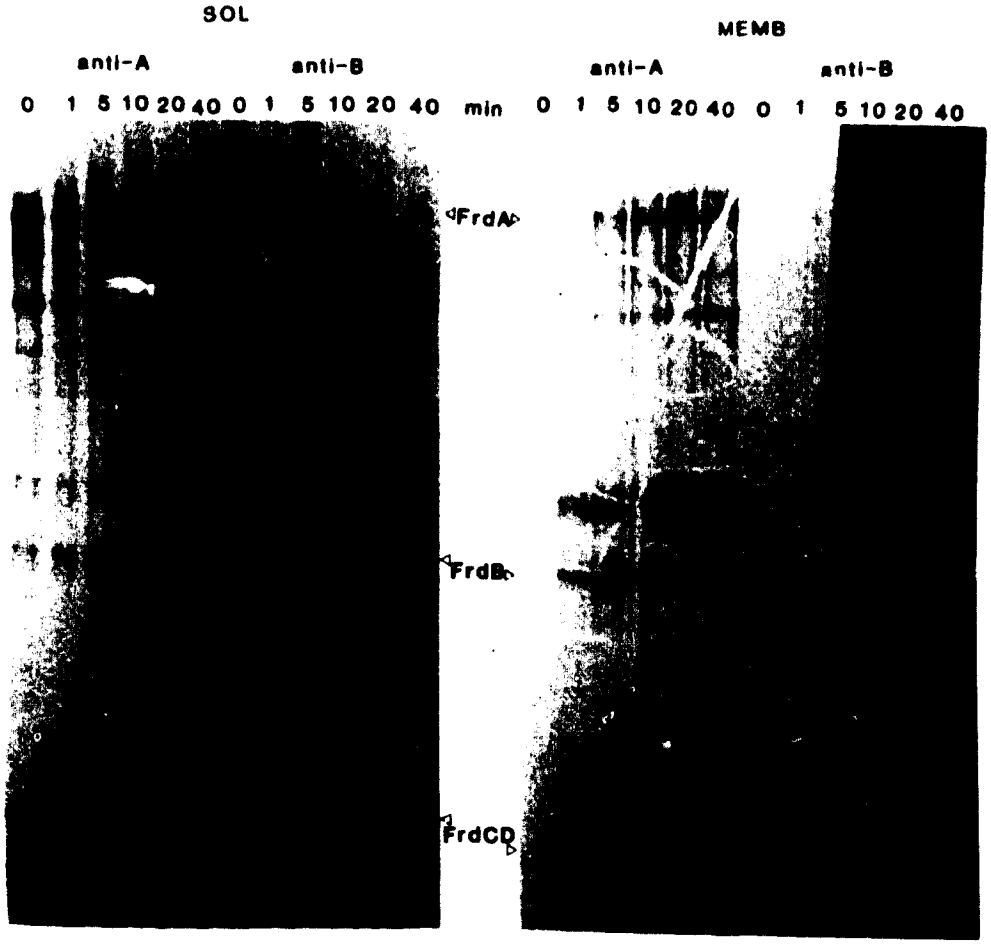

Figure III.5. Subunit assembly at 32°C. DLT111/pDJL6 was pulse labelled with [^{35}S]methionine for one min and chased with 0.1% cold methionine. Aliquots were withdrawn at the indicated times and quenched in ice cold stop buffer. The cells were lysed in a French pressure cell and the soluble fraction and membranes were separated by centrifugation. The membranes were solubilized in PBS, 1% Triton X-100. Duplicate samples were immunoprecipitated with anti-FrdA or anti-FrdB serum. After suspension in sample buffer the proteins were separated on double gradient gels. Markers show the position of the subunits of purified fumarate reductase.

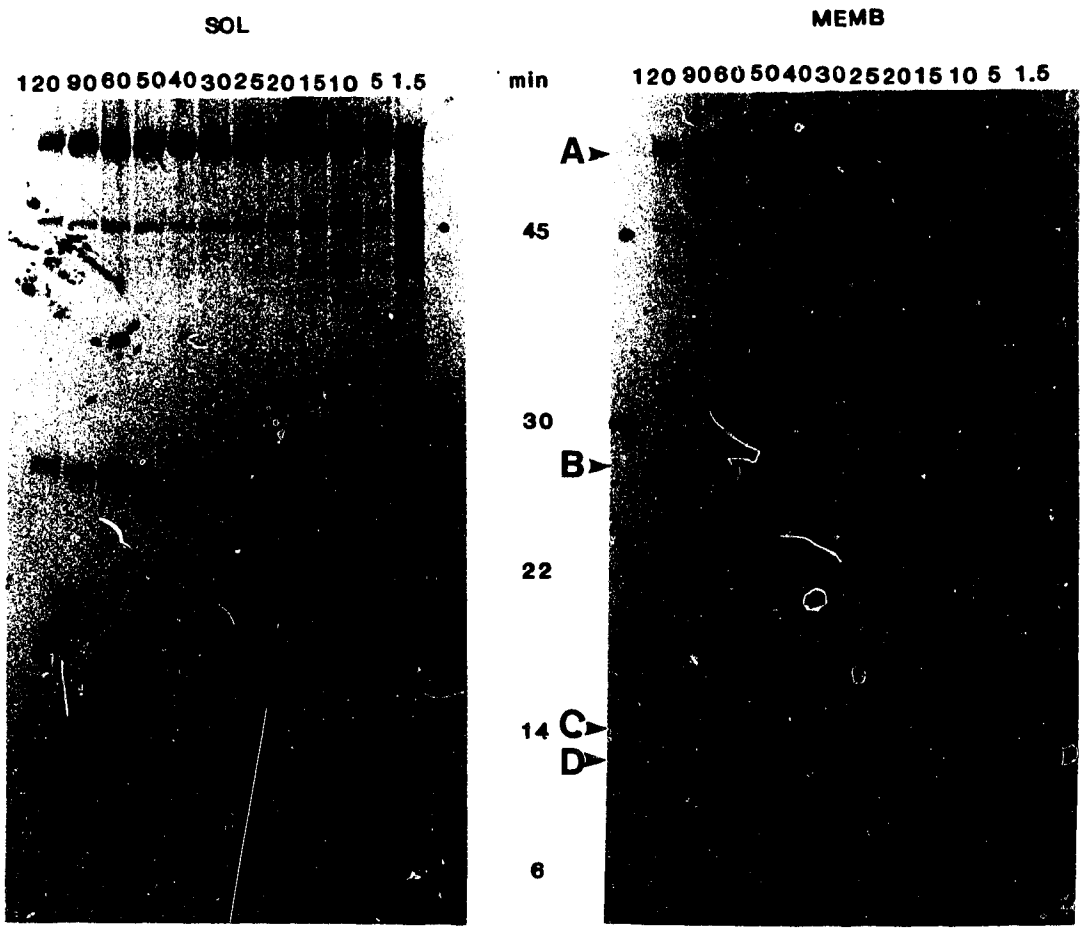

Figure III.6. Membrane insertion of altered fumarate reductase at 32°C. DLT111/pDJL1 was pulse labelled with [^{35}S]methionine for one min and chased with 0.1% cold methionine. Aliquots were withdrawn at the indicated times and quenched in ice cold stop buffer. The cells were lysed in a French pressure cell and the soluble fraction and membranes were separated by centrifugation. The membranes were solubilised in sample buffer. The soluble fraction was precipitated in 10% TCA and suspended in sample buffer. The proteins were separated on double gradient gels. Time reads from right to left. Molecular weight markers are chick ovalbumin [45 kDa], carbonic anhydrase [30 kDa], trypsin inhibitor [22 kDa], lysozyme [14 kDa] and insulin [6 kDa]. Letters mark position of Frd subunits

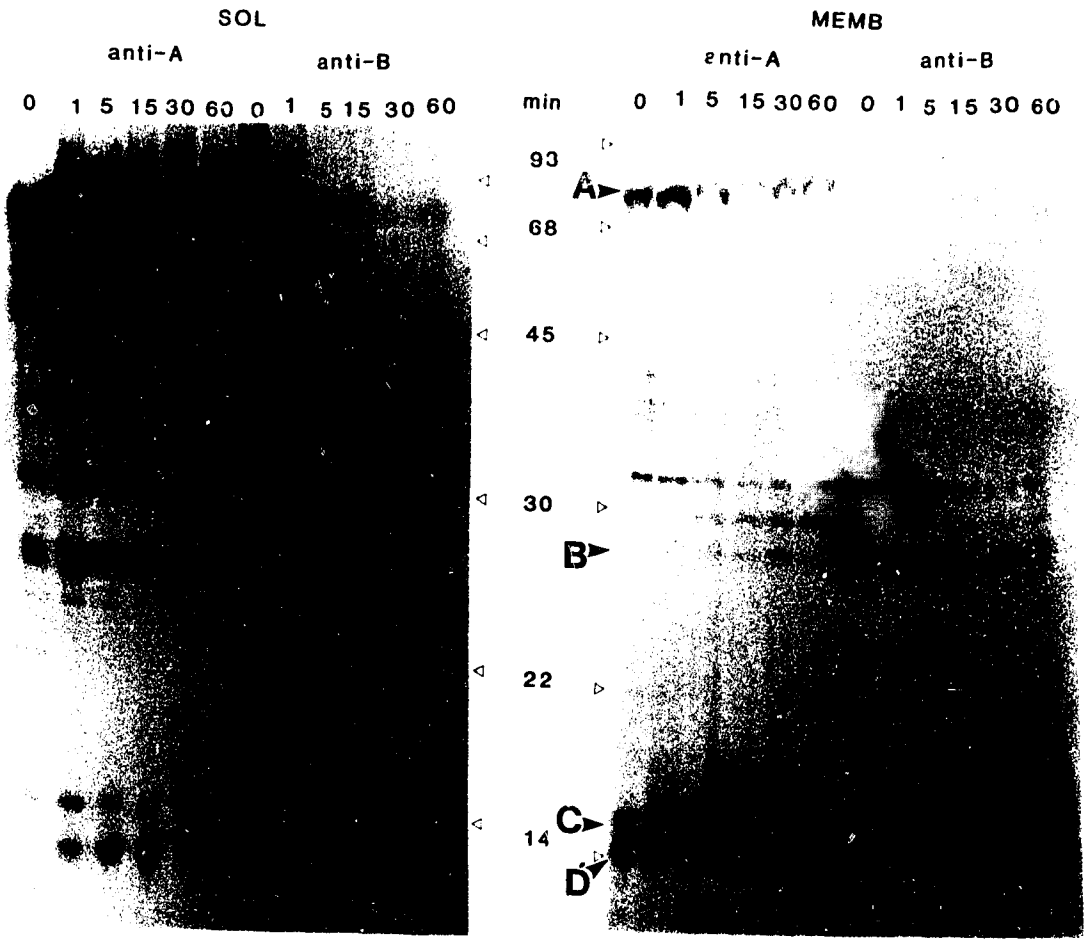

Figure III.7. Subunit assembly of altered fumarate reductase at 32°C. DLT111/pDJL1 was pulse labelled with [^{35}S]methionine for one min and chased with 0.1% cold methionine. Aliquots were withdrawn at the indicated times and quenched in ice cold stop buffer. The cells were lysed in a French pressure cell and the soluble fraction and membranes were separated by centrifugation. The membranes were solubilized in PBS, 1% Triton X-100. Duplicate samples were immunoprecipitated with anti-FrdA or anti-FrdB serum. After suspension in sample buffer, proteins were separated on a double gradient gel. Molecular weight markers are phosphorylase *b* [93 kDa], bovine serum albumin [68 kDa], chick ovalbumin [45 kDa], carbonic anhydrase [30 kDa], trypsin inhibitor [22 kDa], and lysozyme [14 kDa]. Letters mark locations of Frd subunits.

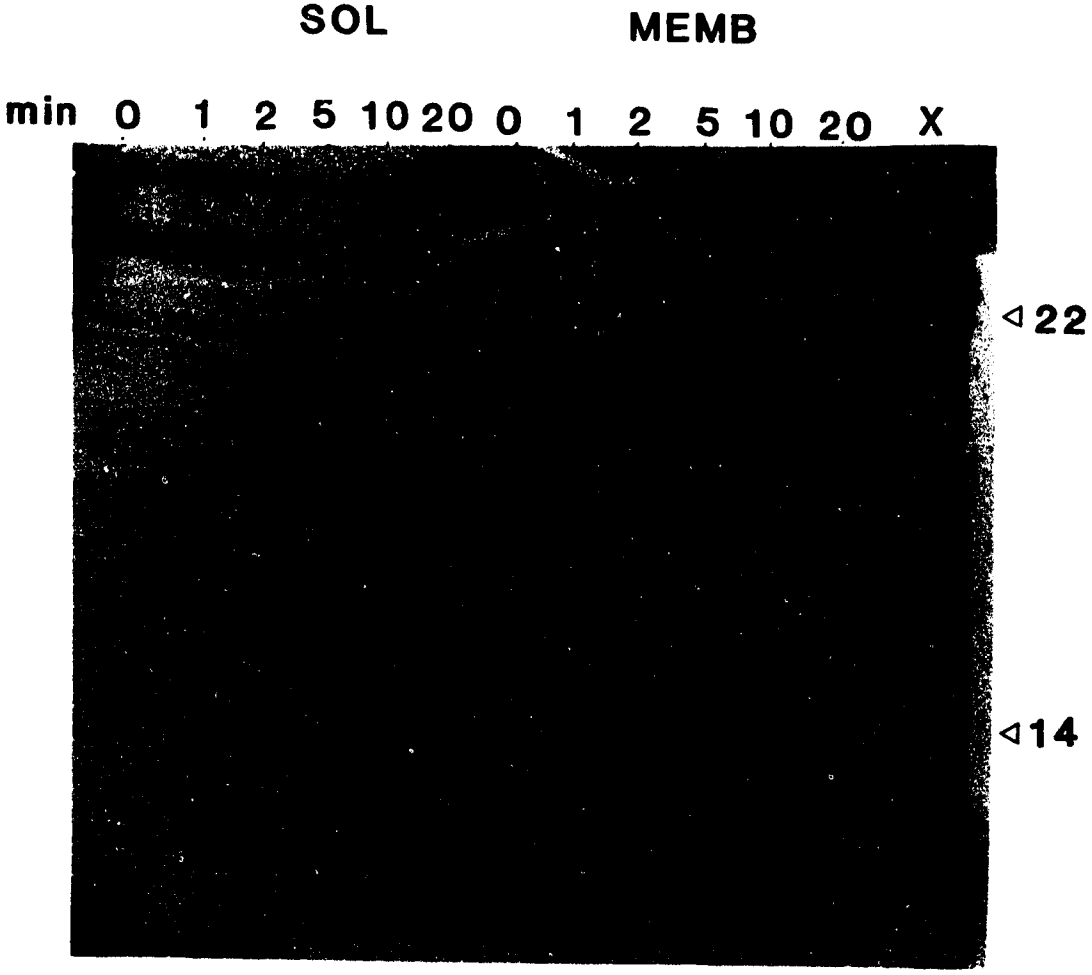

Figure III.8. Localization of membrane anchor subunits at 32°C. DLT111/pDJL22 was pulse labelled with [^{35}S]methionine for one min and chased with 0.1% cold methionine. Aliquots were withdrawn at the indicated times and quenched in ice cold stop buffer. The cells were lysed in a French pressure cell and the soluble fraction and membranes were separated by centrifugation. The membranes were solubilised in sample buffer. The soluble fraction was precipitated in 10% TCA and suspended in sample buffer. Proteins were separated on a double gradient gel. X marks cells expressed without rifampicin. Molecular weight markers are trypsin inhibitor [22kDa] and lysozyme [14 kDa].

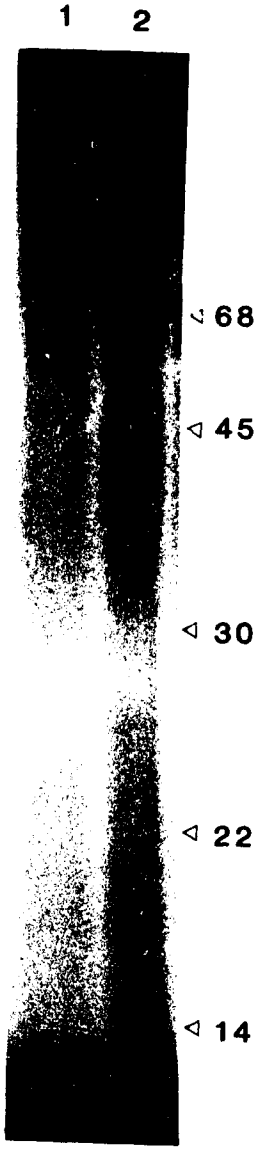

Figure III.9. Labelling the FAD of FrdA with ^{32}P. HB101 alone [lane 1] or harbouring pFRD79 [lane 2] was grown overnight anaerobically as described in Materials and Methods in GF medium containing 46.2 KBq ml^{-1} $^{32}PO_4$. The cells were harvested and French pressed and the membranes were recovered by centrifugation and suspended in sample buffer. Electrophoresis was on a 15% Laemmli gel. Molecular weight markers are bovine serum albumin [68 kDa], chick ovalbumin [45 kDa], carbonic anhydrase [30 kDa], trypsin inhibitor [22 kDa], and lysozyme [14 kDa].

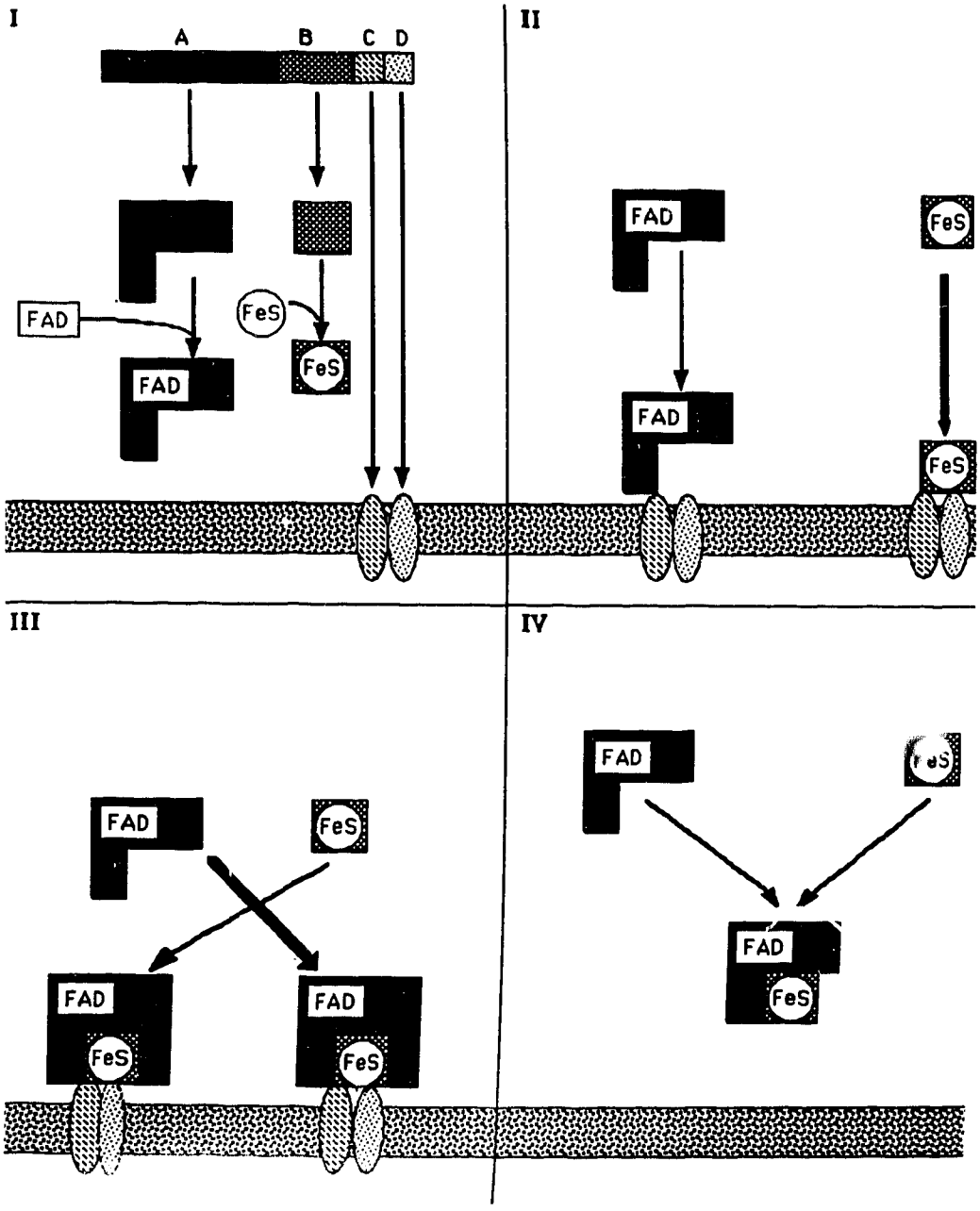

Figure III.10. Proposed assembly pathway for fumarate reductase holoenzyme.

Bibliography

1. Tabor, S. & Richardson, C. C. 1985. Proc. Natl. Acad. Sci. USA. **82**:1074-1078
2. Russel, M. & Model, P. 1985. J. Bacteriol. **159**: 1035-1039
3. Birnboim, H. C. & Doly, J. 1979. Nucl. Acids Res. **7**:1513-1523
4. Miller, J. H. [ed.]. 1972. Experiments in Molecular Genetics. Cold Spring Harbor, N.Y. Cold Spring Harbor Laboratory
5. Latour, D. J. & Weiner, J. H. 1988. Nucl. Acids Res., in press
6. Maniatis,T., Fritsch, E. F., & Sambrook, J. 1982. Molecular Cloning: a Laboratory Manual. Cold Spring Harbor N.Y. Cold Spring Harbor Laboratory
7. Condon, C. & Weiner, J. H. 1988. Molec. Microbiol. **2**:43-52
9. Weiner, J. H. & Dickie, P. 1979. J. Biol. Chem. **254**:8590-8593
10. Weiner, J. H., Lemire, B. D., Elmes, M. L., Bradley, R. B. & Scraba, D. G. 1984. J. Bacteriol. **158**:590-596
11. Dnitzes .1961. Proc. Natl. Acad. Sci. USA. **47**:247
12. Singh, A. P. & Bragg, P. D. 1975. Biochim. Biophys. Acta.**396**:229-241
13. Haddock, B. A. & Jones, C. W. 1977. Bacteriol. Rev. **41**:47-99
14. Cole, S.T., Condon, C., Lemire, B. D. & Weiner, J. H. 1985. Biochim. Biophys. Acta. **811**:381-403
15. Weiner, J. H., Lemire, B. D., Elmes, M. L., Bradley, R. B. & Scraba, D. G. 1984. J. Bacteriol. **158**:590-596
16. Dickie, P. & Weiner, J. H. 1979. Can. J. Biochem. **57**:813-821
17. Cammack, R., Patil, D. S. & Weiner, J. H. 1986. Biochim. Biophys. Acta. **870**:538-544

18. Lemire, B. D., Robinson, J. J. & Weiner, J. H. 1982. J. Bacteriol. **152**:1126-1131
19. Latour, D. J. & Weiner, J. H. 1987. J. Gen. Microbiol. **133**:597-607
20. Mandel, M. & Higa, A. 1970. J. Molec. Biol. **53**:159-162
21. Laemmli, U. K. 1970. Nature **277**:680-685
22. Spencer, M. E. & Guest, J. R. 1974. J. Bacteriol. **117**:954-959
23. Hamm, H.-H. & Decker, K. 1978. Eur. J. Biochem. **92**:449-454
24. Hederstedt, L., Bergman, T. & Jörnval, H. 1987. FEBS Lett. **213**:385-390
25. Brandsch, R. & Bichler, V. 1987. FEBS Lett. **224**:121-124
26. Lemire, B. D., Robinson, J. J., Bradley, R. D., Scraba, D. G. & Weiner, J. H. 1983. J. Bacteriol. **155**:391-397
27. Klionsky, D. J. & Simoni, R. D. 1985. J. Biol. Chem. **260**:11200-11206
28. Friedl, P., Hoppe, J., Gunsalus, R. P., Michelson, O., von Meyenburg, K. & Schairer, H. U. 1983. EMBO J. **2**:99-103.

IV. REGULATION OF *IN VITRO* EXPRESSION OF THE *ESCHERICHIA COLI FRD* OPERON: ALANINE AND FNR REPRESENT POSITIVE AND NEGATIVE CONTROL ELEMENTS.[1]

A. INTRODUCTION

Escherichia coli can use a variety of organic compounds as terminal electron acceptor when grown anaerobically. The choice of electron acceptor is based on its reducing potential, nitrate being preferred over fumarate, dimethylsulfoxide or trimethylamine-*N*-oxide [1,2].

The switching between electron acceptors also requires a switch between terminal electron transfer proteins, from nitrate reductase to fumarate reductase, dimethylsulfoxide reductase or trimethylamine-*N*-oxide reductase. This process is controlled at the gene level by a complex repertoire of regulatory factors. At least four regulators are known to be involved in the induction of the fumarate reductase operon; Fnr [1,3,4,5], a pleiotropic affector of all the terminal reductases, NarL [6], which activates expression of nitrate reductase and suppresses production of fumarate reductase, fumarate [1,2] and cyclicAMP [4,7], both of which can stimulate the expression of fumarate reductase under anaerobic conditions.

The control of operon expression can take several forms. The *trp* operon is negatively controlled by a regulatory protein which prevents initiation of transcription when it binds tryptophan. There is an additional

[1]A version of this chapter has been accepted for publication: Latour, D. & Weiner, J. H. 1988. Nucl. Acids Res., in press.

level of control; translationally-coupled transcription termination, or attenuation [8,9,10], which occurs in several amino acid biosynthetic operons [*trp, ilv, thr, leu, his, phe*].

Immediately 5' to the start of the *trp* operon there is a short stretch of open reading frame coding for a leader polypeptide which contains several Trp codons. This region also forms a set of mutually exclusive hairpin loops in the mRNA, one of which is a Rho-independent terminator. If there are low levels of the appropriate charged tRNAs, the ribosome translating the leader polypeptide will stall at the Trp codons. This leads to continued transcription of the operon. On the other hand, if tRNAs for the amino acid are fully charged, the ribosome will read through the first set of hairpin loops, allowing the alternate loop to form and act as a transcription terminator.

Fnr has been reported to be a positive regulator of *frd* expression [1,3,4,5]. We report that Fnr can function as a repressor of transcription in an aerobic *in vitro* system, probably by mediating a Rho-like termination event, and that the amino acid Ala can function as a positive inducer of the operon.

B. MATERIALS AND METHODS

Plasmids

pDJL6 was constructed by cloning the 4.9 kilobasepair [kbp] *Hin*dIII fragment of pFRD79 containing *frd* [11] into the *Hin*dIII site of pT7-4 [12]. The recombinant plasmid retains the *frd* promoter and 650 bp of 5' sequence. pfnr2 [13] was the kind gift of R. P. Gunsalus.

mRNA secondary structure analysis

The mRNA sequence was deduced from the DNA sequence [14,15,16] and the reported transcription start site [17]. This was analysed for secondary structure by the method of Queen and Korn [18]. Hairpin loop stabilization energies were calculated according to Tinoco *et al* [19]. Basepair [bp] +1 of the DNA sequence is the first A of the *Hin*dIII site [14], while nucleotide [nt] +1 of the mRNA is the first A of the transcript [17].

In vitro protein synthesis

An *in vitro* prokaryotic transcription/translation kit based on an *Escherichia coli* S-30 extract was purchased from NEN Du Pont and used according to the manufacturer's instructions. Plasmids pFRD79 and pfnr2 were added to the final amounts shown in the Tables. Gly or Ala was added to 10 mg ml^{-1} final concentration. 518 kBq of [^{35}S]methionine [Amersham; 41.8 TBq $mmol^{-1}$, or NEN Du Pont; 41.55 TBq $mmol^{-1}$] was added to each 20 µl reaction mixture and incubated aerobically for 1 h at 37°C. Reactions were quenched by the addition of 20 µl sample buffer [60 mM Tris/HCl pH6.8, 2% SDS, 1% 2-mercaptoethanol, 10% glycerol, 0.01% bromophenol blue] and heating to 95°C for 3 min.

Proteins were separated by SDS-polyacrylamide gel electrophoresis in a Laemmli system [20] modified to improve the resolution of small molecular weight differences. Slab gels [19.5 x 15 x 0.15 cm] were cast as linear gradients of 12-17% acrylamide, 0.16-0.91% bis-acrylamide such that there was an increasing degree of cross-linking down the gel. A 2.5 cm 6% acrylamide, 0.08% bis-acrylamide stacking gel was used. Gels were fixed, dried and exposed on Kodak X-Omat AR-5 film at -70°C. The

autoradiographs were scanned on a Chromoscan 3 densitometer [Joyce Loebl, Gateshead, England].

In vitro mRNA synthesis

mRNA analyses were carried out as for protein synthesis except that 1/8 volume of cold methionine [supplied with kit] was added to each reaction. [5,6-^{3}H]UTP [NEN Du Pont; 1.48 TBq mmol^{-1}] was evaporated to dryness under N_2 and redissolved in H_2O to 370 kBq µl^{-1}. 20 µl reaction mixtures were pre-incubated aerobically for 25 min at 37°C and then pulsed for 15 sec with 370 kBq [^{3}H]UTP. Reactions were quenched by the addition of 1.0 ml ice-cold 5% TCA, 0.1M $Na_2P_2O_7$. After incubating 30 min on ice, the labelled RNA was collected on GF/C filters [Whatman; presoaked in 5% TCA, 0.1M $Na_2P_2O_7$], washed thrice with 5.0 ml 1% TCA, 0.02M $Na_2P_2O_7$, once with 5.0 ml 95% ethanol and dried for 2 h at 80°C under vacuum.

10 ml of Aquasol [NEN Du Pont] was added to each filter and they were counted in triplicate in the tritium window to a standard deviation of 2% in an LSC-7800 [Beckman Instruments, Palo Alto, CA]. A standard quench curve was prepared using Beckman [^{3}H]toluene quench standards.

C. RESULTS

mRNA secondary structure

The predicted mRNA sequence downstream of the transcriptional start site at bp 688 [17] of the 4.9 kbp *Hin*dIII fragment carrying the *frd* genes [14] was searched for regions containing imperfect inverse repeats with a minimum stem length of 6 bp and a maximum loop size of 30 nt.

The six bp stem was chosen as the minimum to give a negative stabilization energy [ΔG_{conf}] [AUAUAU = -9.0 kcal mol^{-1} plus a minimum loop of three bp = +8 kcal mol^{-1}], while the maximum loop size was chosen such that both limbs of a six bp stem would be transcribed before the ribosome reached the 5' limb [8, 3, 9]. The ribosome binding sites for the four cistrons were also examined [21,22].

It is a reasonable assumption that control regions in mRNA should contain structures which are significantly different in form or stability from non-controlling structures within the total sequence. The *Hin*dIII fragment contained 374 potential hairpin loops whose mean ΔG_{conf} plus or minus the standard error was determined to be -5.59±0.62 kcal mol^{-1}. The standard deviation of the values was 12.01. Only 14 of the potential hairpin structures had negative ΔG_{conf} values greater than one SD away from the mean, and these are mapped in Figure IV.1 along with the other features located.

Two of the 14 sequences could form mutually exclusive, overlapping hairpin loops and were located at nt 129 to 170 and nt 144 to 202 of the transcript. They had ΔG_{conf} values of -17.4 and -22.0 kcal mol^{-1}, respectively [Fig. IV.2A, B]. These loops contained a fifteenth loop as an imbedded six bp perfect inverted repeat at nt 138 to170 which could form its own hairpin of -15.4 kcal mol^{-1} [Fig. IV.2C]. This region of *frdA* encodes a stretch near the N-terminus of the FrdA subunit which is enriched in Ala [Fig. IV.2D]. These structures and the Ala-rich region were not found in the corresponding sequence of *E. coli sdhA* [23].

An additonal eight of the hairpin structures were also located within *frdA* [Fig. IV.1] at nt 220 to 255, 444 to 483, 790 to 837, 794 to 860, 1164 to 1237,1619 to 1696, 1668 to 1705 and 1812 to 1849 with ΔG_{conf} values

of -17.6,-24.6,-24.8,-26.8,-20.2,-33.6,-19.8 and -17.6 kcal mol^{-1}, respectively. Two of the loops were found within *frdB*, at nt 2039 to 2070 and nt 2474 to 2531 with stabilization energies of -25.2 and -24.2 kcal mol^{-1}. The *frdD* cistron also contained two potential hairpins of -20.8 and -21.0 kcal mol^{-1} at nt 3189 to 3245 and nt 3264 to 3318, respectively. Each area of high structure was followed by a long stretch [>100 nt] of little or no structure, which resemble Rho-dependent termination regions [8]. The -27.6 kcal mol^{-1} terminator for the *frd* operon is at nt 3422 to 3450 [16], immediately downstream of the *frdD* cistron. No haipin loops were located within *frdC*.

FrdA begins with GUG [14], and the Shine-Delgarno sequence was found to consist of two overlapping homologies to the 16S rRNA [21,22] with stabilization energies of -12.3 and -18.5 kcal mol^{-1} [Fig. IV.3]. *FrdB*, *frdC* and *frdD* begin with AUG [1, 16] and their ribosome binding sequences consisted of single homologous regions with stabilization energies of -13.5,-15.1 and -15.1 kcal mol^{-1}, respectively.

The *frd* promoter [24, 17] is located between nt -39 and -9 relative to the transcription start site at nt +1 of the mRNA [Fig. IV.1]. The promoter for *ampC* [16] is located at nt 3375 to 3402, within *frdD*.

In vitro protein synthesis

To test whether the hairpin loops in the Ala-rich region of *frdA* [nt 129 to 202] represented a control region, an S-30 extract was supplemented with 10 mg Gly ml^{-1} or 10 mg Ala ml^{-1} and primed with a plasmid, pDJL6, which bears the entire *frd* operon and 650 bp of sequence 5' to the promoter region.

In the absence of exogenous DNA no polypeptides were produced at appreciable levels [Fig. IV.4A, lane 1]. The vector control [Fig. IV.4A, lane 2] showed that the parent plasmid pT7-4 encoded only the expected β-lactamase polypeptides. Little aerobic expression of fumarate reductase [Table IV.1; Fig. IV.4A, lane 3] is seen with 150 fmol pDJL6 in the presence of Gly. FrdA and FrdB were present at a ratio of 2.6:1. FrdC and FrdD were not detectable. The addition of 10 mg Ala ml^{-1} stimulated the expression of total fumarate reductase polypeptides 17.6-fold [Table IV.1; Fig. IV.4A, compare lane 3 and lane 5]. The subunit ratios for FrdA:FrdB:FrdC:FrdD were 1:0.8:1:1, respectively. Under these conditions, the total amount of β-lactamase produced increased 1.7-fold, while that of total protein increased 4.5-fold.

Expression of fumarate reductase was increased 10.9-fold by doubling the amount of plasmid DNA in the S-30 extract from 150 to 300 fmol. [Table IV.1; Fig. IV.4A, lane 4], but the subunits were present at a ratio of 2.2:1:1:1. The increase in *bla* expression was 1.2-fold. Ala additionally increased total protein expression 1.6-fold, that of fumarate reductase 1.7-fold and the synthesis of β-lactamase 1.5-fold compared to that of 300 fmol DNA with Gly. The Frd subunit ratios became 1:0.9:1:1 [Table IV.1; Fig. IV.4A, compare lane 4 and lane 6].

In vitro mRNA synthesis

To determine whether control was exerted at the translational or transcriptional level, the incorporation of [^{3}H]UTP into mRNA was measured in an S-30 extract.

In the presence of Gly there was little label incorporated into mRNA at 75 or 150 fmol DNA [365 and 315 DPM, respectively; Fig. IV.5, dark

bars]. On titration to 225 fmol DNA there was a 10-fold increase in labeling to 3135 DPM. 300 fmol of plasmid gave 4000 DPM of [^{3}H]UTP incorporated into mRNA. These values were corrected for uptake of label into material precipitable by cold TCA in the absence of exogenous DNA [3030 DPM]. The ratio of mRNA to plasmid DNA varied from 2.1 DPM fmol^{-1} [150 fmol DNA] to 13.9 DPM fmol^{-1} [225 fmol DNA].

Addition of 10 mg Ala ml^{-1} to the aerobic transcription mixture enhanced the incorporation of labelled UTP into mRNA specified by pDJL6 at all concentrations [endogenous uptake was 3040 DPM]. 75 fmol of plasmid DNA directed the increased synthesis of mRNA [1140 DPM]. At 150, 225 and 300 fmol DNA the incorporation of [^{3}H]UTP was increased to 2065, 2520 and 3845 DPM, respectively [Fig. IV.5, gray bars]. In the presence of Ala the ratio of mRNA to exogenous DNA remained essentially constant at 13.3±0.8 DPM fmol^{-1} at all plasmid concentrations.

Effect of Fnr on *frd* protein translation

The Fnr protein has been reported to be a pleiotropic affector of *frd, nar, hyd, fdh* and *tor* expression [3,5]. To examine its effect on the stimulation of expression of fumarate reductase by Ala, a plasmid bearing the *fnr* gene [pfnr2], which expresses the Fnr protein *in vivo* [13], was added to the *in vitro* translation system at the same copy number as *frd.*

In all conditions there was increased polarity of expression in the presence of *fnr* [Table IV.2; Fig. IV.4B]. At 150 fmol of *frd* the molar ratio of FrdA:FrdB:FrdC:FrdD synthesised was 19.4:9.8:1.0:0 in the Gly medium [Fig. IV.4B, lane 1]and 5.1:6.0:3.2:1.0 in the Ala medium [Fig. IV.4B, lane 3] . At the higher DNA concentration of 300 fmol the

ratios became 9.4:3.9:1.0:0 [Fig. IV.4B, lane 2] and 9.5:5.6:4.9:1.0 [Fig. IV.4B, lane 4] when supplemented with Gly and Ala, respectively. The increase in expression due to DNA titration was halved to five-fold from 10.9 fold, while that due to the addition of Ala was reduced an order of magnitude to that seen for β-lactamase.

D. DISCUSSION

Two potential promoters for *frd* have been reported [Fig. IV.1; nt 39 to -34 and -11 to -6 [24] or -37 to -32 and -9 to -4 [17]] which resemble the consensus promoter for many constitutive operons [TTGACA-[16-18bp]-TATAAT] [3, 24]. This suggests that recognition by alternate σ-factors [3, 25] is probably not involved in the anaerobic regulation of this operon . It was observed that transcription is greatly enhanced upon a small increase in *frd* operon concentration, which is consistent with titrating out a repressor protein from the putative *frd* operator region. Also conceivable is the titration of the termination factor responsible for attenuation in the Ala-rich region of *frdA* mRNA .

Under anaerobic conditions *in vivo*, fumarate reductase is always synthesised and assembled in the membrane with one copy of each subunit [26]. Jones and Gunsalus [17] have shown that the *frd* operon is transcribed as a single polycistronic mRNA *in vivo*. *FrdA* begins with the codon GUG, which is reported to be one-half as efficient an initiator as AUG [27]. How, then, is FrdA synthesised at the same level as FrdB, FrdC and FrdD using only translational-level control? The ribosome binding site for *frdA* contains two separate, overlapping homologies to the 16S rRNA [Fig. IV.3]. These may serve to hold the initiation complex in place sufficiently

long to make up for the less efficient binding of $tRNA^{f\text{-}MET}$ to the GUG codon. Also, each of the *frd* cistrons have overlaps between their stop codons and the ribosome binding sites of the following cistron [Fig.IV.1]. This would suggest that translational coupling [28], during which ribosomes restart at the distal cistron without first dissociating from the mRNA after completing the proximal cistron's protein, would ensure that the distal genes would not be transcribed more readily than *frdA*, despite their stronger ribosome binding sites. The remaining three polypeptides, which initiate with AUG, are synthesised *in vitro* in the same ratio as the strengths of their respective Shine-Delgarno sites; 0.85:1:1.

It has already been noted that anaerobically *in vivo* the four fumarate reductase subunits are synthesised in equimolar amounts. Under aerobic conditions *in vitro*, the synthesis of subunits from the *frd* operon showed a different pattern.

Under repressed conditions [150 fmol DNA, 10 mg Gly ml^{-1}] there was some transcription still occuring from the consensus-like *frd* promoter and small amounts of FrdA and FrdB were synthesized from the resulting mRNAs [Table IV.1; Fig. IV.4A, lane 1] indicating read-through of the Ala loop. The ratio of FrdA to FrdB of 2.6 suggested that about 65% of such read-through transcripts terminated at the end of *frdA* and the remainder ended somewhere just downstream of *frdB*. The breadth of the FrdA bands in Fig. IV.3B as compared to Fig. IV.3A may be due to a ragged C-terminus caused by ear' termination. The amount of transcription, as measured by [^{3}H]UTP incorporation, could be stimulated 11.7-fold by increasing the amount of DNA by 50% [Fig. IV.5], as if a repressor protein was being titrated out. However, control over expression was still being exerted downstream of the promoter and 54% of transcripts

appeared to be terminating within *frdB*. The appearance of FrdC and FrdD at equimolar ratio to FrdB must reflect the fact that attenuation downstream of *frdB* was no longer occuring, and therefore that a titratable factor may be involved. We propose that the results discussed above may have been due, in part, to the dilution of an affector protein in the S-30 extract by the excess of *frd* DNA present.

The tripartite hairpin structure in the Ala-rich region at the N-terminus of *frdA* bears a striking resemblence to structures found in the leader regions of the *trp, his, phe, ilv* and *thr* operons [9,29,30]. In these latter cases there is a short 'leader' sequence, encoding a polypeptide containing consecutive codons for the amino acid synthesized by the operon, located upstream of the first cistron . The mRNA transcribed om this region can form multiple, mutually exclusive hairpin loops. If ıe ribosome closely follows the elongation complex and reads through the irst loop in the proximal leader sequence which contains the multiple codons for the appropriate amino acid, then the s d loop in the distal region of the leader sequence can form a Rho-independent attenuator which functions to halt transcription of the downstream operon. If the ribosome stalls at the first loop due to low levels of the appropriate charged tRNA, the terminator cannot form and RNA polymerase continues to transcribe the operon [30,31,32,33].

In the *frd* operon the proposed model is just the opposite. It is envisioned that RNA polymerase is transcribing the DNA template and has reached nt 171 of the message, at which time loop A [Fig. IV.2A] forms, causing the transcription complex to pause [10,9]. The first ribosome catches up to the paused complex and translates $-Val^{10}Gly^{11}$, thereby releasing loop A. The mRNA now forms loop C and the polymerase

continues transcribing the message at least as far as nt 203. If the translating ribosome stalls briefly at Ala^{12} or Ala^{15} due to low levels of charged $tRNA^{ALA}$, loop B forms. This could represent an increased energetic barrier to ribosome translocation, as well as containing additional closely spaced Ala codons at which stalling could occur for extended periods. Meanwhile, the RNA polymerase has transcribed the relatively featureless region downstream of nt 260. At this point termination can occur, mediated either by Rho or by some other protein of like function [8,9,34].

On the other hand, if Ala levels are high and the tRNAs are fully charged, the first ribosome would catch up to the transcription complex at loop A and continue to follow it closely [$\cong$ 40 nt; 9,10] as it moved through this Ala-rich region and onwards. No mRNA devoid of both ribosomes and strong secondary structure would result, and Rho-like termination could not occur [8,34].

Any of the other hairpin loops followed by long structureless stretches could also act as termination areas if the ribosomes are delayed at the early attenuator, making up for the lower efficiency of Rho-dependent termination as compared to Rho-independent termination [8,34]. They could give rise to the patterns of polarity observed in the subunit ratios of the *frd* polypeptides [Tables IV.1 and IV.2; Fig. IV.4]. Rho has been suggested to act on ribosome-free mRNA at areas where cytosine residues are spaced at 12±1 residues [8] or 13±1 residues apart [34a]. Figure IV.6 shows that such spacing of cytosine residues does occur in the *frd* operon in areas of weak structure between the areas of strong structure identified in Figure IV.1. This is additional evidence that either Rho or a protein of like function is involved in the attenuation mechansim of *frd*.

As Fnr has been reported to be a regulator of *frd* expression [3,4,5,13], its effect on the system was examined. The most notable change was the considerable increase in polarity of expression of the operon. Under none of the conditions used were the Frd subunits ever produced in equimolar ratio, and the dramatic increase in synthesis noted on addition of Ala was abolished, being no more than the effect on β-lactamase. In each case the pattern of translation would seem to indicate that approximately half of the transcripts were being terminated within *frdB*, while most of the rest were terminating within *frdC*, if Gly was present, or within *frdD*, if alanine was present. Even in the presence of Ala, less than 13% of transcripts could have been the full length of the operon. However, the addition of Ala did have an effect in reducing the degree of polarity exerted by Fnr on *frd* expression.

In the absence of Fnr, the presence of high Ala concentrations at low DNA concentration relieved both repression of transcription initiation, as indicated by a 6.5 fold increase in [^{3}H]UTP incorporation and by the constant ratio of mRNA to DNA of 13.25 DPM fmol^{-1}, and downstream termination, as indicated by a 17.6-fold increase in production of fumarate reductase polypeptides at equimolar ratios.

The addition of *fnr* to the coupled transcription/translation system not only greatly reduced the effects of Ala on expression, it reduced the magnitude of induction by titration two-fold, also. It would be tempting to speculate that Fnr is therefore acting to repress initiation of transcription, but this effect could as easily be produced by increasing the efficiency of attenuation at the Ala loop region of the transcript. The addition of Fnr has restored to the system the suppression by oxygen, as all of the *in vitro* work was done open to the air.

Fnr is constitutively expressed aerobically but there is some controversy as to its expression anaerobically. Two groups report that there is no change in Fnr expression under anaerobic conditions [4,35]. Spiro and Guest [36] using an *fnr-lacZ* gene fusion demonstrated that there is a 2.7-fold decrease in *fnr-lacZ* expression under anaerobic conditions. Furthermore, this downregulation requires an active *fnr* gene product. There was no effect of Fnr on *fnr-lacZ* expression under aerobic conditions.

The reduction in Fnr seen during anaerobic growth is consistent with the data which shows efficient translation of *frd* mRNA in the absence of Fnr and strong polarity of expression in the presence of Fnr as the basis of regulation of this anaerobic operon. It is proposed that Fnr is acting as a termination factor in the expression of the *frd* operon. Its function appears to be similar to that of Rho or NusA and may, like the latter protein, require the action of additional cofactors.

NusA has a number of effects on transcription [8,34,37]. It can act to increase the efficiency of Rho-mediated termination. It has been implicated in N and Q-dependent antitermination in the lambda phage system, in antitermination at the *trp* attenuator and in termination at sites of transcriptional polarity. In each of these cases it is presumed to bind to the other proteins involved and/or to RNA polymerase. By itself it can cause termination at lambda t_{r2} and *rrnB* t_1 [38]. It may well be that, like NusA, Fnr is multifunctional, mediating both termination and antitermination depending on the operon concerned and the redox state of the cell.

The picture of Fnr as simply an anaerobic switch is further complicated by the observation that *fnr* strains retain several *fnr*-dependent enzyme activities despite being phenotypically deficient for growth [5].

Fumarate reductase was reported to be required in the synthesis of uracil [39] . In contrast, *fnr* strains will grow anaerobically on glucose minimal medium without uracil, implying the presence of adequate levels of fumarate reductase activity for metabolic needs [5]. These authors also showed that *fnr* strains will not grow on formate-fumarate or formate-nitrate media. When the enzyme formate dehydrogenase is assayed in these bacteria a complex pattern of changed activity using artificial electron donors is found. Activity with benzyl viologen is decreased five-fold, activity with dichlorophenylindophenol is increased three-fold and there is no change in activity using methylene blue, as compared to wild-type strains.

These results are inconsistent with the concept of Fnr being a simple positive regulator for anaerobic genes but are entirely consistent with the idea of Fnr being a controller of polarity in polycistronic operons, where proximal subunits required for metabolic needs are produced while distal subunits required for energy transduction are not. In the fumarate reductase system, FrdAB is the catalytic domain, which can exist alone in the cytoplasm [11] while the membrane bound anchors, FrdCD, are required for coupling to electron transport *in vivo* or to quinone analogues *in vitro* [11,17]. The FrdAB dimer has a two-fold higher activity with benzyl viologen as donor than does the FrdABCD tetramer, while it lacks activity with quinone analogues [11].

The previous reports of Fnr as a regulator of *frd* [1,3,4,5] are not in error. In each case the data published is essentially compatible with the model for regulation proposed herein. The confusion lies in the phenotypic selection of *fnr* as a mutation which suppresses growth on nitrate and fumarate as electron acceptors. If Fnr is a negative regulator,

then a deletion or nonsense mutation would lead to an increase in fumarate reductase and not to its loss. Therefore only mutations which cause Fnr to continue its attenuation of the operon under anaerobic conditions will be seen. It is unfortunate that no biochemical characterization of the *fnr* mutants has appeared in the literature to clarify the nature of the lesions in this important control protein.

A rationale for the additional regulation by Ala is not apparent, although it may be that Ala, which is formed from pyruvate and valine by transamination [40], is sensitive to the rate of consumption of pyruvate, which may serve, in turn, as an indicator of the redox state of the electron transport chain. Interestingly, cells grown anaerobically on pyruvate express fumarate reductase 1.4 fold better than cells grown on glucose, reaching 62% of maximal expression in GF medium.

The control of anaerobic expression of operons not involved in amino acid synthesis by amino acid levels is not unique. The *tppB* operon, which is involved in peptide uptake, is induced either by anaerobiosis or by leucine in the medium aerobically [41]. An increase in fumarate reductase activity in complex medium containing casamino acids compared to that expressed in minimal medium without casamino acids has been reported [7]. This supports the observation that, at least *in vitro*, *frd* expression can be controlled by Ala.

We have proposed a model for the expression of the *frd* operon whereby positive control is exerted by Ala and modulated by Fnr acting as a termination factor under aerobic conditions, based on results from an aerobic *in vitro* system. Experiments to extend this observation to the whole cell aerobically and anaerobically are in progress.

AKNOWLEDGEMENTS

The authors wish to thank R. G. Gunsalus for his gift of the *fnr* plasmid.

TABLE IV.1. Aerobic expression of proteins from pDJL6 *in vitro*.

DNA [fmol]	amino acid	FrdA[a]	FrdB[b]	FrdC[c]	FrdD[d]	Bla[e]	total Frd	total protein
150	glycine	1.79	0.69	ND	ND	11.60	2.48	14.08
150	alanine	11.16	9.62	11.4	11.6	19.70	43.78	63.48
300	glycine	11.47	5.15	5.20	5.30	14.10	27.10	41.20
300	alanine	12.26	10.15	12.1	11.8	20.90	46.41	67.31

a 10 mg ml^{-1} final conc.
b area under scanned peak/19 Met per polypeptide.
c area under scanned peak/13 Met per polypeptide.
d area under scanned peak/4 Met per polypeptide.
e area under scanned peak/6 Met per polypeptide.
f area under scanned peak/10 Met per polypeptide. Pre-Bla and the two processed peaks were always present in constant ratio, therefore the area of pre-Bla only was used as a measure of total *Bla* expression.
ND not detected

TABLE IV.2. Effect of Fnr on aerobic expression of proteins from pDJL6 *in vitro*.

DNA [fmol][a]	amino acid[b]	FrdA[c]	FrdB[d]	FrdC[e]	FrdD[f]	total Frd
150	glycine	1.55	0.78	0.08	ND	2.41
150	alanine	1.42	1.68	0.90	0.28	4.29
300	glycine	7.96	3.31	0.85	ND	12.11
300	alanine	9.24	5.46	4.75	0.97	20.41

a pfnr2 and pDJL6 each present in this amount.
b 10 mg ml^{-1} final conc.
c area under scanned peak/19 Met per polypeptide.
d area under scanned peak/13 Met per polypeptide.
e area under scanned peak/4 Met per polypeptide.
f area under scanned peak/6 Met per polypeptide.
ND not detected.

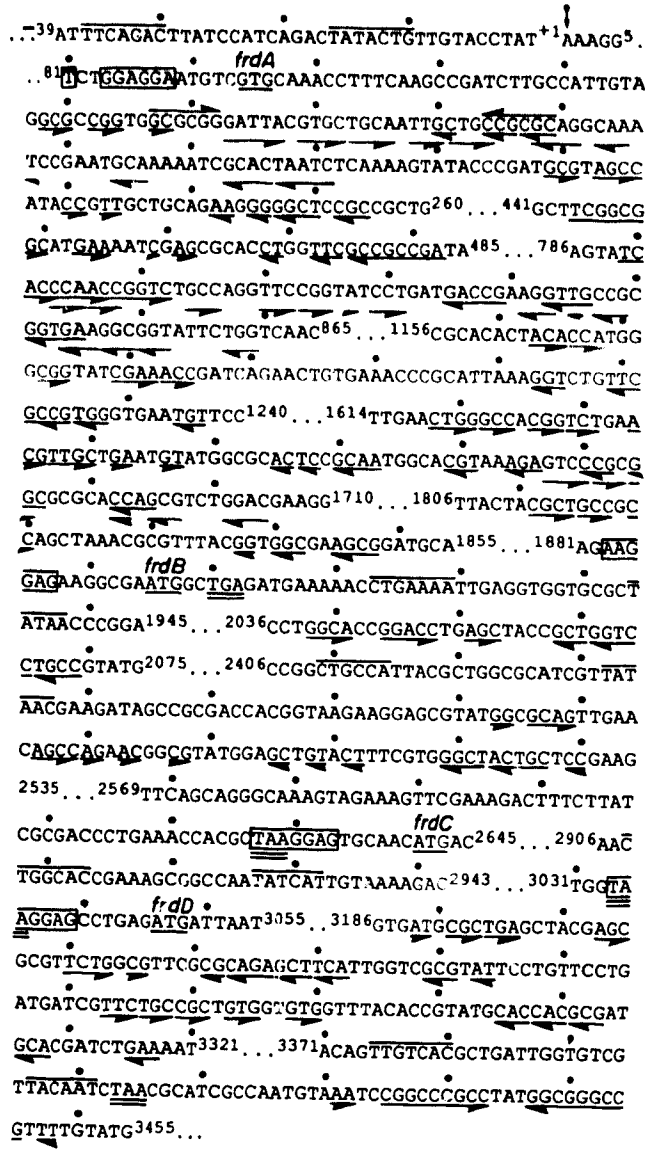

Figure IV.1. The DNA sequence of the *frd* operon. Ellipses mark gaps in the sequence left for clarity's sake, the superscript numbers being the position in the mRNA of the attached nucleotide. Overlines mark promoter sequences, single underlines initiation codons and double underlines termination codons. Shine-Delgarno sequences are boxed. Arrows beneath the sequence indicate the matched bases of the imperfect inverted repeats. Arrows above the sequence mark the perfect 6 bp inverted repeat. The vertical arrow at +1 marks the beginning of the mRNA transcript.

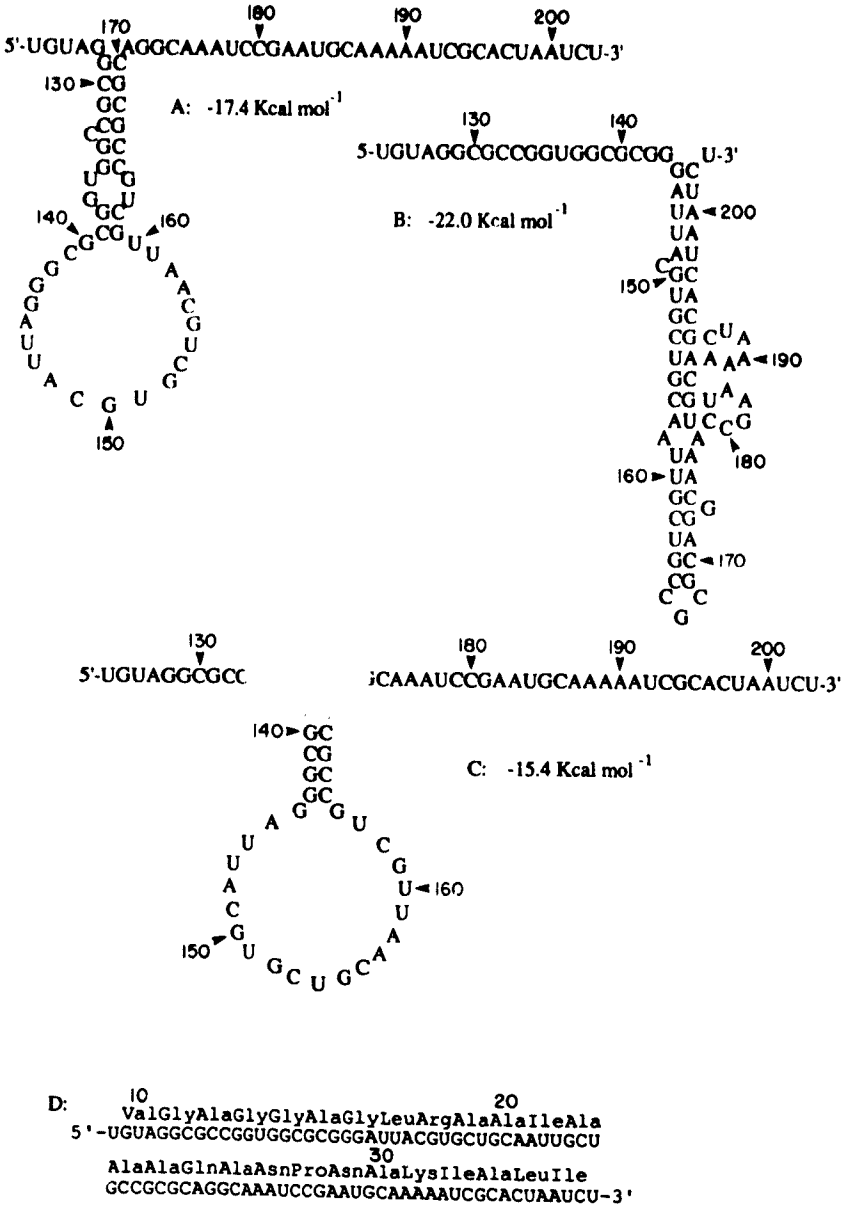

Figure IV.2. The attenuator region of the *frd* mRNA. A, B and C show the three mutually exclusive hairpin loops described in the text, together with their ΔG_{conf} values. The numbering is from the start of transcription. D shows the same linear RNA sequence and the protein sequence encoded thereby, with the numbering relative to the initiating Met.

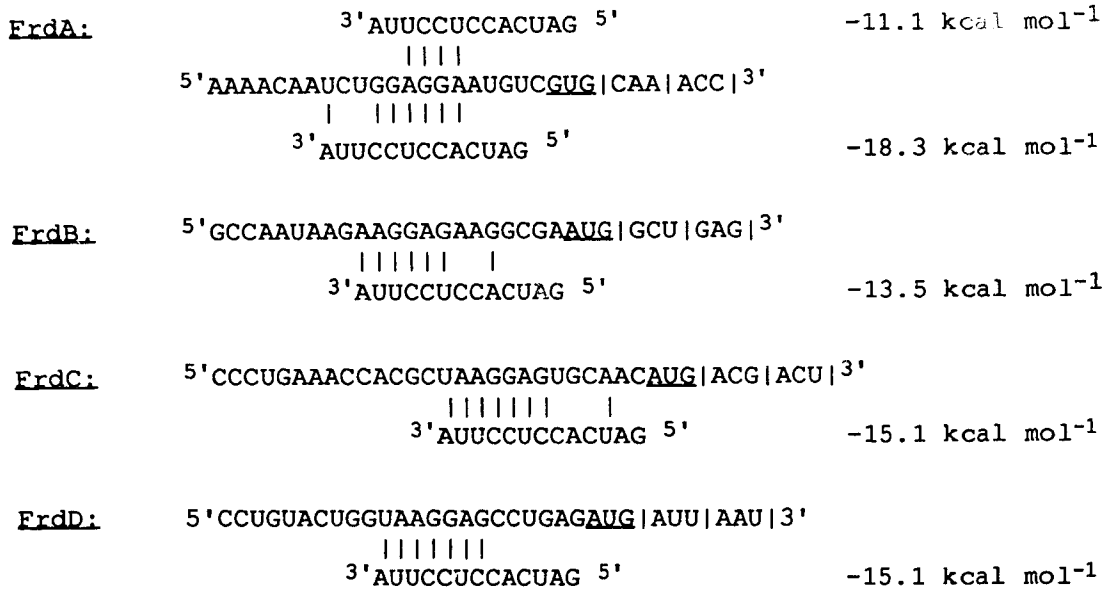

Figure IV.3. The Shine-Delgarno sequences of the *frd* operon.

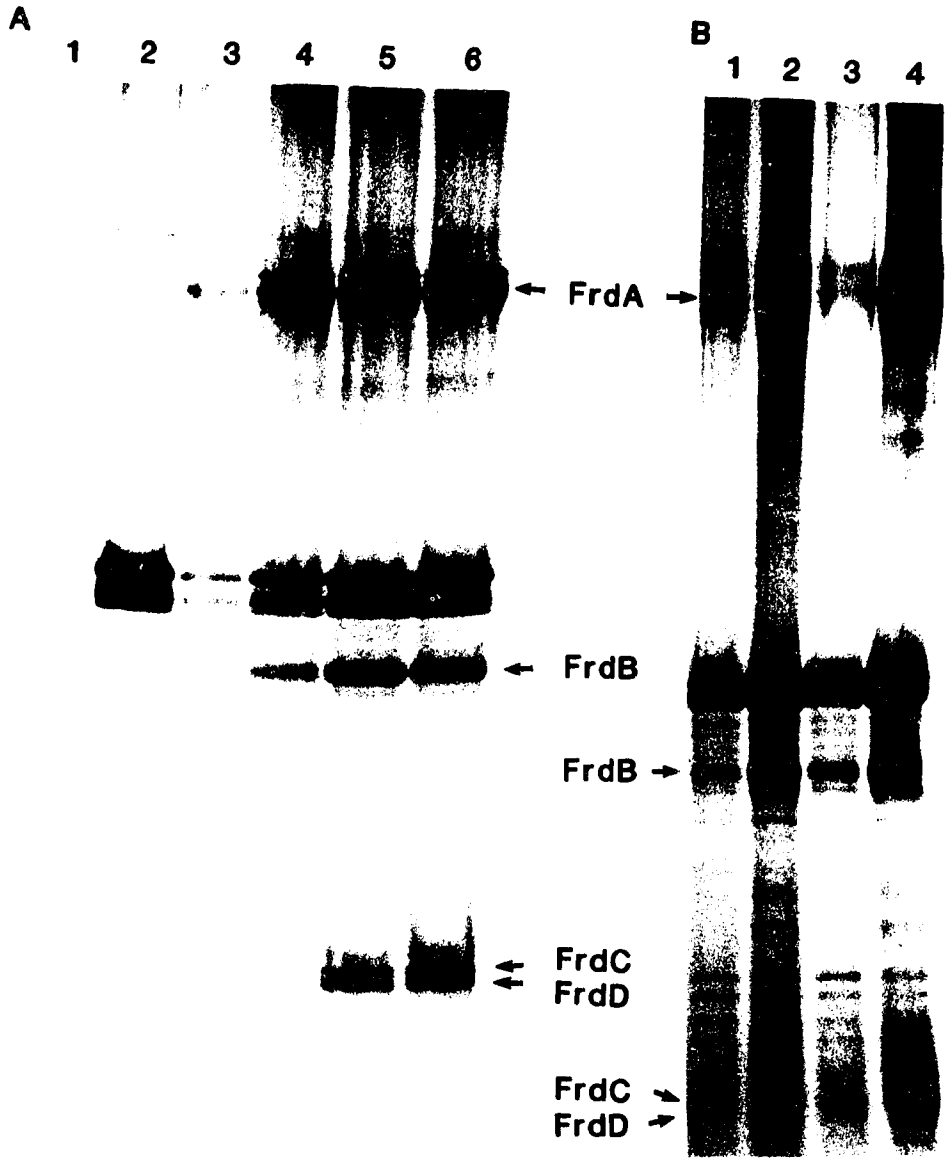

Figure IV.4 Protein expression from pDJL6. Shown are autoradiographs of double-gradient polyacrylamide gels. Proteins were translated and labelled with [^{35}S]methionine as described in Materials and Methods. 10 µl of S-30 extract containing the indicated quantities of plasmid DNA and 10 mg of the specified amino acid per ml were loaded into each well. [A] Translation in the absence of *fnr*. [lane 1] no plasmid, [lane 2] 600 fmol pT7-4 plus Gly, [lane 3] 150 fmol pDJL6 plus Gly, [lane 4] 150 fmol pDJL6 plus Ala, [lane 5] 300 fmol pDJL6 plus Gly, [lane 6] 300 fmol pDJL6 plus Ala. [B] Translation in the presence of *fnr*. [lane 1] 150 fmol pDJL6 and pfnr2 plus Gly, [lane 2] 300 fmol pDJL6 and pfnr2 plus Gly, [lane 3] 150 fmol pDJL6 and pfnr2 plus Ala, [lane 4] 300 fmol pDJL6 and pfnr2 plus Ala.

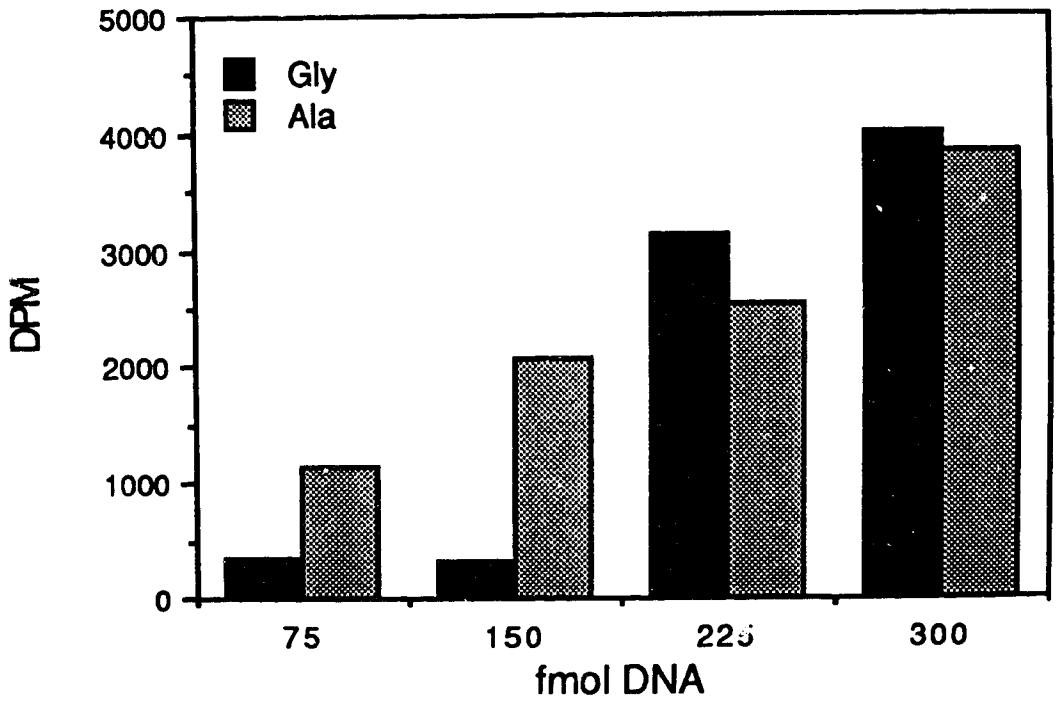

Figure IV.5. mRNA expression from pDJL6 in vitro. S-30 extracts were pulsed for 15 sec with [^{3}H]UTP, mRNA was precipitated in cold 5% TCA, 0.1 M $Na_2P_2O_7$, collected on GF/C filters and counted. Data are corrected for non-specific incorporation in the absence of exogenous DNA [3032.0 DPM in Gly or 3041.7 DPM in Ala].

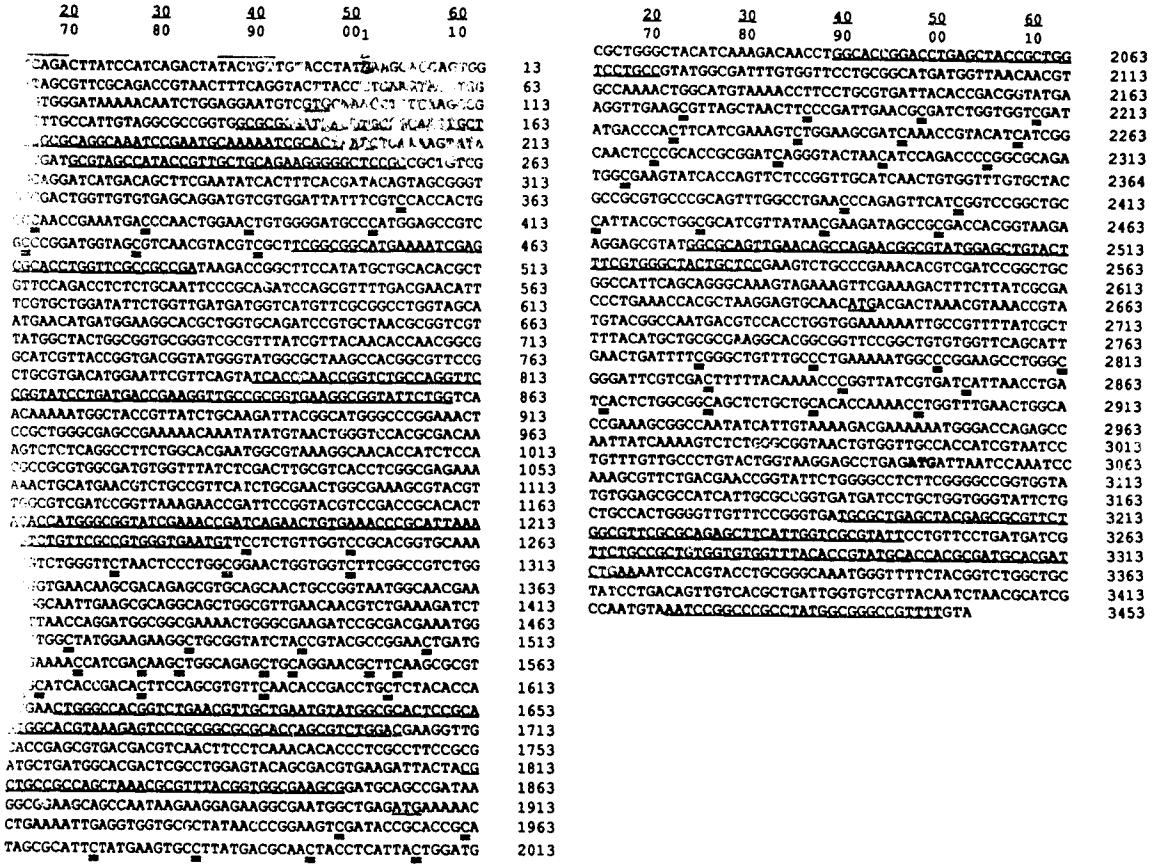

Figure IV.6. Rho binding sites in the *frd* operon. Shown is the sequence of the *frd* operon from promoter to terminator. Numbering is relative to the start of transcription which is marked by: **A**. The promoter is marked by overlines. Start codons are marked by wavy underlines. Hairpin-forming regions are marked by single underlines. Possible Rho-binding residues are marked by double underlines.

Bibliography

1. Cole, S.T., Condon C., Lemire B.D., & Weiner, J. H. 1986. Biochim. Biophys. Acta. **811**:381-403.
2. Lin, E.C.C. & Kuritzkes, D.R. pp 201-221. 1987. *In* Neidhardt , F. C. [ed.-in-chief], *Escherichia coli* and *Salmonella typhimurium*, cellular and molecular biology. American Society for Microbiology, Washington, D.C.
3. Hoopes, B. C. & McClure, W. R. 1987. pp. 1231-1240.*In* Neidhardt , F. C. [ed.-in-chief], *Escherichia coli* and *Salmonella typhimurium*, cellular and molecular biology. American Society for Microbiology, Washington, D.C.
4. Unden, G. & Duchene, A. 1987. Arch. Microbiol. **147**: 195-200.
5. Lambden, R. R. & Guest., J. R. 1976. J. Gen. Microbiol. **97**: 145-160.
6. Iuchi, S. & Lin, E. C. C. 1987. Proc. Nat. Acad. Sci. USA. **84**:3901-3905.
7. Unden, G. & Guest., J. R. 1984. FEBS Lett. **170**:321-325.
8. Platt, T. 1986. Ann. Rev. Biochem. **55**:339-372.
9. Landick, R. & Yanofsky, C. 1987. pp.1276-1301. *In* Neidhardt , F. C. [ed.-in-chief], *Escherichia coli* and *Salmonella typhimurium*, cellular and molecular biology. American Society for Microbiology, Washington, D.C.
10. Yanofsky, C. 1981. Nature. **289**:751-758.
11. Latour, D. J. & Weiner, J. H. 1987. J. Gen. Microbiol. **133**:597-607.
12. Tabor, S. & Richardson, C. C. 1985. Proc. Natl. Acad. Sci. USA. **82**:1074-1078.
13. Jones, H. M. & Gunsalus, R. P. 1987. J. Bacteriol. **169**:3340-3349

14. Cole, S. T. 1982. Eur. J. Biochem. **122**:479-484.

15. Cole, S. T., Grundström, T., Jaurin, B., Robinson, J. J. & Weiner, J. H.. 1982. Eur. J. Biochem. **126**:211-216.

16. Grundström, T. & Jaurin, B. 1982. Proc. Natl. Acad. Sci. USA. **79**:1111-1115.

17. Jones, H. M. & Gunsalus, R. P. 1985. J. Bacteriol. **164**:1100-1109.

18. Queen, C. & Korn, L. J.1984. Nucl. Acids Res. **12**:581-599.

19. Tinoco, I., Jun., Boyer, P. N., Dengler, B. & Levine, M. D. 1973. Nature New Biol. **246**:40-41

20. Laemmli, U. K. 1970. Nature **277**:680-685.

21. Shine, J. & Delgarno, L. 1974. Proc. Natl. Acad. Sci. USA. **71**:1342-1346.

22. Steitz, J. A. & Jakes, K. 1975 Proc. Natl. Acad. Sci. USA. **72**:4734-4738.

23. Wood, D., Darlison, M. G., Wilde, R. J. & Guest, J. R. 1984. Biochem J. **222**:519-534.

24. Harley, C. B. & Reynolds, R. P. 1987. Nucl. Acids Res. **15**:2343-2361.

25. Helmann, J. D. & Chamberlin, M. J. 1987. Proc. Natl. Acad. Sci. USA. **84**:6422-6424.

26. Lemire, B. D., Robinson, J. J., Weiner, J. H. 1982. J Bacteriol. **152**:1126-1131.

27. Klionsly, D. J., Skalnik, D. G. & Simoni, R. D. 1986. J. Biol. Chem. **261**:8096-8099.

28. Gold, L. & Stormo, G. 1987. pp.1302-1307. *In* Neidhardt , F. C. [ed.-in-chief], *Escherichia coli* and *Salmonella typhimurium*, cellular

and molecular biology. American Society for Microbiology, Washington, D.C.

29. Rosenberg, M. & Court, D. 1979. Ann. Rev. Genet. **13**:319-353.
30. Lee, F. & Yanofsky, C. 1977. Proc. Natl. Acad. Sci. USA. **74**:4365-4369.
31. Zurawski, G., Elselviers, D., Stauffer, G. V. & Yanofsky, C. 1978. Proc. Natl. Acad. Sci. USA. **75**:5988-5992.
32. Morse, D. E., & Morse, A. N. C. 1976. J. Mol. Biol. **103**:209-226.
33. Yanofsky, C. & Soll, L. 1977. J. Mol. Biol. **113**:663-677.
34. Yager, T. D. & von Hippel, P. H. 1987. pp.1241-1275. *In* Neidhardt , F. C. [ed.-in-chief], *Escherichia coli* and *Salmonella typhimurium*, cellular and molecular biology. American Society for Microbiology, Washington, D.C.

34A. McSwiggen, J. A., Bear, D. G. & von Hippel, P. H. 1988. J. Mol. Biol. **199**:609-622.

35. Pascal, M.-C., Bonnefoy, V., Fons, M. & Chippaux, M. 1986. FEMS Microbiol. Lett. **36**:35-39.
36. Spiro, S. & Guest, J. R. 1987. J Gen Microbiol. **133**:3279-3288.
37. Ralling, G. & Linn, T. 1987. J. Bacteriol. **169**:2277-2280.
38. Schmidt, M. C. & Chamberlin, M. J.1987. J. Mol. Biol. **195**:809-818.
39. Ruch, F. E., Kuritzkes, D. R. & Lin, E. C. C. 1979. Biochem. Biophys. Res. Comm. **91**:1365-1370.
40. Reitzer, L. J. & Magasanik, B. 1987. pp. 302-320. *In* Neidhardt , F. C. [ed.-in-chief], *Escherichia coli* and *Salmonella typhimurium*, cellular and molecular biolog American Society for Microbiology, Washington, D.C.

41. Jamieson, D. J. & Higgins, C. F. 1984. J Bacteriol. **160**:131-136.

V. CONCLUSIONS

The studies reported in this thesis were directed towards an understanding of the expression and assembly of the fumarate reductase from anaerobically grown *E. coli.* Much of the work was stimulated by the sequencing of the *frd* operon and the identification of the membrane anchor subunits of the holoenzyme. These polypeptides held the enzyme to the membrane, induced increased stability and allowed interaction with quinone analogues. It was of interest to know why two dissimilar subunits were required for these functions.

In Chapter II I showed that each subunit contributed its own suite of characteristics to the holoenzyme. FrdA alone was sufficient to allow flavinylation of its own His^{44}, but not for catalytic activity. The addition of FrdB conferred activity on the enzyme. FrdC stabilized the enzyme against alkali and conferred anion insensitivity. FrdD was required for membrane insertion, thermal stability and quinone oxidase activity.

It would be interesting to further examine the FrdC and FrdD subunits to see which residues are involved in their various properties. It is already known that His^{84} of FrdC is important in electron transfer from menaquinone to FAD within the complex. It may be possible to purify these two subunits by hydrophobic exchange chromatography of the purifed tetramer. Once isolated, classical biochemical techniques involving residue modification and reconstitution may yield interesting answers. It has become technically feasible to examine the conformation of proteins of about 100 residues in size in solution by ^{13}C-NMR [1]. There is interest in the lab in pursuing such studies if a purified anchor subunit were available.

In the course of this study I generated several transposon insertions in the *frdA* and *frdB* genes. These may be used in the future to address the

question of how much of the relevant polypeptide chain is required before insertion of the FAD or assembly of the iron-sulphur clusters can occur. As the truncated proteins involved are rapidly degraded, the T7 expression system may also be used to produce adequate levels of polypeptides.

Fumarate reductase strongly resembles *E. coli* succinate dehydrogenase in terms of subunit composition, cofactors present, catalytic mechanism and primary structure of the catalytic subunits [2]. The 15kDa SdhC subunit has been identified as cytochrome b_{556} and presumably it mediates electron transfer from the FAD to ubiquinone. There is no evidence to date that a *b*-type cytochrome is associated with fumarate reductase, although much effort in this lab has been directed toward this end. Also, fumarate reductase has been shown to interact directly with quinone analogues, suggesting that a cytochrome is not, in fact, required. This difference may reflect the fact that the midpoint potential of the ubiquinone/quinol couple [+40mV] is more positive than that of the succinate/fumarate couple [+30mV], while the menaquinone /quinol couple [-74mV] is more negative [3].

I have developed an aerobic assay for quinol oxidase activity which is superior to the anaerobic assays previously required to work with these readily oxidized substances. This should allow the study of the kinetics of the enzyme using substrates which are more realistic than the organic dyes previously used as electron donors. Preliminary results showed that the K_m for fumarate is different when using DMN than when using benzyl viologen.

It was already known that FrdA and FrdB could assemble in solution to form a catalytic dimer, and that this dimer could bind to anchor subunits which previously had been assembled normally in the membrane as part of

the holoenzyme and then stripped of their catalytic heads. The studies in Chapter III addressed the question of subunit assembly in more detail. The assembly pathway indicated by this work was the preassembly of FrdC and FrdD immediately after synthesis, with the later association of FrdB and FrdA, in that order.

While this conclusion is probably valid, a note of caution must be introduced. The level of polypeptides expressed by the *in vivo* T7 transcription/translation system in a very brief time is much greater than would normally be obtained. Also, the four fumarate reductase subunits are normally expressed in equal amounts, while in the T7 system the anchor subunits predominate. So that while the immunoprecipitated complexes indicate the pathway described, it may be that the excess of anchor subunits interferes with proper assembly of the catalytic head. Additionally, it has been shown that for proper assembly of holoenzyme to occur the *frdC* and *frdD* genes must be present in *cis*. If they are present in *trans* on different plasmids a non-functional tetramer results [4]. This argues that FrdC and FrdD must interact strongly at the time of synthesis to form the normal membrane anchor.

Frd is one of about 50 genes which are specifically expressed during anaerobiosis [5]. The substance which signals anaerobic conditions is probably different for different operons. The control of *frd* was known to involve at least two proteins, Fnr and NarL. Surprizingly, alanine was found to regulate *frd* expression *in vitro*, as discussed in Chapter IV. While this effect can be rationalised by saying alanine concentration varies directly with pyruvate concentration, which in turn may reflect the activity of the aerobic electron transport chain, it would be instructive to know the alanine concentration *in vivo* under both aerobic and anaerobic conditions.

Toward this end I am engaged in a series of NMR experiments involving cells grown on [^{13}C]alanine.

One lesson learned from the expression studies was that simplicity is a human concept, and not a driving force in evolution. Natural selection only works against lethal conditions, and not for any given trait. Thus, any system which works adequately will get conscripted. Given this, it should not have been surprizing to find such a unique method of regulation in the *frd* operon. A second lesson was one in scepticism. With the revelation that *frd* expression was translationally coupled and involved sequences in the mRNA well downstream of the promoter I begin to question the validity of claims based on the use of operon fusions for the study of gene expression. Such research may well be missing vital control elements for want of distant sequences.

Our goal of reconstituting an active electron transport chain is now closer than ever. With the characterization of the tetrameric fumarate reductase, the knowledge that it reacts directly with quinones and the renewed study of glycerol-3-phosphate dehydrogenase with the discovery of its membrane anchor subunit, we are now at a stage where reconstitution experiments in proteoliposomes might begin.